CASE STUDY OF NORMAL AND HIGH GLUCOSE LADEN CELL RESPONSE TO CELLULAR PHONE RADIATION USING GTEM CELL

A Dissertation

presented to

the Faculty of the Graduate School

at the University of Missouri-Columbia

In Partial Fulfillment

of the Requirements for the Degree

Doctor of Philosophy

---

by

NATTAPHONG BORIRAKSANTIKUL

Dr. Naz E. Islam, Dissertation Supervisor

JULY 2012

The undersigned, appointed by the Dean of the Graduate School, have examined the dissertation entitled

CASE STUDY OF NORMAL AND HIGH GLUCOSE LADEN CELL RESPONSE TO CELLULAR PHONE RADIATION USING GTEM CELL

presented by Nattaphong Boriraksantikul,

candidate for the degree of Doctor of Philosophy,

and hereby certify that in their opinion it is worthy of acceptance:

_____

Professor Naz E. Islam

_____

Professor Guilherme DeSouza

_____

Professor Mahmoud Almasri

_____

Professor H. R. Chandrasekhar

_____

Professor John A. Viator

ACKNOWLEDGEMENTS

I would like to give special thanks to Dr. Naz E. Islam, who is my academic advisor while I am pursuing the Ph.D. degree in Electrical and Computer Engineering at University of Missouri-Columbia (MU), Missouri, USA. His advices and assistance were valuable and beneficial. I would also like to thank all members of my graduate committee for their great comments and supports.

Thanks also go to my laboratory colleagues and friends for providing a good learning experience. I would also like to sincerely thank my colleagues at the Viator Institute of Acoustic, Thermodynamic, and Optics Research for all their great support in this dissertation. I also thank all of my friends in MU and at Thailand for their truly friendship.

Finally, I am very thankful to Mr. Narklom Boriraksantikul (my father), Ms. Wilailuck Boriraksantikul (my mother), Mr. Pholdee Boriraksantikul (my elder brother), Mr. Pholboon Boriraksantikul (my younger brother), and Mr. Krittinard Boriraksantikul (my younger sister) for their selfless love and supports. They always cheer me up and provide mental supports when I am facing the difficult time. Without their love, affection and prayers, I would not have completed my Ph.D. degree.

Nattaphong Boriraksantikul
July, 2012

CASE STUDY OF NORMAL AND HIGH GLUCOSE LADEN CELL RESPONSE TO CELLULAR PHONE RADIATION USING GTEM CELL

Nattaphong Boriraksantikul

Dr. Naz E. Islam, Dissertation Supervisor

ABSTRACT

The primary objective of this dissertation is twofold. First, to study the response of red and white blood cell and normal and high glucose blood to cellular phone radiation exposures at frequencies of 850 and 900 MHz. Secondly, to analysis the design and fabrications of an in-house GTEM cell. The simulation study of the GTEM cell was carried out by using the Computer Simulation Technology (CST) Microwave Studio 2011 software [1]. The GTEM cell characterizations include the degree of uniformity of electromagnetic fields, voltage standing wave ration (VSWR) and return loss calculations. In the biological effects studies, the blood samples were placed at the testing area inside the GTEM cell operated at 850 and 900 MHz and at 2 W and 60 W power levels; the frequencies and power respectively represent radiations from a hand held cell phone and the cell phone tower.

The simulated return loss and the VSWR values cell from 0 to 4.0 GHz for the GTEM are > 10 dB and < 2, respectively and provided perfect conditions for EM field exposures of experimental subjects. At 850 MHz statistical results on blood cell showed that there was only one significant change in red blood cell viability compared to the control, while there were five significant changes in the white blood cell viability. At 900 MHz exposure, the statistical results on the blood cell viability showed a significant difference in red blood cell viability when compared with the control samples.

Table of Contents

LIST OF FIGURES

Chapter 1: Introduction

Cellular phones emit electromagnetic (EM) radiation, and without proper shielding, the radiation could be harmful to humans and other biological elements. With the introduction of a new generation of mobile telecommunication system, with enhanced bandwidth and power, the biological effects of electromagnetic radiation from these gadgets is a real concern to many. Besides cell phones, there are other sources of EM radiation. For example:

A tablet personal computer or tablet PC is an EM sources. The tablet is a kind of computer which can be carried everywhere conveniently due to its size. It has the key features of a full-size PC. All programs and functions shown on the tablet screen are equipped with a touch screen. Some products have specific features including front and back cameras, Bluetooth and Wi-Fi.

A smart phone, which is a high-end cell phone, also emits the electromagnetic fields. The smart phone has more advanced computing ability and connectivity than other general cellular phones. It also provides more feature functions, such as video cameras, audios, Wi-Fi and some PC software, than other general mobile phones. It sometimes can serve as a mobile PC.

A computed tomography (CT) scan is also a good example of the EM sources which many of us may have contact with. It is a medical imaging technology which is the special x-ray tests using x-rays and high resolution computer. It can provide the 3-dimension (3D) scans of the patient's organ or even full body, for the doctor to diagnose

the illness. However, the CT scan may cause of the possible risks of the cancer for the patient in the future.

The radar is another EM sources. The radar is used to detect the objects using the electromagnetic waves, specifically radio waves. The radar transmits the signal to bounce off any object in the path. The reflection of the signal then returns to the received radar. It can be used to forecast the weather as well as indicate the range, altitude, direction and speed of both moving and fixed objects such as vehicles, ships and aircrafts.

EM radiation can be harnessed for useful application as well. EM fields from an anechoic chamber and a TEM cell can be used to improve the germination of the soybean seeds. The soybean seeds are placed inside the chamber with appropriate operating power, frequency, and time duration to enhance germination rate [2].

In this study emphasis is on the negative effects of electromagnetic fields [3, 4], specifically on humans with high glucose sugar levels. Previous studies have point towards such a possibility. For example, the classification of the WHO/International Agency for Research on Cancer (IARC) has suggested that cell phone radiation could possibly increase risks of developing brain tumor [5]. Exposure to GSM 900 MHz radiation for 35 minutes could increase the blood pressure of 5 mm Hg to 10 mm Hg [6]. The 900 MHz cell phone radiation also negatively affects human sperm motility, including a decrease in the rapid progressive and slow progressive movement of human sperm [7]. Ionizing electromagnetic fields cause changes in cell membrane structure, including an increase ion permeability, damage of cell membrane and loss of ion-homeostasis [8]. It has been reported that the extremely low frequency and radiofrequency fields influence stimulation of protein synthesis of DNA, and at higher

exposure levels, it causes DNA damage [9]. There are many other researches being studied on the mobile phone radiation effects [10, 11] as well as control of prostate and breast cancer [12, 13].

The current degree of proliferation of electromagnetic radiation is now unprecedented in our daily life. The EM fields are all around us; from cell phones, computers, or wiring in the home. Some believe that it significantly contributes to diseases of today. An example is diabetes ; Havas et al presented her interesting case studies that electromagnetic fields caused increases in plasma glucose levels of her diabetic patients [14, 15]. However, EM fields and its biological effects is still a question mark. Thus, more experiments on the response of blood sugar to uniform electromagnetic fields are need. An anechoic chamber or a TEM cell can provide such a field.

Basically, an anechoic chamber is a large shielded cavity, which provides the uniform electromagnetic fields and the shield environment. Even though the anechoic chamber can be used for the radiated emission and the immunity tests of the electronic devices, the large test areas of such anechoic chamber or open area test site (OATS) are not efficient for conducting the biological experiment, where the size of the biological sample is very small [16]. Certainly, the smaller testing areas provide minimum interference and reflection of the EM signal area, which is better condition to perform experiments on the smaller samples and where the large test chambers cannot offer.

On the other hand, a gigahertz transverse electromagnetic (GTEM) cell, which is a pyramidal coaxial waveguide, is a better choice and provides a uniform EM field and a shielded environment. The testing area of the GTEM cell is one-third of volume between the inner conductor and the bottom floor of the outer conductor. The GTEM cell is the

today instrument that is widely used for radiated immunity and emission tests of electronic devices and biological applications [17].

In this dissertation, a modified technique to use an in-house designed GTEM cell that operates at a wide range of frequencies for study of the response of sugar laden blood cells to cellular phone exposure at 850 and 900 MHz is proposed. In order to see the effects of cell phone radiation to normal and high glucose blood, the GTEM cell will be used to generate the EM field at 850 and 900 MHz with operating input power of 2 watts for the mobile phone signal, that of 60 watts for the cell phone base station signal. The exposure duration for each sample in the experiment will for 10, 30, 60 minutes. Normal and high glucose blood samples will be placed in the testing area inside the GTEM cell, which provides shielded environment. The red blood cell and white blood cell counts, the glucose level will be analyzed and compared with the controls.

Following this brief introduction, Chapter 2 will start with a review of GTEM cell design, biological and health related issues related to electromagnetic field exposure, and studies on EM exposure on living organisms. In Chapter 3 the several theories related to GTEM cell, diabetes, blood cells and biological effects of electromagnetic fields are described. The simulation and experiment configurations, including GTEM cell design, developed GTEM cell and experimental setup, of the work are detailed in Chapter 4. The simulated and experimental results of the GTEM cell, developed GTEM cell and the blood response analysis are discussed in Chapter 5. The last chapter, Chapter 6, includes the discussion, conclusion and future work.

Chapter 2: Literature Review

The central theme of this research work is to study the effects of electromagnetic stimulation, using a GTEM (gigahertz transverse electromagnetic) cell as the radiation source, on blood cells with high sugar concentration. The GTEM cell will be designed and characterized in the laboratory for this research and thus is a part of the report. As such, a brief review of the research related to the use of GTEM cell and its usage in biological effects studies is discussed here. This chapter thus specifically deals with a description and the application of GTEM cells, as well as the electromagnetic stimulation of biological subjects, specifically diabetic blood cells.

The objective in the design of a GTEM cell is to generate uniform electromagnetic fields inside a shielded environment. The GTEM cell was developed from a TEM (transverse electromagnetic) cell as its high frequency variant and therefore the principle of the GTEM cell design is quite similar to that of a TEM cell. A brief discussion of the TEM cell is therefore provided first.

The TEM cell was designed by Myron L. Crawford at the National Bureau of Standards in 1973 [18]. In 1974, Crawford realized that the potential interfering signals in the open systems could affect the accuracy of the electronic or electromechanical measurements. Hence, the TEM cell was introduced in order to provide a uniform electromagnetic fields in a shielded environment [19]. The TEM cell can operate at broadband frequency. The frequency usage is restricted with the TEM cell size, where is designed based on the waveguide concept [20].

The TEM cell, as shown in Fig. 2-1, is a coaxial transmission, which consists of a rectangular coaxial transmission section tapered with coaxial connectors on the both ends section (one end for input feeder port and another for signal terminator port). Ideally, the characteristic impedance of the TEM cell is 50 Ω. The TEM cell was designed to maximize the cross-sectional testing areas as well as maximize usable frequency, reduce impedance mismatch of the cell or voltage standing wave ratio (VSWR), and enhance the uniform electromagnetic fields or eliminate the EM field distortion [21, 22].

Figure 2 - 1 The design laboratory TEM cell [20].

Crawford also provided the equation for the characteristic impedance of the TEM cell, which is approximately similar to the equation for the characteristic impedance of the shielded strip line, given as [19]:

$$z_0 \cong \frac{94.15}{(\varepsilon_r)^{1/2}\left[\frac{w}{b\left(1-\frac{t}{b}\right)}+\frac{C^{f'}}{0.0885\varepsilon_r}\right]} \quad (ohms) \qquad (2.1)$$

where ε_r is the relative dielectric constant of the medium between the conductors, $C^{f'}$ is the fringing capacitance in picofarads per centimeter, and the parameters w, b, and t are shown in Fig. 2-2.

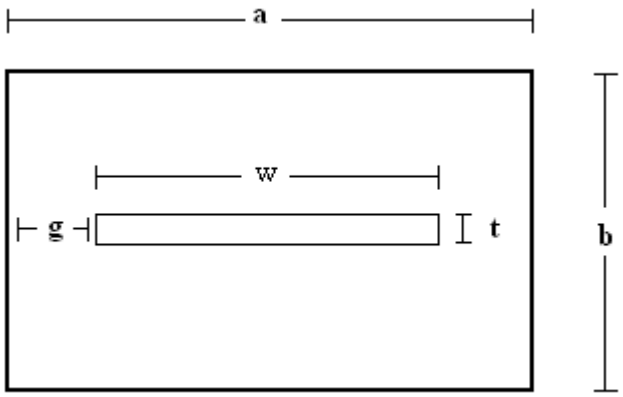

Figure 2 - 2 Cross section view of the TEM cell.

The GTEM cell was introduced by D. Koenigstein, and D. Hansen in 1987 [23]. Since the TEM cell consists of a rectangular coaxial transmission section which is tapered with the coaxial connectors of both sides. As a result three different sections need to be considered in the analysis, which has its disadvantages causing resonances due to the complex relations between the actual outer length and the working volume. The

distributed currents of the travelling wave also cannot propagate to the terminated load simultaneously, so the reflections and non-TEM modes occur. Moreover, the TEM cell is not appropriate for use in systems that are several meters in length due to the association of the frequency of the modes to its size. For these reason, the GTEM cell was developed. The design principles, necessary calculations and technical data of the GTEM cell will be presented in the next chapter, while a review of the research using the GTEM cell is discussed here.

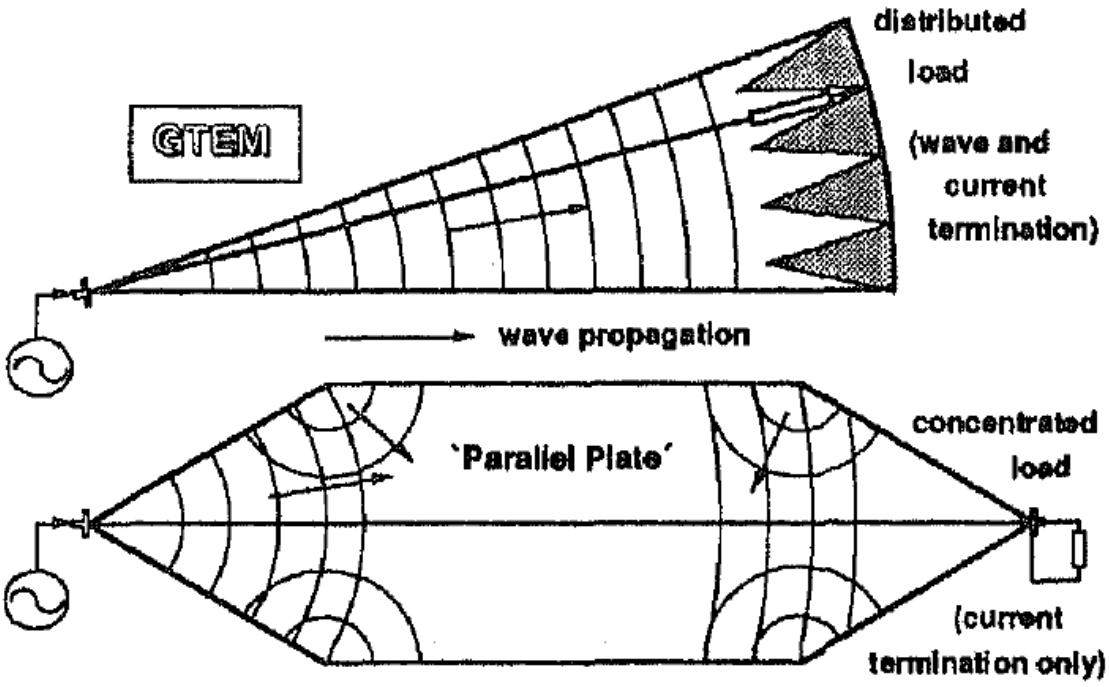

Figure 2 - 3 EM wave propagation: GTEM cell (top) and TEM cell (bottom) [24].

In 1989, D. Hansen, P. Wilson, D. Koenigstein, and H. Schaer presented results from a comparative study of the conventional TEM cell and GTEM cell. First, the authors compared the differences between wave propagation in a GTEM cell and in a conventionally designed TEM cell, as shown in Fig. 2-3. In the GTEM cell, the travelling

time from the source to the terminated load is equal for all parts of the test volume. In addition, there is no source of non-TEM modes inside the cell. On the other hand, the travelling time from source to the load in the conventional TEM cell is not equal for all parts, and the sources of the non-TEM modes can be generated, as well [24].

While the usage frequency of the TEM cell is limited to its mechanical dimensions, such basic limitations are not considered for the GTEM cell. In addition, the GTEM cell has the additional advantage of high power and high voltage capability. The authors also mentioned that the GTEM cell can be used for radiated emission and radiated susceptibility measurements. The measurements can be conducted on small electronic devices, such as from printed circuit board, up to such auto-mobiles. The test can be performed both in frequency and time domain. Compared to anechoic chambers, for the same performance in field homogeneity, the GTEM cell has the advantage of being compact in size. Also, like the anechoic chambers the tests are not influenced by interfering signal like an open area tests (OATS). Additionally, the measurements is repeatable and a cost effectiveness.

Since its introduction, the GTEM cell has been used in many applications. Applications include electromagnetic radiation effects to biological objects, radiation immunity test for telecommunication equipments, interference evaluation between an ultra wideband system and a wireless local area network (LAN), integrated circuit (IC) electromagnetic compatibility (EMC) testing, and gain and impedance measurement of microstrip patch antennas, dipole excitation and scattering by spherical objects, and directivity test of radio-frequency identification (RFID) tag and more.

An important application of GTEM research related to this work is the study of electromagnetic pulse's effects on insulin's bioactivity and mechanism, as discussed by Y. -B. Chen, J. Tan, X. Miao, J. Li, and G. -Z. Guo in 2009 [25]. Here the authors investigate the effects of the electromagnetic pulse (EMP) to the insulin's bioactivity on fasting blood glucose of type I diabetic mice using the GTEM cell.

In the experiment the EMP was generated at 400 kV/m, 0.5 pps and a total 2000 pulses. The pulse was generated through a spark gap and transmitted into the GTEM cell. The average specific absorption rate (SAR) used for the test samples was 0.04 mW/mL. The mice were randomly divided into 2 groups, which were sham-exposed insulin and EMP-exposed insulin. The mice were then placed into the GTEM cell for 15 minutes and later the blood glucose was measured.

The results showed that the effects of EMP exposure on insulin's bioactivity, binding affinity between insulin and its receptor, and fluorescence intensity of insulin were significantly reduced in the mice of EMP-exposed insulin group. For the reason, the authors believed that EMP exposure caused the alteration of insulin's conformation. However, they also suggested that the further studies are needed to confirm their studies.

Another important GTEM cell usage and application is the study of the effects of pulsed electric fields (PEFs) on the viability of Culex quinquefasciatus using the GTEM cell. This study was presented by N. Pinpathomrat, T. Kaweeferngfu, A. Laphodom, N. E. Islam, and P. Kirawanich in 2011 [26]. The experimental setup in Fig. 2-4 consisted of the nsPEF system and the GTEM cell. The PEL was connected to the input port of the GTEM cell in order to delivering the pulses to the treaded objects placed inside the GTEM cell. The samples were separated into 24 groups of 20 larvae each for viability

tests. There were four experimental sets for 4 different combinations of exposure parameters, including pulse amplitude and duration. All larval samples were put in the cup filled with 20 ml of water.

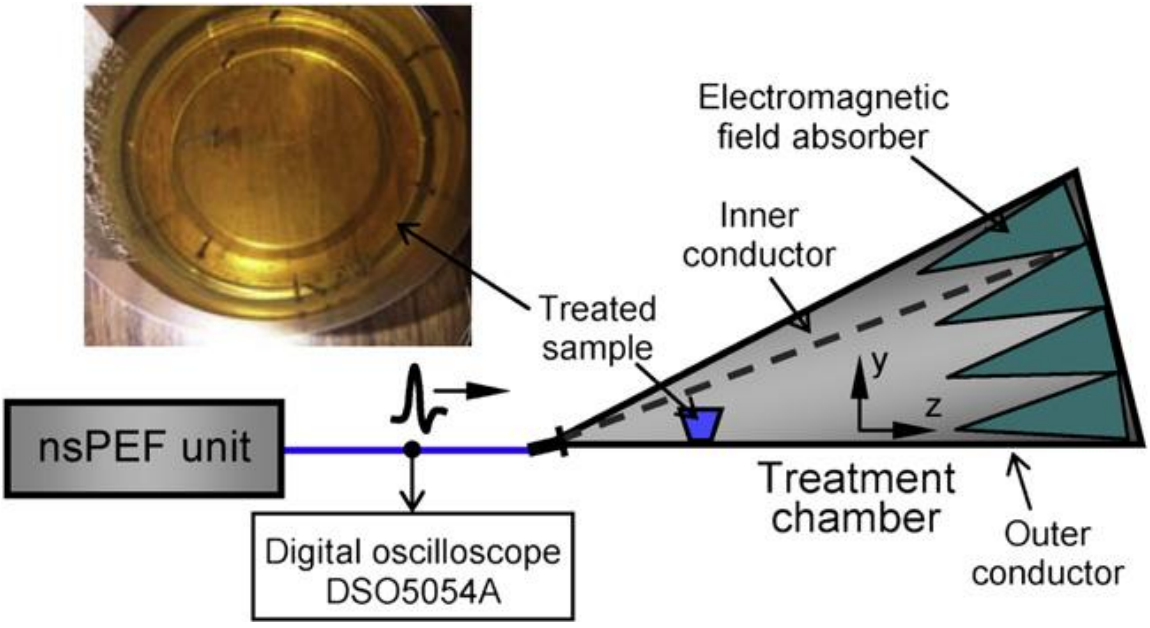

Figure 2 - 4 Experimental setup with the nsPEF system transmitting the pulses to the treated samples placed inside the GTEM cell [26].

The results showed that the number of survived mosquitoes was decreased by 20 percents with exposure energy density of up to 17.76 J/m^3. The average developmental rate into adult forms of the treated fourth-instant larvae was lower comparing to the control, corresponding to a 25% reduction. The authors finally suggested that the electric pulse could decrease in mosquito viability.

The next paper of the GTEM cell application researched in this study is that of gain and impedance measurement of microstrip patch antennas, which was presented by Z. Zivkovic, and A. Sarolic in 2010 [27]. The authors presented the method for measuring gain and impedance of the rectangular and circular microstrip antennas in the

GTEM cell. The measurement setup for gain was depicted in Fig. 2-5(a) as well as the measurement setup for impedance was shown in Fig 2-5(b).

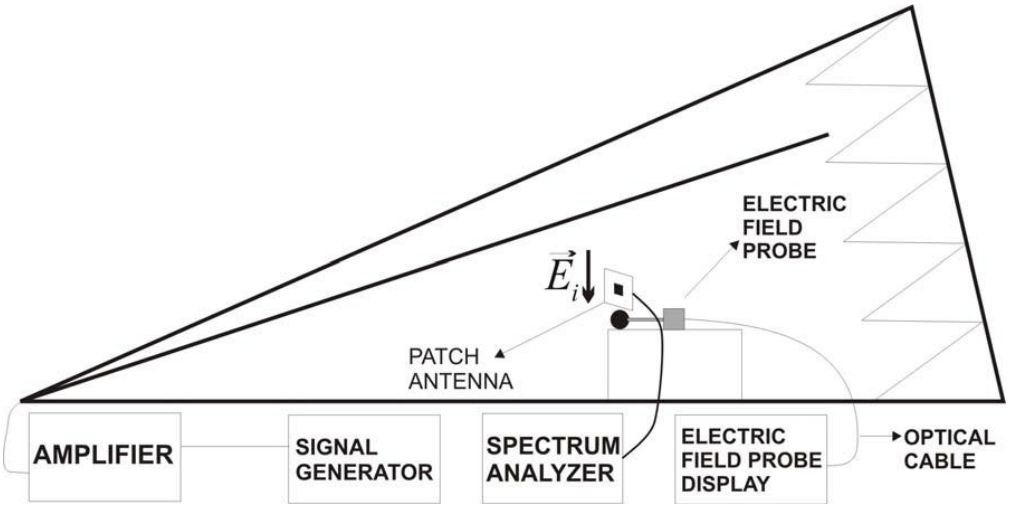

(a)

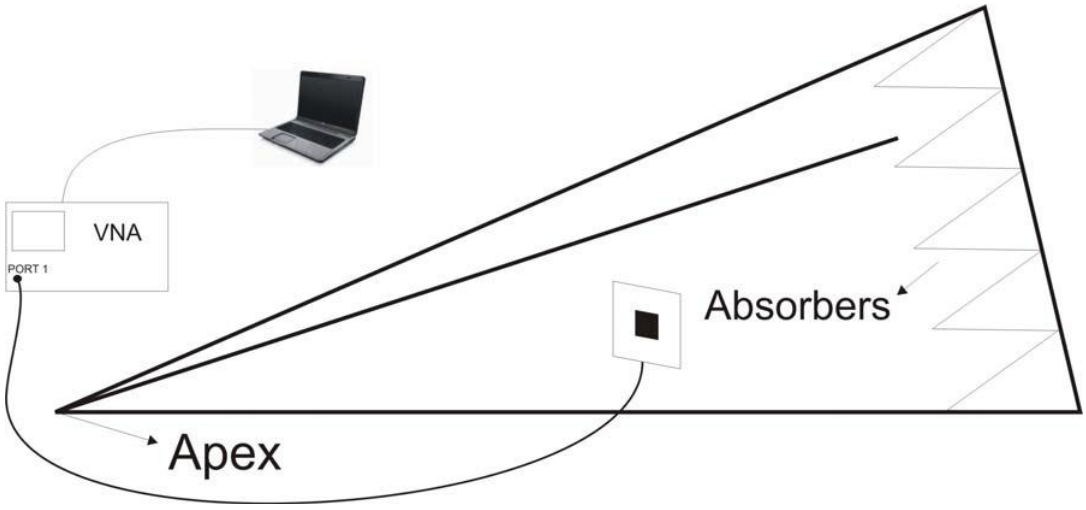

(b)

Figure 2 - 5 Experimental setup: (a) gain measurement and (b) impedance measurement [27].

The antennas were mounted on styrofoam support inside the GTEM cell. The measurements were performed at the frequency range of 2 GHz to 2.8 GHz. The measurements were performed for different orientations of the antennas in the GTEM

cell, including direction toward the RF absorbers and the input port of the cell. The input impedance of the antennas was obtained for magnitude and phase of the reflection coefficient S_{11} results. The measurement and simulation results were compared.

The results showed that the measured gains are agreement with the simulation results. The impedance measurements showed good matching at the resonant frequency. Therefore, the authors suggested that the GTEM cell could be used as a low-reflective indoor environment for such small antenna measurements.

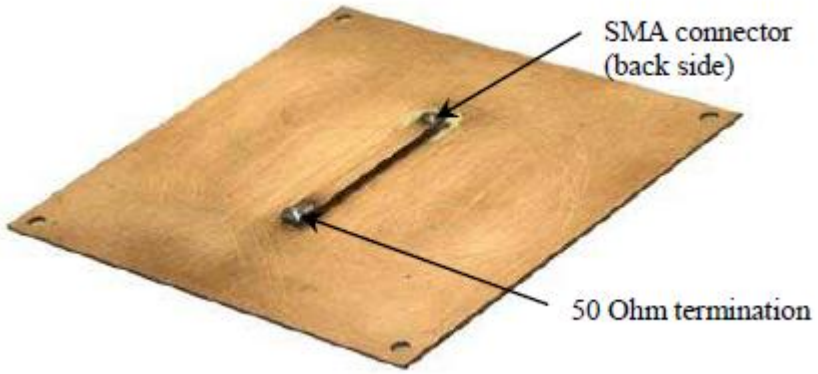

Figure 2 - 6 Test board [28].

R. Heinrich, V. Mullerwiebus, A. Lange, B. Deutschmann, U. Karsten, and F. Klotz presented the application of the GTEM cells for IC EMC testing in 2008 [28]. The authors proposed the method to characterize the EMC behavior of integrated circuits (IC) emission tests and immunity tests. The authors stated that in the present the clock speeds of the ICs increased above 1 GHz. This then required testing at higher frequencies. Due to the upper frequency limit of μTEM cells, the GTEM cell was an alternative tool for the measurements.

A special test PCB, which was clamped on a special opening in the wall of the GTEM cell, was designed for the purpose of the GTEM investigations, as shown in Fig. 2-6. The PCB was tested as a function of four different orientations, as shown in Fig. 2-7. The measurements were conducted by using the network analyzer. The results showed that the return loss results of the orientation 1 and 3 were about -15 dB to -20 dB. On the other hand, the return loss results of the orientation 2 and 4 were about -35 dB to 60 dB, which was good return loss. The authors concluded that this test system could be used up to 18 GHz, and could be successfully applied for IC EMC testing.

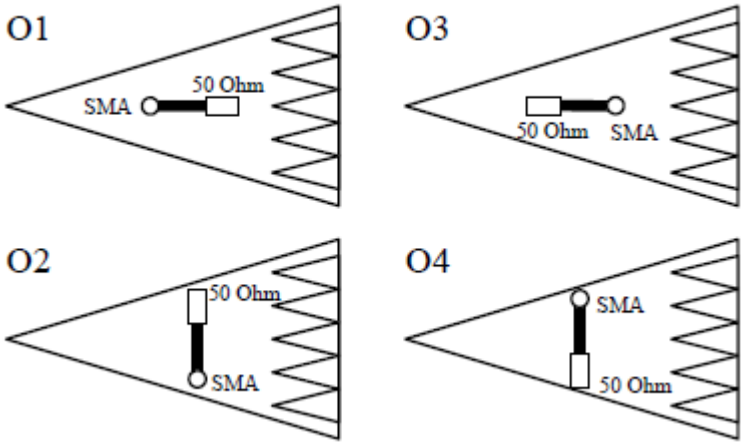

Figure 2 - 7 PCB orientations in GTEM cells [28].

In 2011, M. Alvarez-Folgueiras, M. M. Minana-Maiques, E. Moreno-Piquero, F. Jorge-Barreiro, E. Lopez-Martin, and F. Ares-Pena presented the paper on the experimental system for the study of multi-frequency dosimetry [29]. The primary purpose of this paper was to provide the experimental system for RF exposing small animals to radiation using the GTEM cell. The frequencies of 900 and 2450 MHz were

mixed for multiple simultaneous exposures to EM signals from various sources. The specific absorption rate (SAR) in the body and brain of the animals was calculated by using the FDTD method and SEMCAD commercial software.

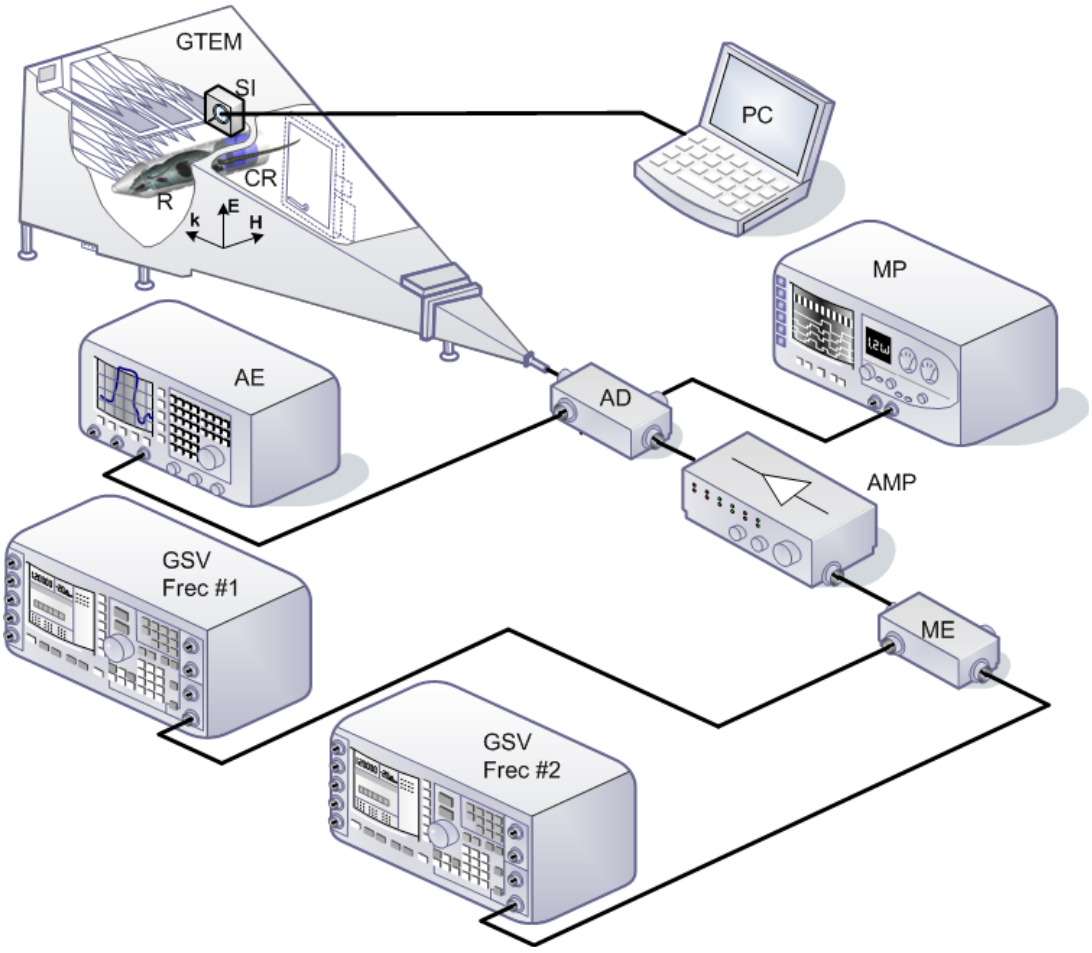

Figure 2 - 8 System configuration of the multi-frequency dosimetry study [29].

The experimental system setup is shown in Fig. 2-8. Two vector signal generators were used for generating each pure sinusoidal signal of 900 and 2450 MHz at the power level required during the treatment. The signal from both generators was connected to a signal mixer, and its output was then passed through an amplifier. The amplified signal

was sent into the directional coupler and then delivered to the GTEM chamber. The animals were placed at 21.5 cm height with irradiated power of 2 W. The incident power value was measures by using the power meter. The reflected power value was monitored from the spectrum analyzer.

The results showed that the relative SAR numerical model affected in various anatomical areas of the rat, including cerebral cavity, cerebral hemispheres, hypophysis, cerebellum, muscle, thymus, testicles, fat tissue and tongue. The SAR brain and body values were averaged for 1 g of tissue. The authors suggested that the SAR results established the initial biological study for exposure to multi-frequency radiation in these mammals. The EM exposure could impact the harmful health of living organisms, as well.

The next paper is the study of absorber and resistor contribution in the GTEM cell, which presented by K. Malaric, J. Bartolic, and B. Modlic in 2000 [30]. The authors investigated the influence of absorbers and resistors to standing wave ratio (SWR) and return loss. The measurements were performed on the GTEM cell as well as on the GTEM cell without resistors, absorbers, and with open and metal end. The GTEM cell in this paper was designed with the Finite element method (FEM).

As stated in several other papers, the authors mentioned that the terminated load section consists of the RF absorbing material for EM wave termination and the distributed resistive load for current termination. The absorber will attenuate the incident wave at high frequencies, while the resistive load will primarily operate at low frequencies. For this reason, the GTEM cell can perform from DC to several GHz.

The experimental results were achieved by the network analyzer. The measurements were conducted without resistors and absorbers in various combinations. The results of the frequency ranges up to 1 GHz, and up to 20 GHz were shown. The experimental results indicated that the influence of the absorber is more important at higher frequencies, especially above 50 MHz, while the resistors have more influence at the frequencies below 400 MHz. The GTEM cell without the absorbers and the rear end metal covering performed similarly to the full GTEM cell.

In addition, the time domain measurements were also performed. They were carried out with the low pass filter. The results suggested that the greatest discontinuity appeared at the N-type connector, and at the dielectric supporters of the inner conductor. However, the discontinuities of the dielectric supporter were smaller than those of the connector. The dielectric supporter, which was placed in the vicinity of the absorbers, and the test area, significantly caused the disturbance of the EM field inside the GTEM cell. Finally, the results showed that the door did not cause the significant impact to the homogeneous EM field inside the cell.

In 2009, X. Zhou, Q. –X. Jiang, and H. Q. Jiang presented the influences of cable under test (CUT) on the VSWR of the GTEM cell [31]. For measuring shielding effectiveness of such cable using the GTEM cell by the ANSI/SCTE48-3 2004 test standard, as shown in Fig. 2-9, the authors realized that the CUT's parameters, such as size, position, shape and direction, could result in the error of VSWR. However, this consideration had not been analyzed.

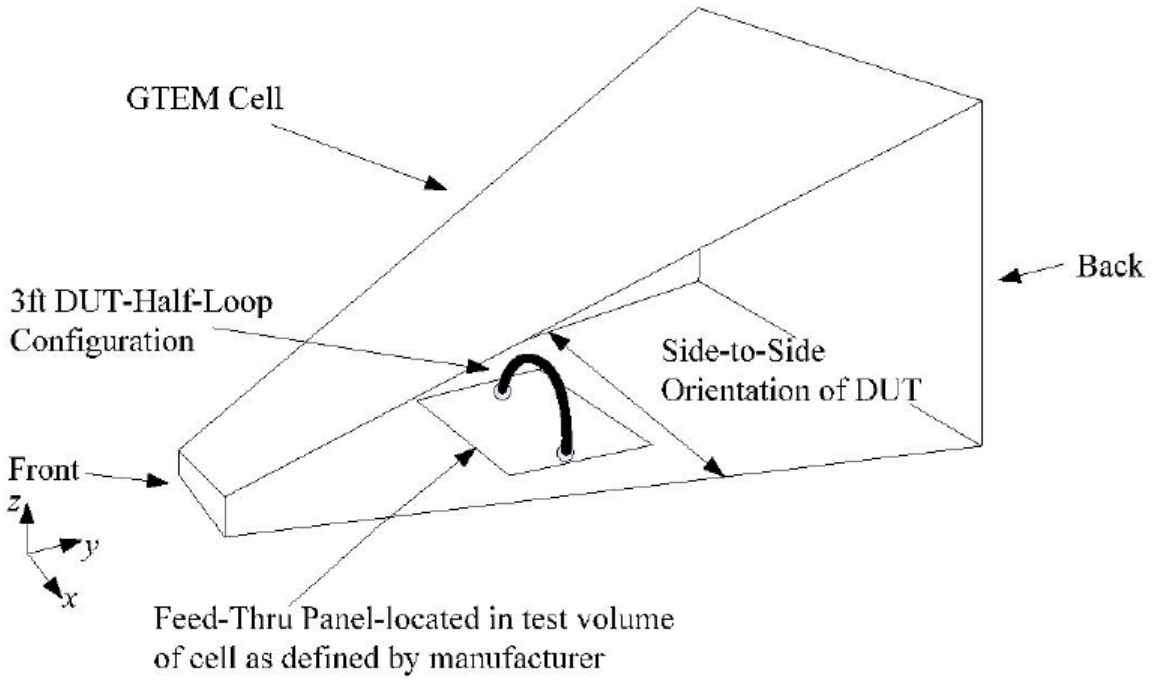

Figure 2 - 9 Measuring shielding effectiveness of CUT by ANSI/SCTE48-3 2004 test standard [31].

The authors investigated the arc radius, shape, direction and radius of CUT. The simulated and experimental results of were conducted for the analysis. Both simulations and measurements showed that larger arc radius and larger radius of the CUT resulted in higher VSWR. The different shape and different position of CUT influenced in the different VSWR. The CUT in parallel direction caused a little higher VSWR. Finally, the authors suggested that before test the VSWR should be measured in order to avoid using the resonant frequencies, resulting in dramatic measure error.

H. X. Araujo, and L. C. Kretly studied the impacts of the apex to the impedance matching of the GTEM cell [32]. The authors presented the concept and models for matching the APEX and the GTEM cell. They have pointed out that in designing the GTEM cell, where the difficult part is to establish the correct size of the apex. The apex

works in the transition from the coaxial input feeder to the septum of the GTEM cell. The length of the apex section is usually about 10 percents of the overall length of the GTEM chamber. Mismatching between the input feeder and the inner conductor significantly induce reflection inside the chamber.

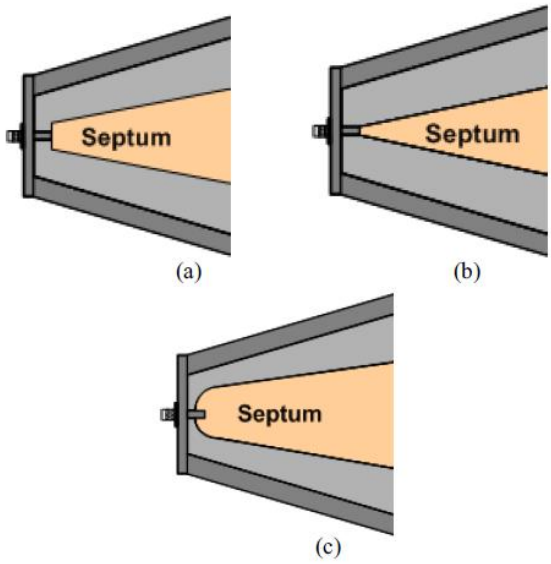

Figure 2 - 10 Apex section with different septums: (a) wide, (b) direct, and (c) round corner [32].

To obtain the best connection between the apex and the GTEM body, three different apexes, as shown in Fig. 2-10, were analyzed. The GTEM cell in the study was designed by the EM software based on Finite Element Method (FEM). The length of the designed GTEM cell was based on the given equation,

$$L = 3\left(T_V + D_{TA} + L_A\right) \tag{2.2}$$

where T_V is the testing volume, D_{TA} is the safety distance between the testing volume and the absorbers, and L_A is the length of the absorbers. The height of the RF absorbers is

obtained from the equation of the lowest frequency attenuated by the RF absorbers, given as

$$f_{\min} = \frac{c}{2h} \tag{2.3}$$

where f_{min} is the lowest frequency attenuated by the absorbers, c is the speed of light and h is the height of the absorbers.

The results showed that at frequencies from 500 MHz to 18 GHz all septums provided very low return loss. The wide septum resulting in the smoother behavior was more appropriated to use. While the round corner septum provided the oscillatory values compared to the others. This suggested that the septum was an important factor on the field distribution and reflection inside the GTEM cell.

The next paper is the study of the measurement method to determine the impulse response of ultra-wideband (UWB) antennas inside the GTEM cell by S. Sczyslo, H. Thye, G. Armbrecht, S. Dortmund, and T. Kaiser in 2009 [33]. A cone antenna, as shown in Fig. 2-11, was chosen for this study. The excited UWB pulse system consisted of the pulse generator connected to the GTEM cell and a cone antenna was placed into the testing area of the GTEM cell.

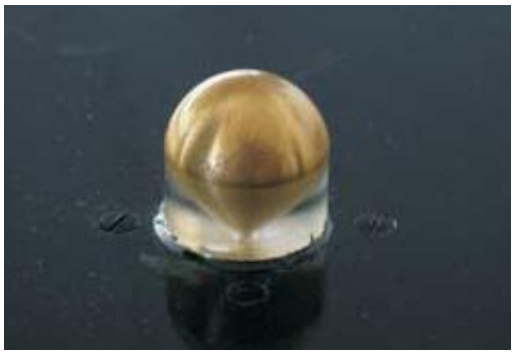

Figure 2 - 11 A cone antenna [33].

The impulse response of the GTEM cell could occur by the distribution within a distinct time interval. Within this interval, an approximately plane TEM wave then transmitted to the antenna located in the testing area without distortion of the parasitic multimode wave propagation. The size of the cone antenna and estimated impulse response length were carefully designed based on the GTEM cell's properties, so that the received cone antenna could detect the impulse response within this distinct time interval.

The results of the antenna impulse response by using the GTEM cell were verified with simulation as well as by the two antenna reference measurement. The results, in terms of the shape and the amplitude of the impulse response, showed good agreement. The results suggested that the GTEM method could be alternatively used for characterizing the absolute impulse response of UWB antennas.

In 2006, A. I. Yurekli, M. Ozkan, T. Kalkan, H. Saybasili, H. Tuncel, P. Atukeren, K. Gumustas, and S. Seker presented the effect of the transmitted GSM cellular phone base station radiation to the oxidative stress and generation of the free radicals in rats [34]. The free radical is a molecule or ion with an unpaired electron in its outer orbit. The unpaired electrons of free radicals can be transferred from one molecule to another. Most common free radicals can be produced from oxygen metabolism.

The young adult male Wistar albino rats were used as the treated samples. The rats contained in two metabolic cages were subjected to 945 MHz EM fields inside the GTEM cell. A power density of 3.67 W/m^2, which provided SAR value of 11.3 mW/kg, was used. The experiment was conducted for seven hours per day for a period of eight days. The malondialdehyde (MDA), reduced glutathione (GSH) and superoxide dismutase (SOD) levels of the samples were measured. MDA were determined in order to

evaluate lipid peroxidation. GSH and SOD were monitored for the analysis of the antioxidant status in the blood samples.

The results showed that the MDA, GSH and SOD levels in the treated rat have been changed significantly after EM exposure. The MDA and SOD level was increased significantly when compared to the control groups. However, GSH concentration decreased significantly when compared to the control. The authors described that the decrease of the GSH level related to free radicals. The higher GSH consumption produced more free radicals. The increase of SOD activity could have some relation to the low concentration of GSH. The GSH provided a protective function in scavenging radicals and in molecular repair. Such scavenging could create a superoxide-dependent chain production of H_2O_2 and oxidized glutathione, which would cause oxidative stress in the cell. For this reason, the increased SOD concentration responded to the increase of chain oxidation of GSH. The balance between GSH-Px and SOD was essential for the cellular resistance to oxidative stress.

The author concluded that EM radiation from the cellular phone tower affected the oxidative stress of free radicals. It enhanced the lipid peroxidation and reducing the GSH level. The reactive oxygen species might be a probable cause of the effects from the EM fields at cell phone frequencies. The author also suggested that the future study related to their work was required for confirmation.

T. Jorge-Mora, M. J. Misa-Agustino, J. A. Rodriguez-Gonzalez, F. J. Jorge-Barreiro, F. J. Ares-Pena, and E. Lopez-Martin studied the effects of 2.45 GHz radiofrequency on the paraventricular nucleus (PVN) of the rat hypothalamus in 2011 [35]. The authors investigated the following:

(1) Whether or not the PVN would respond the non-thermal (<4 W/kg) SAR from RF exposure,

(2) Which cell regions in the nucleus would be activated by different power levels.

The experiments were conducted by using the GTEM cell at 2.45 GHz and at power levels of 3 and 12 watts. A total 60 of the adult female Sprague–Dawley rats weighing 230–250 g were placed in individual cages with free access to food and water inside the GTEM cell. The temperature was maintained at 22 ºC under a 12:12 light/dark cycle regime. The rat samples were divided into 3 groups, 20 rats for each group. The simulated SARs were calculated by the finite difference time domain (FDTD) software.

The response of the hypothalamic nucleus to the effect of non-ionizing radiation was analyzed from the SARs and the immunohistochemical morphological results of the c-Fos protein in different regions of the PVN of the postmortem brain. The experimental procedure is shown in Fig. 2-12 (a) and the simulation of SARs in rat samples at 2.45 GHz and at 3 W is shown in Fig. 2-12(b).

The results showed that after 90 minutes and 24 hours treatment the high SAR increased the c-Fos. In addition, after 24 hours exposure the low SAR also increased the c-Fos counts compared to the controls. At 3 W operated power, the cellular activation of PVN in the multi irradiated rats increased by more than 100% compared to the single irradiated rats and to repeated non-radiated controls.

The authors concluded that PVN significantly responded to 2.45 GHz microwave radiation at non-thermal SAR levels in diverse neuronal populations. The power levels and the time of exposure to single or repeated doses of radiation were important factors that might influence a response in the nucleus.

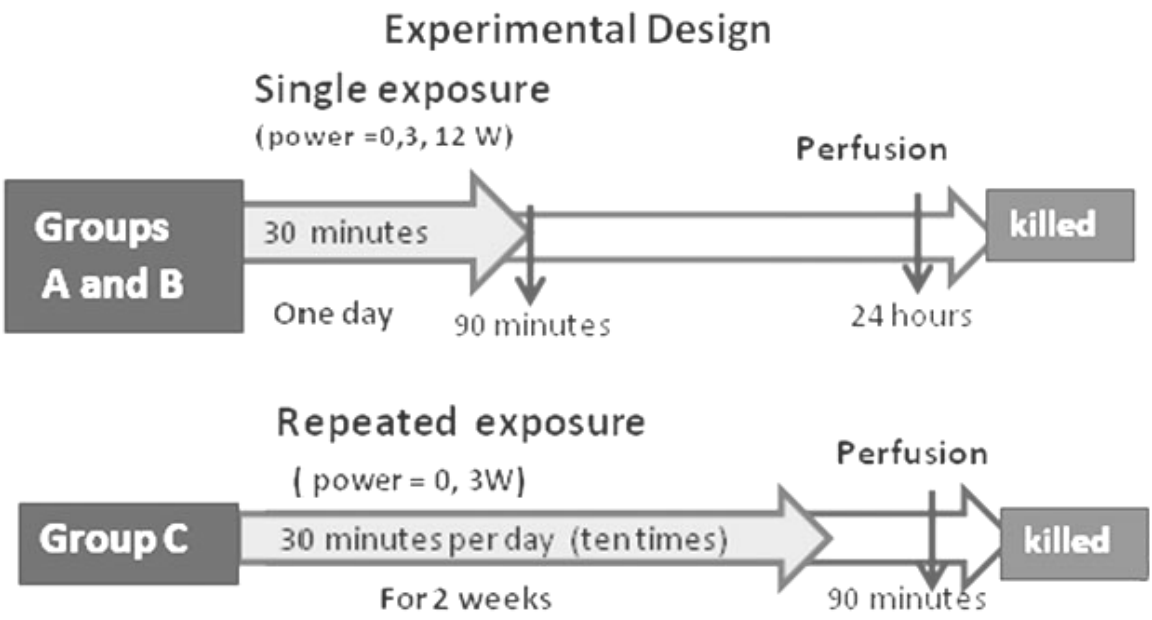

(a)

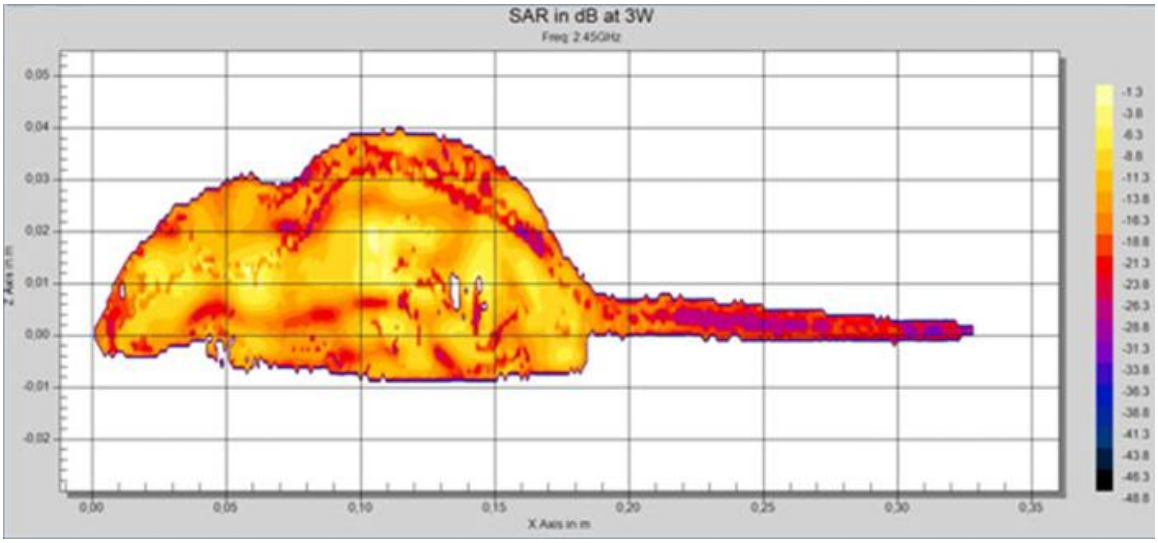

(b)

Figure 2 - 12 (a) Diagram of experiment design and (b) FDTD simulation of SARs in a rat at 2.45 GHz [35].

K. Malaric, A. Sarolic, V. Roje, J. Bartolic, and B. Modlic studies the electric fields distribution inside the GTEM cell in 2001 [36]. The numerical model of the E field

was performed with the finite element method (FEM) and compared with measured results.

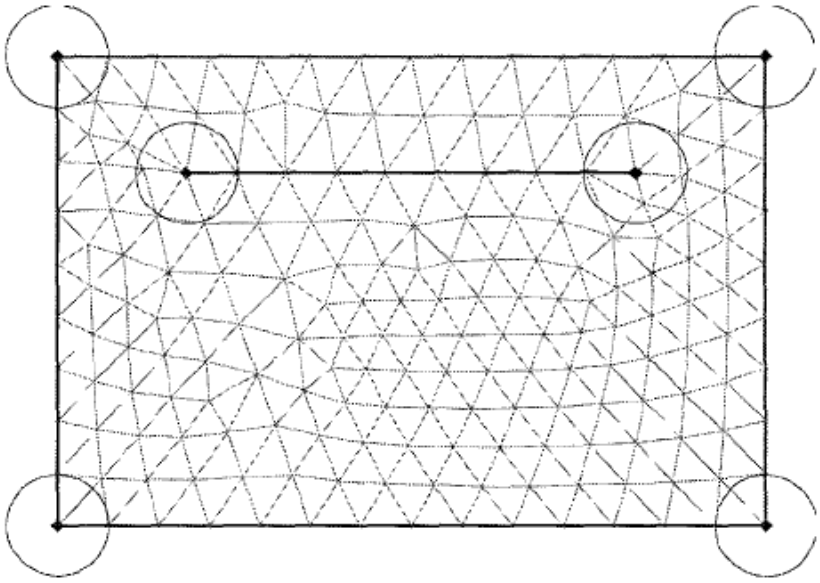

Figure 2 - 13 Finite element method of GTEM cell [36].

The authors described that the FEM could be powerfully used for solving complex, especially nonlinear problem in electromagnetic compatibility (EMC). To start the simulation, the cross section area of the GTEM was divided into small elements as shown in Fig. 2-13. The FEM parameters included the device geometry, material constants, excitations, mesh cells and boundary constraints.

The simulated E field and the H field vectors in the GTEM cell were shown in Fig. 2-14(a) and 2-14(b), respectively. It showed that the E field should be in horizontal or parallel to the side wall of the GTEM cell. The H field should be in vertical or parallel to the top ceiling and the base of the GTEM cell. The usable area inside the GTEM cell was about 80% of the volume between the septum and the floor of the cell. In their study, only the E field in the center area of the cell was measured and it was carried out by using

the E field probe. At 100 MHz and at ½ septum height, the E field was nearly constant, less than 3 dB different. The measured result also showed good agreement with the FEM simulation.

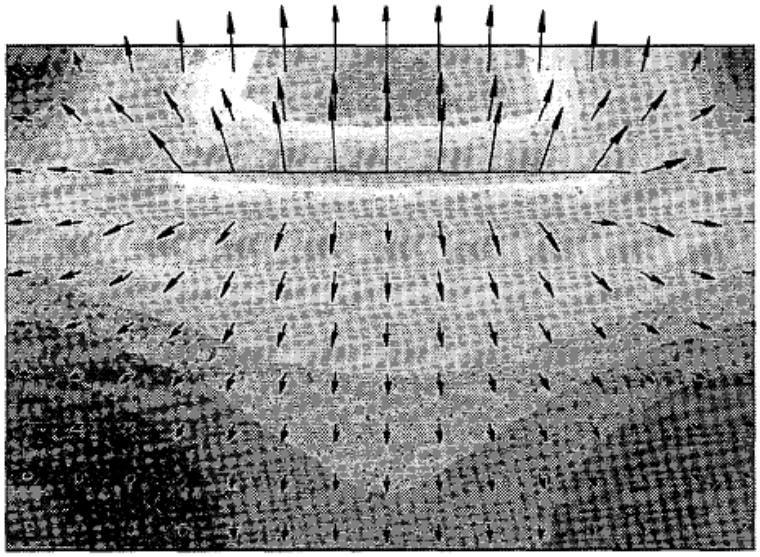

(a) E field distribution inside GTEM cell

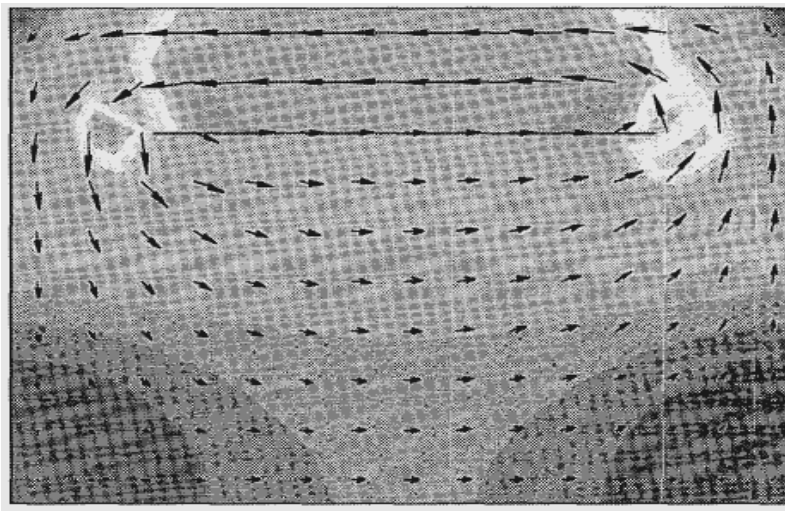

(b) H field distribution inside GTEM cell

Figure 2 - 14 E and H fields distribution inside GTEM cell: (a) E field and (b) H field [36].

S. T. Lu, S. P. Mathur, Y. Akyel, and J. C. Lee presented the effect of the ultrawide-band (UWB) electromagnetic pulses to the cardiovascular system, including heart rate, systolic, mean arterial pressure, and diastolic pressures, in 1999 [37]. The UWB is a RF signal with a few nanosecond ultrashort pulse width and very fast rise time which is less than 200 picoseconds. The UWB devices can generate an extremely high peak electric field and very low duty cycle. This can cause the extremely high temporal peak SAR, but the average SAR will be very low when applying the time-average procedure. The authors mentioned that the ratio of peak to average SARs would be much greater than those of narrowband RF radiation.

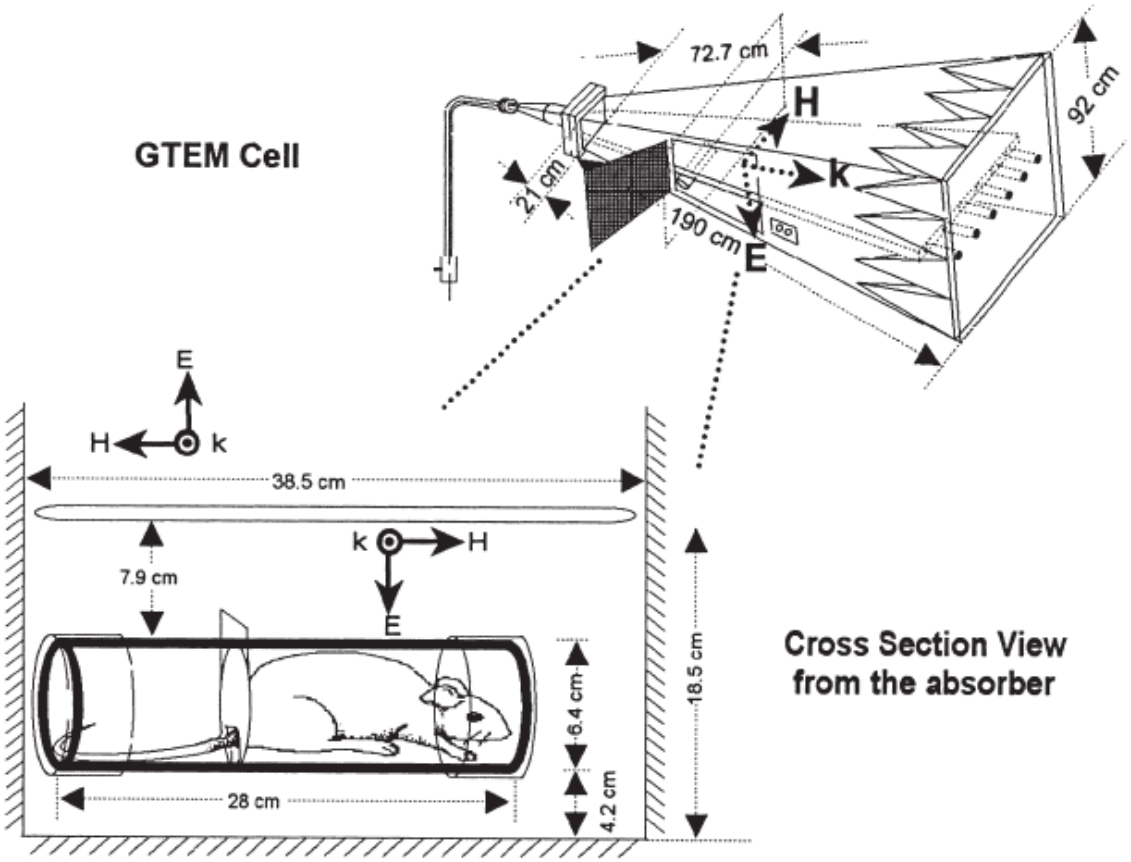

Figure 2 - 15 The UWB pulse system [37].

For the experimental setup, the fifteen male Wistar-Kyoto rats were used. The UWB system consisted of a spark gap pulse generator connected to the GTEM cell, as shown in Fig. 2-15. At 500 Hz, the rise time of 180 ps and the pulse width of 1 ns were used. At 1000 Hz, the rise time of 200 ps and the pulse width of 1.03 ns were used. The rats were placed in an acrylic tube and polyethylene endcaps. The tube located at 72.7 cm from the input feeder and at 4.2 cm from the floor. The rat samples were treated for 6 minutes. The cardiovascular system of the rats was measured immediately before and after the treatment.

Results showed that the exposed rats gain weight after treatment at 500 Hz. The average heart rate was not affected at any treated frequencies. The systolic pressure increased in the sham-exposed group, while it was lower in rats exposed to 500 or 1,000 Hz UWB fields. The mean arterial pressure increased in the sham-exposed rats, while it decreased in rats exposed to 500 or 1,000 Hz UWB. The changes in the diastolic pressure, which was obtained from the systolic and mean arterial pressure, were similar to both measurements. The authors stated that the decrease in arterial pressures without changes in the heart rate in rats was uncommon. The changes might be due to a robust, consistent, and persistent from the UWB radiation-induced hypotension.

M. Tkalec, Z. Vidakovic-Cifrek, B. Pevalek-Kozlina, K. Malaric, and R. Malaric presented the effect of 900 MHz electromagnetic field on *Allium cepa* seeds using the GTEM cell in 2007 [38]. In their study, the germination and root growth as well as on mitotic index and mitotic of *Allium cepa* exposed to 900 MHz EMF were investigated. 15 seeds soaked for 12 hours on moist sterile filter paper in plastic Petri dishes were used for each EM treatment. For all experiments, the seeds were placed in the GTEM cell for 2

hours. The 5 W MiniCircuits amplifier were used to generate the EM fields. Four electric field strengths of 10, 23, 41 and 120 V/m were investigated. In addition, the effect of longer exposure (4 hours) with modulation and E-field strength of 23 V/m was also monitored. The temperature inside the GTEM cell was controlled to not vary more than ± 0.1 ºC. After treatment in GTEM cell, the seeds were grown in the dark at 20–24 °C. The germination percentage and lengths of the primary roots were measured on 7^{th} day.

Results show that there was no significant change in the germination rate and root length after EMF exposure. However, the treatments at higher EMF strengths (41 and 120 V/m) and with modulation as well as longer exposure could significantly improve mitotic index, including percentage of mitotic abnormalities, mainly consisting of laggards, anaphase bridges, C-mitosis, vagrants and unequal distribution, when comparing to corresponding controls.

K. Malaric, J. Bartolic, and R. Malaric studied the cut-off and resonant frequencies of the higher order mode in the TEM cell and GTEM cell in 2000 [39]. It is well known that the TEM cell and GTEM cell can propagate uniform TEM mode. The higher order modes of the TEM cell are at sharply defined frequencies. On the other hand, the resonance, induced the field distortion inside the cell, in the GTEM cell is attenuated by the RF absorbers. The usage of frequency range depends on the cell's size. The smaller size of the cell provides higher frequency range.

The first cutoff frequency (f_c) of the TEM cell, which is TE_{10} mode, can be obtained from the given equation,

$$f_c\left(TE_{10}\right) = \frac{c}{2a} \tag{2.4}$$

where c is the velocity of light, and a is the width of the TEM cell as shown in Fig. 2-2. The cutoff frequency for any higher mode can be obtained as given,

$$f_c\left(TE_{m,n}\right) = \frac{c(b^2m^2 + a^2n^2)^{1/2}}{2ba} \tag{2.5}$$

where b is the width of the TEM cell as shown in Fig. 2-2. The authors also provided the equation of the resonant frequency. The resonance in the TEM cell occurs from which the waves propagate in the higher-order mode undergoing multiple reflections from end to end within the cell until the wave is dissipated. Therefore, the resonance frequency $f_{R(mnp)}$ of the TEM cell can derived from the cell's effective length, as given,

$$l_{(mn)} = \frac{p\lambda_{g(mn)}}{2} \tag{2.6}$$

where p is the mode for the half guide wavelengths long (p = 1,2,3,…), and λ_g is the half guide wavelengths, which can be obtained by

$$\frac{1}{\lambda^2} = \frac{1}{\lambda_g{}^2} + \frac{1}{\lambda_{c(mn)}{}^2} \tag{2.7}$$

where λ is the light's wavelength, and $\lambda_{c(mn)}$ is the cutoff wavelength value. Therefore, the resonant frequencies of the TEM cell can be calculated as given,

$$f_{R(mnp)}^2 = f_{c(mn)}^2 + \left(\frac{pc}{2l_{(mn)}}\right)^2 \tag{2.8}$$

where

$$f_{c(mn)} = \frac{c}{\lambda_{c(mn)}} \tag{2.9}$$

For the GTEM cell, the higher order modes are not considered because they are attenuated by the absorbers. For this reason, the GTEM cell is not a cell with high Q factor. The authors pointed out that when the waves traveling along the propagation axis move away from the feed connector, the higher order modes will increase. The modes excited are the TEM mode, and the non-essential modes are excited by the geometrical discontinuities. The first essential mode is H_{10} mode, but the first propagation mode is H_{01} mode, which is the non-essential mode. The cutoff frequencies can be found as given,

$$f_c = \frac{k_c c}{2\pi} \tag{2.10}$$

where k_c is the wave number.

R. De Leo, L. Pierantoni, T. Rozzi, and L. Zappelli studied the signal termination of the GTEM cell in 1996 [40]. The authors stated that the termination of the GTEM cell consists of the combination of resistors, working at frequencies lower than 100 MHz, and of tapered RF absorbers, working at frequencies higher than 100 MHz. However, the number of resistive loads and the dielectric property and geometry of the absorbers need to be considered. The authors suggest that the width of the septum should not permit connection to just one resistor.

The theoretical and the experimental results show that to optimize the characteristic impedance, a large number of teeth, which are the connections between the resistors and the septum, in Fig. 2-16, are required. The length of the transition (t) did not significantly change the matching, while changing the length of the resistive load (s) would influence the characteristic impedance at high frequency. Increasing the length of the resistive load would result in a lower resonant frequency. In addition, they also

concluded that higher permittivity (ε), and longer length of the bulk and cones of the absorbers would provide better reflection coefficient.

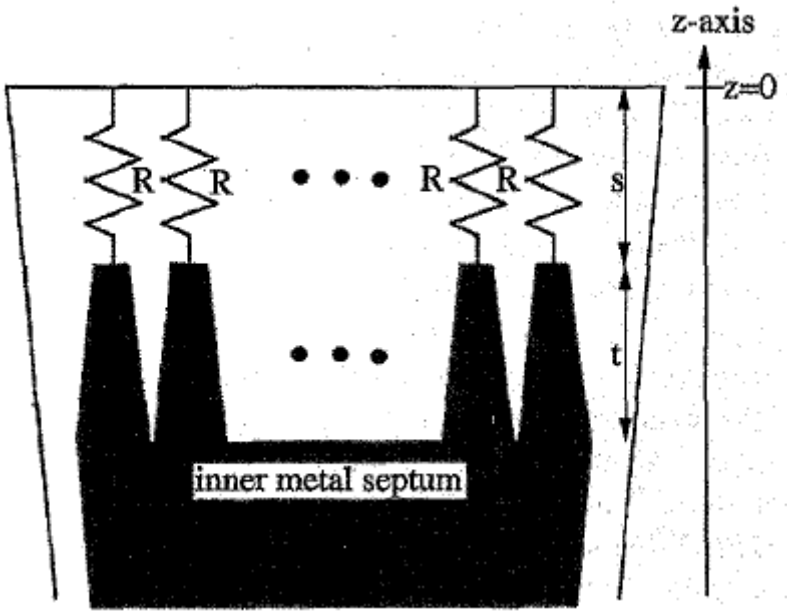

Figure 2 - 16 Top view of the resistive network inside the GTEM cell [40].

R. N. Perez-Bruzon, A. del Moral, C. Perez-Castejon, M. Llorente, A. Vera, and M. J. Azanza proposed a method to expose human cell in microwave and to grow the cell in the non-energized environment using the GTEM cell in 2011 [41]. The cell properties, including cell morphology, expression and distribution of cytoskeleton proteins, genotoxicity, viability and cell cycle progression were observed and compared with the cell samples grown inside a standard incubator (control samples).

The authors show that mammalian cell normally grow under the temperature of 37 ºC and 5% CO_2 in a humidified atmosphere. However, in growing the cell inside a standard-incubator, the cell exposed to RF-EMF was performed at room temperature, which was dropped from 37 ºC. To solve this problem, the authors introduced the

GTEM-incubator to control the temperature and CO_2 in a humidified atmosphere at 37.0 ± 0.1 ºC and 5% respectively.

Two series of experiments for the GTEM-incubator validation were performed by growing cells for 6 and 24 hours. Human normal astrocytes and cells from human astrocitoma, human astrocytes tumor, were used. In order to control other possible thermal effects on cells under EMF treatment, the cells were maintained in sub-thermal conditions at low powers of 0.34 and 0.60 mW. For this reason, the experiments needed to be conducted at 9.6 GHz carrier frequency, modulated by short pulses with widths of 100 and 120 ns, with pulse repetition frequency of 100 and 800 Hz.

The results showed that there was no significant effect on cell morphology, either on astrocyte or astrocytoma cells for either after 6 and 24 hours incubation times. There was no genotoxic effect, normal nuclei, neither necrosis nor apoptosis alterations between control and test samples. There was also no significant difference in the expression and distribution of GFAP, tuc-4, α- or β-tubulin proteins either after 6 or 24 hours incubation times. In addition, the viability of normal astrocyte or astrocitoma cells was not significant different for incubation times of 6 and 24 hours either in control samples or in test samples. Therefore the authors concluded that GTEM-incubator could be used to culture the human normal astrocyte and astrocytoma cells. The GTEM-incubator allowed the cell growth in physical conditions comparable with standard incubator.

G. Duranti, A. Rossi, N. Rosato, G. Fazio, G. Sacerdoti, P. Rossi, R. Falsaperla, V. Cannelli, and R. Supino investigated the effects of 900 MHz radiation on human keratinocytes in 2005 [42]. The authors realized that skin is usually exposed to electromagnetic radiation, especially at cell phone frequency, more than inner tissues.

HaCaT cells, spontaneously immortalized human keratinocytes cells developed through long-term culture of derived from normal human adult skin keratinocytes, were used and exposed to a pure sinusoidal field at the frequency of 900 MHz (average SAR levels ranging from 0.04 to 0.08 W/kg) inside the GTEM cell for 18 hours at the temperature of 37 ºC. Both controls and exposed cells were kept at 37 ºC without CO_2. After EM exposure, the medium was changed and the cells were incubated at the temperature of 37 ºC in 5% CO_2 for the growth, proliferative and citotoxicity assay analysis at 0, 24, 48 and 72 hours recovery.

The results from experiments by G. Duranti et. al. showed a reduction of survival cell numbers in treated samples, compared to controls: 12% after 24 hours, 21% after 48 hours, and 30% after 72 hours of recovery time. There was no significant change in the number of dead cells found at any recovery time. The dead cells were 10% of the total number both in control and treated samples at any exposed time. After exposure to 900 MHz radiation, the HaCat cells tended to stop dividing. Expression of involucrin and keratin 1 in exposed cells increased compared to controls. Therefore, these results suggested that the exposure to 900 MHz electromagnetic field at non-thermal level could affects the dermal tissues, in particular on HaCaT cells.

Finally, there are several reports on the study of EM radiation on blood sugar. One of significance is the study of "dirty electricity" which tends to elevate blood sugar among electrically sensitive diabetics which explains the concept of 'brittle' diabetes, as presented by Magda Havas in 2008 [14]. Havas stated that the transient electromagnetic fields, known as dirty electricity, are generated by electronic equipment's and wireless devices and is ever-present in the environment. It might influence the glucose levels in

blood among diabetics and pre-diabetics. For example, exercise on a treadmill, which produces dirty electricity, can possibly increase the blood sugar levels.

Havas introduced her case studies on four diabetic patients. The results show that in the clean EM field environment, type 1 diabetics needed less insulin and type 2 diabetics had lower levels of plasma glucose levels. She pointed out that the EM exposure might account for higher plasma glucose levels and might contribute to the misdiagnosis of diabetes. The study also concluded that in some diabetics, in order to better regulate their blood sugar with less medication and borderline or pre-diabetics to remain non-diabetic longer, they should avoid staying in the EM pollution and/or use some special undesirable EM radiation filters to reduce EM exposure from the electric devices.

N. J. Maclver, S. R. Jacobs, H. L. Wieman, J. A. Wofford, J. L. Coloff, and J. C. Rathmell studied the regulation of lymphocyte metabolism and the consequences of disrupting normal metabolism in T cells in 2008 [43]. The authors state that the lymphocytes or white blood cells need glucose uptake and metabolism for normal survival and function. Glucose can be taken by the cell-surface expression of a group of glucose transporters. For example, the glucose transporter 4 (GLUT4), which is one of glucose transporters, is expressed in muscle, liver, and adipose tissue, and its surface expression is controlled by the insulin receptor activation. For lymphocytes, they rely on the surface expression of glucose transporter 1 (GLUT1), found to be over expressions in cancers, especially in the human T cell leukemia virus.

The authors state that the glucose and glutamine are primary resources for T cells. The glucose helps cell survival, size, activation, and cytokine production. The glucose

can also serve as a primary substrate for the generation of Adenosine triphosphate (ATP), supply a carbon source for the synthesis of such nucleic acids and phospholipids, and be metabolized by the pentose phosphate pathway to generate Nicotinamide adenine dinucleotide phosphate (NADPH). For resting T cells, they need extracellular signals, such as cytokines, hormones, and growth factors, or low-level TCR stimulation for adequate glucose uptake to maintain housekeeping functions. Without the extracellular signals, resting T cells internalize and degrade GLUT1 and the viability of the T cells cannot be maintained.

The authors also explained that in general, glucose metabolism and aerobic glycolysis are essential needs for the activated T cells to support the energy and biosynthetic for growth, proliferation, and other functions. Therefore, activation of T cells dramatically increases the demand in GLUT1 expression and surface localization. If glucose uptake is less or not enough, glycolytic flux will drop down to which the viability no longer maintains, and proapoptotic B-cell lymphoma 2 (Bcl-2) members are activated, promoting cell death. On the other hand, over glucose uptake can cause hyperactive immune responses and possible immune pathology. To keep immune homeostasis, the tight regulation of glucose uptake is necessary needed. Finally, the authors suggested that understanding of these metabolic pathways may help to figure out therapeutic strategies for some forms of cancer or autoimmunity.

R. Otton, J. R. Mendonca, and R. Curi investigated the glucose and glutamine metabolism in lymphocytes obtained from mesenteric lymph nodes of alloxan-induced diabetic rats in 2002 [44]. The authors mentioned that the metabolisms of glucose and glutamine are the major fuels for lymphocytes or white blood cells in the biosynthesis of

ATP, DNA, RNA and phospholipids. To determine the change of these metabolisms in lymphocytes, the Wistar rats, weighing 220 ± 20 g, were used in this study. The samples were separated into two groups: alloxan-induced diabetic and control rats. Both samples were kept under same conditions. Before analyzing each key enzyme activity, the lymphocytes obtained from control and diabetic rats were cultured at 37 ºC in an air/CO_2 atmosphere at a density of 10^7 cells in 1 ml RPMI-1640 medium supplemented with 10% foetal calf serum, containing 5.6 mM glucose, 2 mM glutamine and antibiotics in the presence of 1 mU/ml insulin for 6 hours. The major enzyme activities of glycolysis (hexokinase and phosphofructokinase), pentosephosphate pathway (glucose-6-phosphate dehydrogenase; G6PDH), Krebs cycle (citrate synthase), glutaminolysis (phosphate-dependent glutaminase), and decarboxylation of metabolites [U-^{14}C]-, [1-^{14}C]- and [6-^{14}C]-glucose, [1-^{14}C]- and [2-^{14}C]-pyruvic acid, [U-^{14}C]-palmitic acid and [U-^{14}C]-glutamine were monitored.

Results from this study show that the activity of phosphofructokinase was increased, while the activities of hexokinase, G6PDH and citrate synthase were decreased by the diabetic state, In addition, the results also indicated a decrease of the metabolite decarboxylation of [U-1^{4}C]- and [6-^{14}C]- glucose, [1-^{14}C]- and [2-^{14}C]-pyruvate and [U-^{14}C]- glutamine in lymphocytes from diabetic rats, while [U-^{14}C]-palmitic acid was raised. Finally, the authors suggested that the insulin administration *in vivo* or added to the culture medium caused the reversed changes in freshly obtained lymphocytes. Alloxan-induced diabetes significantly affected lymphocyte metabolism and this possible important mechanism might lead to mortality of lymphocyte function.

I. Buhler, R. Walter, and W. H. Reinhart studied the effect of glucose on blood rheology in 2001 [45]. The authors described that blood glucose could cause and increase in cardiovascular mortality of diabetic patients. Morbidity and mortality of diabetes directly depend on the degree of glycemic control. However, the mechanism of how hyperglycemia affects both the macro- and microcirculation was not clear. The authors mentioned that one of mechanisms might be haemostatic factors, increased circulating adhesion molecules and cytokine-mediated monocyte adhesion and endothelial dysfunction. Another mechanism might be an impairment of blood rheology, leading to an increase of the mechanical stress and the structural changes of the vessel wall. The other mechanism might be haemorheological abnormalities, increased blood viscosity and decreased red blood cell (RBC) deformability.

In this paper, the authors mainly considered on the haemorheological abnormalities. It has been showed that the glucose levels can cause decreased membrane deformability and increased RBC cytoplasmatic viscosity. For this reason, the authors investigated the increasing glucose concentrations on RBC shape and volume, blood viscosity at high shear rate (94.5 s^{-1}), blood viscosity at low shear rate (0.1 s^{-1}), and the viscosity of haemoglobin solutions. The blood samples were incubated with various concentrations of D- and L-glucose for 1 hour at 37 ºC and the haemoglobin solutions were incubated with D-glucose for up to 96 hours.

The results showed that the after adding D-glucose dissolved in H_2O and isotonic NaCl to the blood, the RBC was swelling and the blood viscosity at low shear rate increased. On the other hand, there was no effect when adding L-glucose, since the L-glucose was not transported into RBC by the D-glucose-specific transport protein

GLUT1. There was no change of haematocrit and viscosity when adding D-glucose dissolved in H_2O and autologous plasma to the blood, whereas adding L-glucose to the blood decreased haematocrit and viscosity values. The glycosylated haemoglobin (HbA1C) increased up to 8 % and the viscosity remained when haemoglobin solutions incubated with D-glucose at 37 ºC.

Finally, K. B. Levine, T. K. Robichaud, S. Hamill, L. A. Sultzman, and A. Carruthers presented results by characterizing human erythrocyte glucose transport protein GLUT1 expression and function in a Saccharomyces cerevisiae (RE700A) in 2005 [46]. As membrane mentioned in many papers, the authors stated that the glucose could cross through the family of integral proteins known as glucose transporters (GLUTs). Especially, the glucose transport protein GLUT1 mediates the glucose across the red blood cells. In fact, the membrane-associated GLUT1 is multimeric, and cytoplasmic ATP associated directly and cooperatively with GLUT1 changes the transporter affinity for substrate and net sugar flux through the transport complex.

However, the carrier-mediated sugar transport GLUT1 and the transport complex were not clear. For this reason, the authors proposed the characterization of human GLUT1 expression and function in RE700A. First, the transfecton of the RE700A was carried out with the p426 GPD yeast expression vector containing DNA encoding the wild-type human GLUT1, mutant GLUT1 ($GLUT1_{338\text{-}A3}$), or carboxy-terminal hemagglutinin-polyHis-tagged GLUT1 (GLUT1-HA-H6).

The results showed that GLUT1 and GLUT1-HA-H6 were accomplished at the yeast cell membrane. GLUT1 and GLUT1-HA-H6 refreshed 2-deoxy-D-glucose (2DG), 3-*O*-methylglucose (3MG), and D-glucose transport capacity to RE700A. Interaction of

GLUT1-HA-H6 with GLUT1-specific sugar transport characteristics to transfected RE700A included inhibition by cytochalasin B and high-affinity transport of the nonmetabolized sugar 3MG. $GLUT1_{338\text{-}A3}$ was expressed but could not raise RE700A sugar uptake capacity or growth on glucose. In addition, in human enthrocyte transport, the concentration at the maximal rate of sugar uptake in nM per 10^9 cells per minute for 2DG uptake equaled the concentration of sugar (mM) or cytochalasin B (nM) reducing sugar uptake by 50% of the maximal inhibition for 2DG inhibition of 3MG uptake. On the other hand, in human RBC transport transfected with GLUT1-HA-H6, the sugar uptake was not inhibited and was not stimulated by intracellular sugar.

The references cited above cover a large variety of experiments using GTEM cells and evidences of the EM field effects to the diabetes. Results from the studies cited will serve as a guideline for this research work.

Chapter 3: Theoretical Background

This chapter provides an overview of the GTEM cell, diabetes, blood cells, and biological aspects of exposure to electromagnetic fields. The topics covered are tailored to develop the information background necessary in the study of biological effects of electromagnetic radiation at cellular phone frequencies. The theoretical background related to GTEM cells is presented in section 3.1. Signal termination, including current and field termination, is discussed in section 3.2. Brief overview of diabetes and blood cells is given in section 3.3 and section 3.4, respectively. Finally, the theories and effects of biological exposure to EM fields are explained in section 3.5.

3.1 Giga-hertz Transverse Electromagnetic Cell

The giga-hertz transverse electromagnetic (GTEM) cell, shown in Fig. 3-1, was developed from the TEM cell, and is essentially a tapered coaxial waveguide which provides uniformity of EM fields in a shielded environment. The concept behind the GTEM cell design was to eliminate the restriction on upper frequency limit of the TEM cell. The GTEM cell can be operated at frequencies from DC up to several gigahertzes, and the main volume of a GTEM cell consists of only one section of a pyramidal transmission line. Since its inner conductor, or septum, and outer conductor have the same length, the travel time along each conductor is equal [47].

Because GTEM cells can provide accurate and repeatable measurements, they are used mainly for radiation emission and immunity measurements. In immunity testing, a

GTEM cell can provide a uniform EM field, so it will prevent any potential interferences or field distributions.

An EM wave travels from the source to the 50 ohms quadratic shielded transmission line and to the hybrid termination without reflection or field distortion of the TEM wave. The GTEM cell is a pyramidal quadratic transmission line with a characteristic impedance of 50Ω and is tapered with its coaxial connectors on a precise apex, as shown in Fig. 3-1.

Figure 3 - 1 GTEM cell model GTEM EMC – 1500 by EMC TEST Technologies [48].

The GTEM cell's EM waves are terminated with a distributed load made from absorption material to prevent resonance and reflection, and a 50 Ω resistance, which is a number of resistors in parallel, is used to terminate low frequency currents. Hence, the matching impedance from DC to a few tens of gigahertz is due to the cell having 50 Ω for

the low frequencies and the absorber attenuating the incident wave for higher frequencies.

At low frequencies, the influence of resistance is considered to be important. If resistors are placed close to the middle of the septum, the VSWR worsens at lower frequencies and increases the non-uniformity of the field. The resistors, therefore, should be positioned closer to the septum edges so that the currents in the area will flow close to the edges and will not cause a non-uniformity of the EM field in the testing area.

The equation of the impedance, which is derived from the relevant geometrical parameters of the GTEM cell, is given by [49, 50]

$$z_0 = \frac{\eta_0}{4\left[\frac{W}{b} + \frac{2}{\pi}\ln\left(1 + \coth\frac{\pi a}{2b}\right)\right]} \tag{3.1.1}$$

where z_0 is the GTEM cell characteristic impedance, a is the width of the outer conductor, b is the height of the outer conductor, W is the septum width, and η_0 is the intrinsic impedance dependent on the dielectric permittivity and magnetic permeability of the material spacing the inner and outer conductor. In this case, η_0 is equal to 377 Ω due to the free space inside the GTEM cell. These parameters are labeled in Fig. 3-2(a), which is a cross-sectional view of the GTEM cell.

The geometrical parameters of the GTEM cell can be determined from the GTEM cell characteristic, as follows [51]:

The characteristic impedance (z_0) of the GTEM cell, which theoretically equals 50 Ω, depends on the geometrical parameters of the structure as shown in Fig. 3-2. The septum is located at ¾ of the cell height. The height/width ratio (b/a) of the inner GTEM

cell is 2/3. In this case, the height (b = 39.7 cm) and the width (a = 58.7 cm) are given. The intrinsic impedance (η_0) equals 377 Ω due to the free space inside the GTEM cell. With this information, the septum width can be determined from equation (3.1.1). The angle between the septum and the lower shield is 15°, and the angle between the septum and the upper shield is 5°. The septum must be supported by the dielectric material.

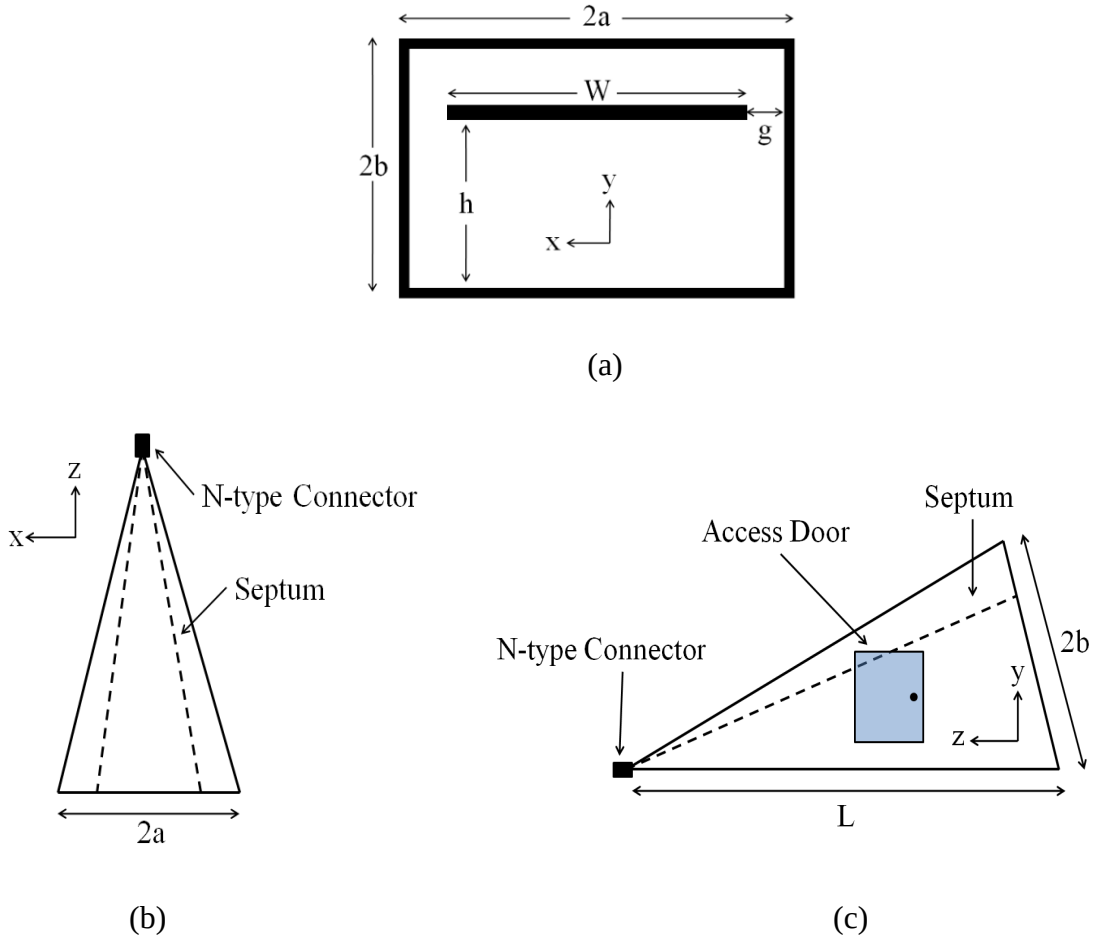

Figure 3 - 2 GTEM cell configurations: (a) cross-sectional view, (b) top view, and (c) side view. The parameters of the GTEM cell dimensions are a = 58.7 cm, b = 39.7 cm, W = 88.9 cm, g = 14.1 cm, h = 69 cm, and L = 222.1 cm.

The E field strength (E) at the position of the testing area is given by [52]

$$E = \frac{\sqrt{P \cdot z_0}}{h} \tag{3.1.2}$$

where z_0 is the GTEM cell characteristic impedance, P is the respective input power, and h is the distance between the inner conductor and the bottom outer wall.

The area where tests can be performed in a GTEM cell is one-third of the volume between the septum and the lower outer wall [51]. The testing sample area should be approximately 20 to 45 cm away from the absorbers inside the GTEM cell.

3.2 Signal Termination

The signal termination in a GTEM cell is a key factor in establishing a wideband impedance match for all frequency range. As mentioned in the previous section, the current in the inner conductor, at frequencies lower than a few hundred megahertz, can be terminated by a large number of parallel resistors between the center conductor and rear wall.

At frequencies where half the wavelength is smaller than the cross-sectional dimensions of the GTEM cell, the higher order modes are excited [52]. The higher order modes, defined as waveguide modes, cannot be terminated by the resistors. Therefore, the pyramidal RF absorbers are used to terminate higher order modes at higher frequencies, especially at frequencies higher than 200 MHz [52]. These absorbers are positioned at the rear wall.

3.2.1 Current Termination

The resistive termination needs to have a high return loss property for frequencies of at least 200 MHz. There are two primary considerations taken into account in designing the resistive termination. The first consideration is that the number of parallel resistors directly affects the current distribution in the septum. The effect of the use of different numbers of parallel resistors was investigated by C. Icheln and is shown in Fig. 3-3 [52].

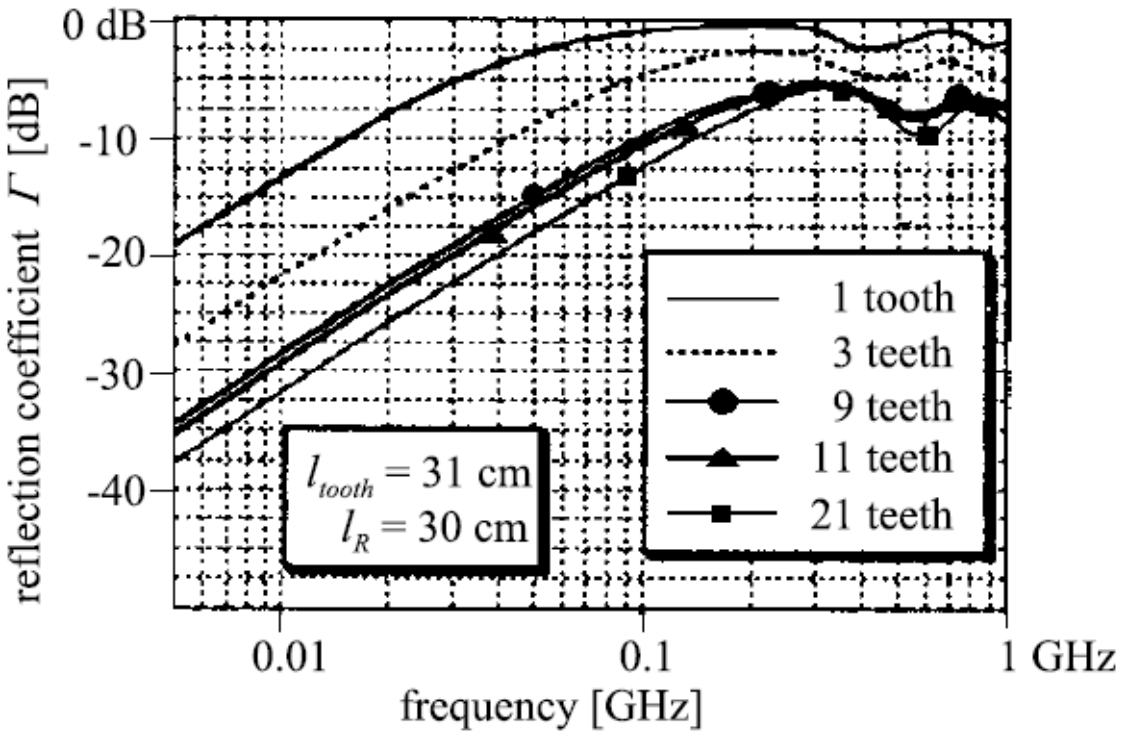

Figure 3 - 3 The return loss results of the different numbers of parallel teeth and resistors without RF absorbers in the GTEM cell. l_{tooth} is the length of the tooth and l_R is the length of the resistor [52].

The second consideration is that the cross section at the rear wall is filled by RF absorbers, which normally have high conductivity. This causes an increase in the distributed capacitance of the GTEM cell, resulting in a decrease in the characteristic

impedance of the GTEM cell towards the rear end. Therefore, the current-terminating section can help to maintain the characteristic impedance of 50 Ω and compensate the effect of the distributed capacitance.

3.2.2 Field Termination

RF absorbers are widely used for electromagnetic compatibility (EMC) applications to attenuate or absorb the energy of an incident wave. The RF absorbers are lossy material, which consists of carbon loaded polyurethane foam. Generally, the RF absorbers are pyramidal shaped, as shown in Fig. 3-4.

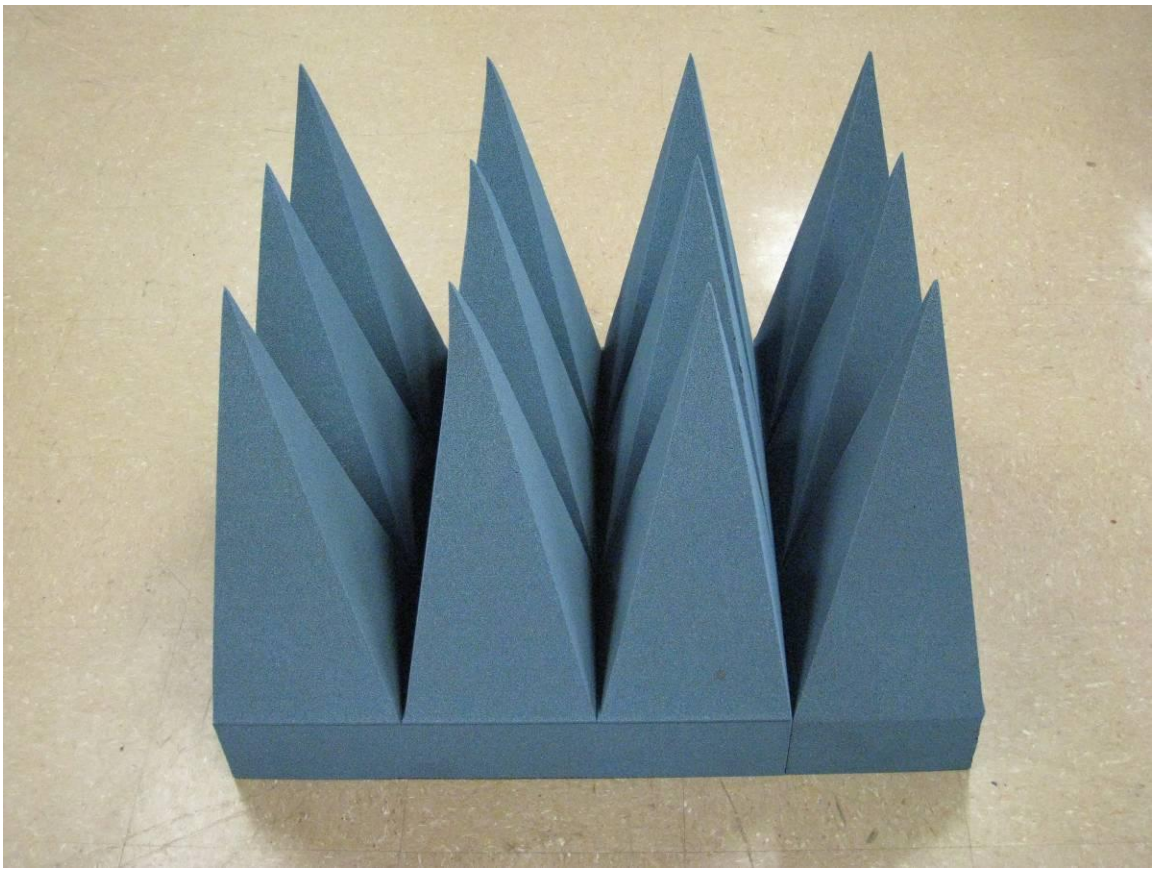

Figure 3 - 4 EMC-24PCL microwave absorbers by ETS-Lindgren L.P.

The tapered geometry of the RF absorbers can provide good low-reflection properties because the pyramidal tips can change the impedance of the incident wave and thus reduce the Q factor [53]. The incoming wave will be reflected and scattered from the surface of the absorbers rather than reflected back into the GTEM cell. Since the absorbers are made of absorbant material, the reflected wave will be absorbed continuously.

In addition to the material, the height of the absorbers should be considered. Usually, the height of the pyramidal absorbers equals half of the wavelength [32]. The lowest frequency where the pyramidal absorbers can be used is when the height of the absorbers equals half the incident wavelength.

3.3 Diabetes

Diabetes, which is a kind of metabolic disease, causes high levels of sugar in blood. Diabetes can occur when the body does not produce enough insulin, when cells do not respond to insulin, or as a result of both the conditions. In normal people, their blood plasma glucose is between 70 to 110 mg/dL. On the other hand, for people who have diabetes, their blood plasma glucose exceeds 126 mg/dL [54].

Diabetes is a chronic and global public disease. In the present, there are 346 million people worldwide with diabetes [55]. More than 80 percent of diabetes deaths occur in low and middle income countries. The WHO estimates that diabetes deaths will double between 2005 and 2030. In the USA, 25.8 million people, 8.3 percent of the U.S. population, have diabetes [56]. It is the seventh leading cause of death in the USA.

There are five major types of diabetes [54]:

1. **Type 1 Diabetes** – is found in 5 – 10 percent of all diabetes cases. Most type 1 diabetes is because of a failure of the pancreas to produce insulin and leads to absolute insulin deficiency resulting from the destruction of the pancreatic islet beta-cells. Symptoms include weight loss, thirst, vision changes, fatigue, and excessive excretion of urine. These symptoms may occur suddenly. Type 1 diabetes can be treated by directly injecting the insulin to the body.

2. **Type 2 Diabetes** – is found in 90 – 95 percent of all cases. It occurs when the body resists insulin. However, the causes of insulin resistance are still not clear. Some believe that it results from the genes, age, stress, or the failure of the pancreatic islet beta-cells. It can be found largely in people who have excess body weight and physical inactivity. The symptoms are similar to type 1 diabetes.

3. **Gestational Diabetes** – is defined as glucose intolerance. It is found during the pregnancy period, especially during the second and third trimesters of pregnancy. In the USA, approximately 7 percent of all pregnancies have this diabetes. The causes of this diabetes are not clear.

4. **Other types of Diabetes** – may be due to genetic defects in beta-cell function or insulin action, genetic mitochondrial defects, diseases of the exocrine pancreas, endocrinopathies, drug or chemical-induced diabetes, and other conditions.

5. **Other Disorders of Glucose Regulation** – are referred to as prediabetes. People who have impaired glucose tolerance (IGT) and impaired fasting glucose (IFG), are at risk for diabetes that can develop into type 2 diabetes.

3.4 Blood Cells

Blood is red liquid which flows in blood vessels and is a specialized form of connective tissues. Blood consists of free cells, including blood cells, and fluid intercellular substances, including blood plasma. The blood acts as the vehicle to transport essential nutrients to cells and transport metabolic waste out of cells. People have approximately five liters of blood in their body. In males, 40 – 54 percent of blood consist of blood cells while in females, blood cells are 37 – 47 percent of the blood [57].

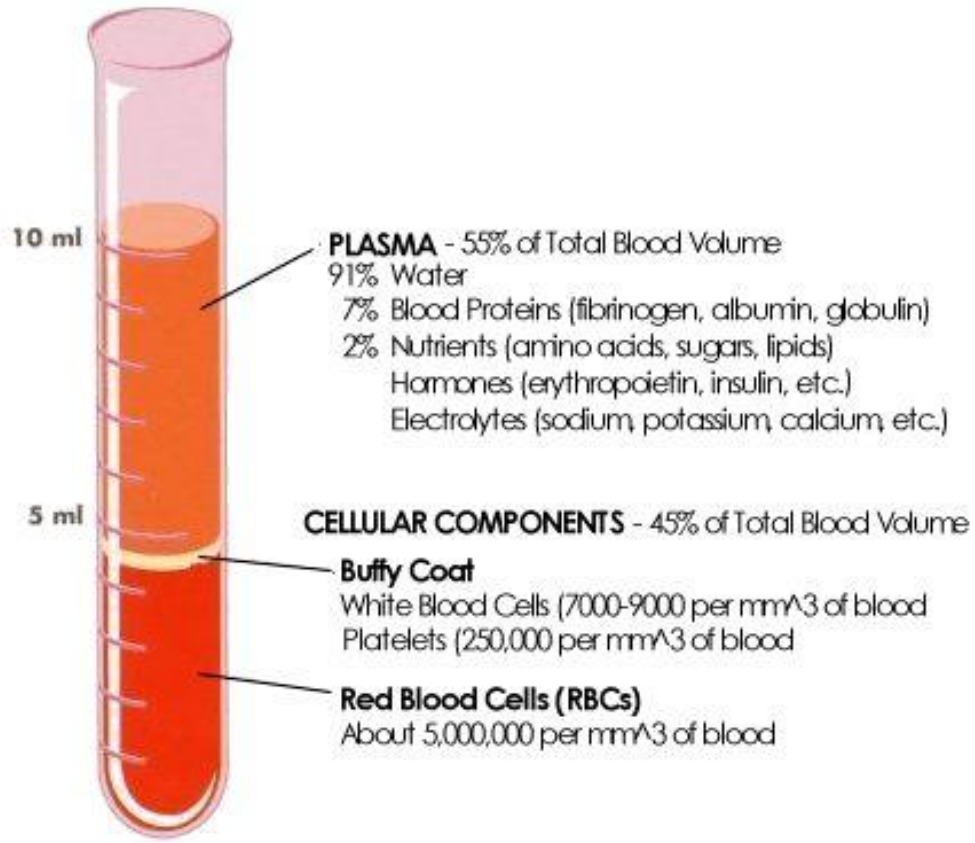

Figure 3 - 5 Blood elements by National Space Biomedical Research Institute [58].

Blood cells can be divided into three major elements: red blood cells, white blood cells, and blood platelets in plasma. The red blood cells are sometimes called erythrocytes, and the white blood cells are called leukocytes.

Red blood cells deliver oxygen to body tissues and pass carbon dioxide to lungs. They are flexible biconcave disks which lack a cell nucleus and most organelles. The diameter of a red blood cell is around 7 to 8 micrometers. Red blood cells can be produced in bone marrow and destroyed in the spleen. The lifespan of red blood cells are approximately 90 to 120 days. In general, a male has 5 million red blood cells per 1 mm^3 of blood, and a female has 4.5 to 5 million red blood cells per 1 ml^3 of blood. Hemoglobin is an important element in red blood cells because it binds oxygen. Each red blood cell has 280 million molecules of hemoglobin. However, if the hemoglobin in blood is high, the blood will become sticky and cause flow problems.

Unlike red blood cells, white blood cells provide an immune system to defend the body against pathogens, including contagious diseases. There are several types of white blood cells, classified into granuler and agranular. The diameter of the white blood cells is around 8 micrometers, causing them to be bigger than red blood cells. White blood cells are produced in bone marrow like the red blood cells are. People generally have 6,000 to 9,000 white blood cells per 1 ml^3 of blood.

Another free cell in blood is the blood platelet, which us biconvex disc-shaped bodies 2 to 4 micrometers in diameter. They are found only in mammals. Platelets help to stop excessive bleeding. A low number of platelets cause excessive bleeding, and a high number of platelets cause the obstruction of blood vessels, resulting in such events as a

myocardial infarction, stroke, pulmonary embolism, or the blockage of blood vessels to other parts of the body like the extremities of the arms, legs and fingers.

3.5 Biological Effects of Electromagnetic Exposure

A large proliferation of electronic devices, such as microwaves, laptops, and mobile phones, has also increased dramatically the possibility that radiation from such devices would produce harmful health effects on individuals who use these devices or or work around them.

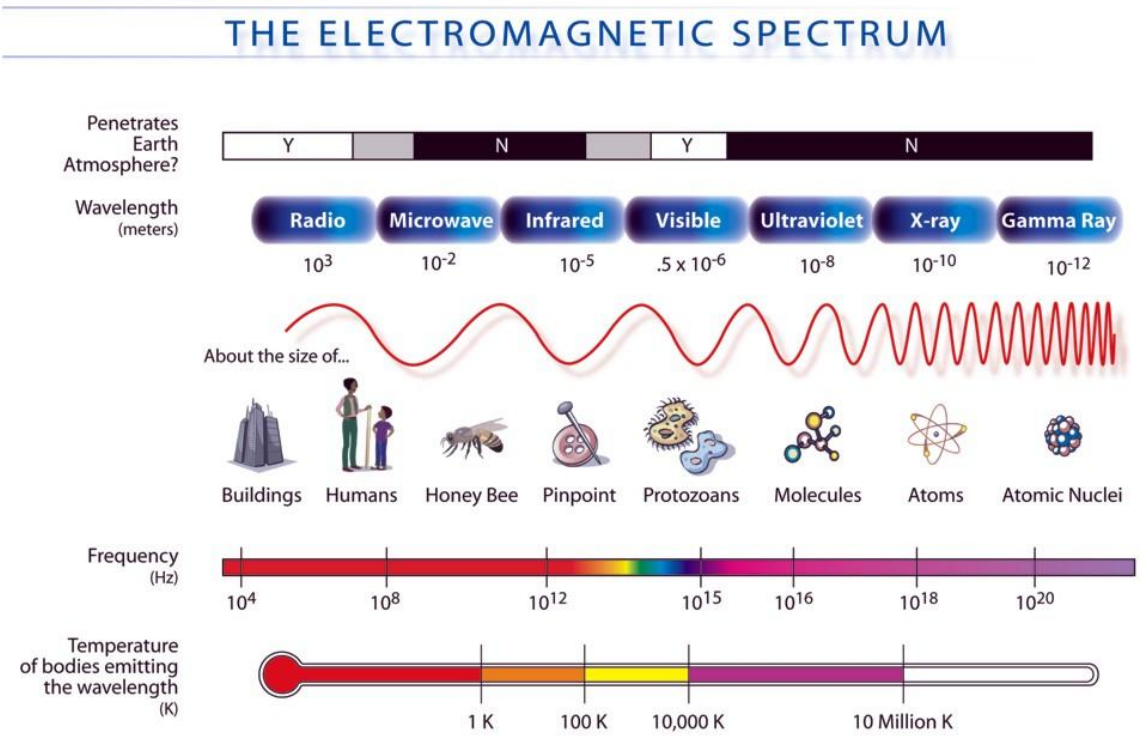

Figure 3 - 6 Electromagnetic spectrum by NASA [59].

In general, electromagnetic radiation is a form of energy wave traveling through space. Electromagnetic radiation has both electric and magnetic field components oscillating perpendicularly to each other along the direction of wave propagation. The electromagnetic fields has a large frequency spectrum, which can be divided into zones, as shown in Fig. 3-6.

An excellent source of information on the biological effects of electromagnetic fields is the book entitled the *Biological Effects of Electromagnetic Fields: Mechanisms, Modeling, Biological Effects, Therapeutic Effects, International Standards, Exposure Criteria* by Peter Stavroulakis [60]. According to this book, EMF frequencies greater than 300 GHz, including the solar spectrum as well as *x* and gamma rays, have been deeply studied to raise awareness of their possible biological effects. We are well informed the harmful effects of sun radiation. If we are exposed to the sunlight for long periods of time, our risk of developing skin cancer increases. We are also made aware of the catastrophic effects of nuclear bombs, nuclear reactor leaks, and diagnostic X-rays which can all increase the risk of cancer, especially leukemia. On the other hand, the biological effects of static field and electromagnetic radiation at frequencies lower than 300 GHz, which some segment of the population are exposed to on a daily basis, are not been well documented [60].

There are many electronic devices used in our daily lives that can generate electromagnetic radiation at frequencies up to 300 GHz, which is non-ionized electromagnetic radiation that cannot ionize atoms: satellite TV antennas; electric power networks; radios; wireless internet routers; wireless Wi-Fi repeaters; and all electric or electronic appliances, including microwave ovens, heating appliances, electrical heating

resistances for floors, wireless electronic games, mobile electronic computers, electric blankets, heated waterbeds, and wireless Bluetooth headsets.

For the measurement of such non-ionized electromagnetic radiation, knowledge of the exposed frequencies is required. For the frequencies below 500 Hz, defined as low frequencies, measurement of the electric and magnetic fields is necessary because they are uncoupled. For the frequencies higher than 3 MHz the electric field is measured only due to interrelations connecting the electric field and magnetic field as well as due to the power density, which defines the power per surface unit (W/m^3). The magnetic field and power density can be obtained from the electric field, whereas at lower frequencies both electric and magnetic fields must be determined individually [60].

In effect, the weak electromagnetic fields results in an increase in the heat in the tissue of living organisms. The electromagnetic fields affect the interaction of the neural cells, whose electric pulse is 1.5 MV/m. This can consequently cause considerable harm to organisms. Usually, there is a 50 MV/m electric field difference between the inside and outside of a cell membrane. Weak EMFs should not be able to affect the cell membrane functions, but they do. The therapeutic effects in which the electric field is used for Parkinson's therapy are good examples of this phenomenon [60].

The explanation of these therapeutic effects is that electromagnetic fields at certain intensity levels can possibly create windows, resulting in movement in and out of calcium and potassium ions. Melatonin is a hormone secreted into our body by the pineal gland that is at the rear side of the cerebrum. The cerebrum is used to regulate other hormones, support the immune system, and maintain the body's circadian rhythm, a biological "clock" that affects when we fall asleep and when we wake up. The melatonin

levels in our body can decrease when we are exposed to electromagnetic fields. This decrease of melatonin levels can then cause harmful effects in humans [60].

Non-ionizing electromagnetic radiation is electromagnetic energy with frequencies ranging from approximately 0 to 300 GHz and not exceeding visible light frequency. Most non-ionizing electromagnetic radiation is emitted from man-made technology. Electromagnetic fields with frequencies lower than the frequency of visible light cannot ionize living or non-living matter. Only EM fields that have frequencies greater than the frequency of visible light can cause ionization in a single photon [60].

The differences between the man-made electromagnetic waves from electronic devices like oscillating electric circuits and natural light are that the artificial electromagnetic fields have frequencies lower than infrared radiation (less than 300 GHz). Man-made EM waves are typically linearly polarized and can be radiated continuously by the oscillating circuits [60].

On the other hand, electromagnetic waves from natural light are not polarized waves. The natural EM waves are generated by excitations and de-excitations, and they are the form of discontinuous waves. In addition, the frequencies of natural electromagnetic waves are equal or higher than infrared (equal or greater than 300 GHz) [60].

Polarized waves from artificial EM waves can affect bioactive organisms, but non-polarized waves cannot. The free ions, mainly K^{+}, Na^{+}, Cl^{-}, and Ca^{+2}, on both sides of each cell membrane [60]:

1. Control the entrance or exit of water to maintain cell volume,
2. Function in different metabolic cell processes-signal transduction processes,

3. Create the potential difference of a very intense electric field about 10^7 V/m between the inside and outside of the cell membrane.

The free ions on both sides of a cell's plasma membrane can be energized by the oscillating force from the external electric field, resulting in vibration of the free ions. The gating channels for matter moving in and out the cell membrane are electrically sensitive. Disordering in gating channels occurs when the amplitude of the ions' forced-vibration reaches the critical value, and the oscillating ions can give a false signal, resulting in the electrochemical balance of the plasma membrane and consequently the cell functions [60].

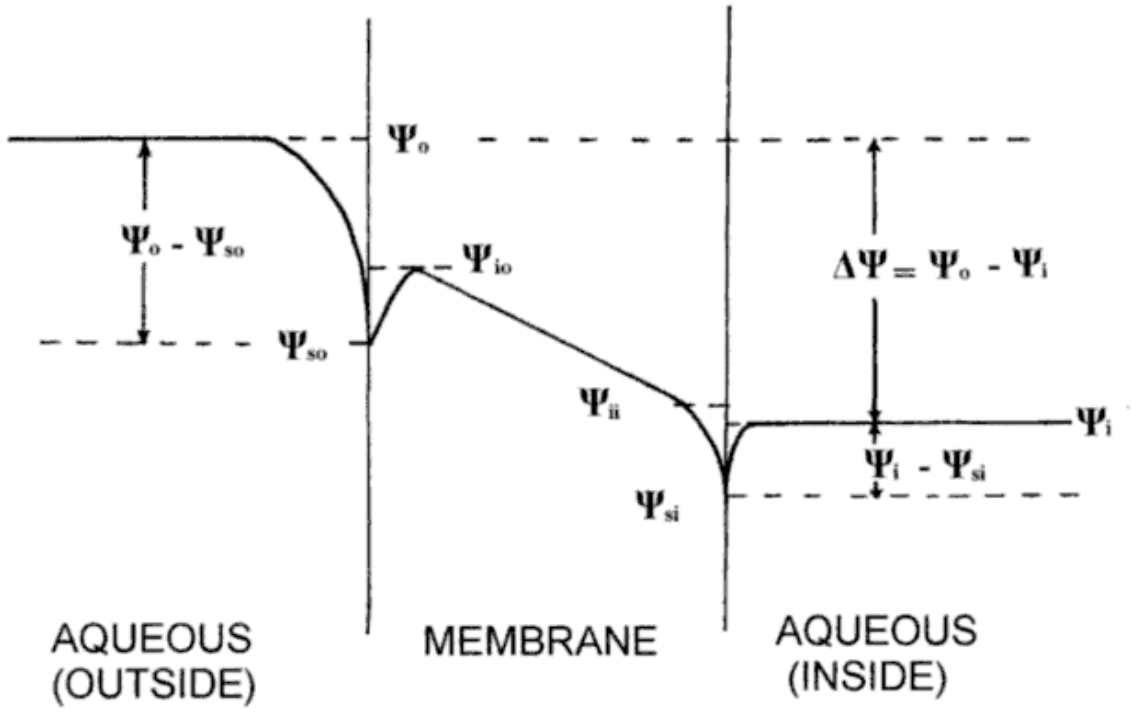

Figure 3 - 7 The characteristic of the voltage across the cell membrane [60].

The characteristic of the electric field across the cell membrane is shown in Fig. 3-7. The aqueous solutions, including the plasma membrane, mitochondria, chloroplasts, endoplasmic reticulum, and Golgi apparatus are surrounded by the cell membrane and present negative potential in relation to the aqueous solutions outside the cell membrane [60].

In Fig. 3-7, the voltage across the cell membrane occurs when there are electric charges of the membrane lipids located at the surface. The voltage at the surface is negative, about -10 mV to -100 mV, due to the negatively charged lipids, including phosphatidylserine, phosphatidylinositol, and diphosphatidyl-glycerol. In addition, the voltage of the inner surface is always negative due to the distribution of the lipid dipoles as well as due to the hydrophobic ion binding within the cell membrane [60].

The total electric potential difference between the outside and inside of the cell membrane, $\Delta\Psi = \Psi_o - \Psi_i$, is usually from the concentration differences of positive ions, mainly Ca^{2+} and K^+, between the aqueous solutions outside and inside the cell membrane. Hence, the difference in electrical potential between the aqueous solutions outside the cell membrane and the membrane's surface outside the cell membrane, $\Psi_o - \Psi_{os}$, is greater than the difference in electrical potential between the aqueous solutions inside the cell membrane and the membrane's surface inside the cell membrane, $\Psi_i - \Psi_{si}$ [60].

The total electric potential across the cell membrane of living organisms is between 20 mV and 200 mV. The intensity of the transmembrane electric field, $E_m = \Delta\Psi/s$, is 10^7 V/m, assuming the width of the membrane equals 10^{-8} m and the total electric potential difference between the outside and inside of the cell membrane ($\Delta\Psi$) equals 100 mV [60].

The total electric potential across the cell membrane under equilibrium conditions due to a certain type of ion can be determined by the "Nernst equation" [60]

$$\psi_o - \psi_i = -\frac{RT}{zF_c} \ln \frac{C_o}{C_i} \tag{3.5.1}$$

where Ψ_o and Ψ_i, are the electrical potential on the external and internal surfaces of the membrane, respectively. R is the global constant of the perfect gases. T is the absolute temperature (ºK). z is the ion's electric charge (in electrons) or the ion's valence. F_c is the Faraday's constant. C_o and C_i are the respective concentrations of the ion on the external and internal side of the membrane, when the net flux of the ion is zero [60].

As mentioned previously, the total electrical potential difference across the cell membrane is due to the summation of the contributions from the ions in the membrane. Therefore, when these ions absorb the external electric field, two consequences can occur [60].

1. If the electric field is static, it will cause a polarization of constant magnitude and direction in the cell [60].
2. If the electric field is an oscillating field, it will cause a forced-vibration of the free ions [60].

However, as it was shown above, in this dissertation I mainly focus on the second case, which is the most complicated according to the book by Peter Stavroulakis [60].

The plasma membrane is surrounded by a free-ion layer that isolates the membrane from external fields. When the external oscillating electric fields exert force on every ion on the plasma membrane, including the ions within channel proteins, the ions will have forced vibration. When the vibrational movement amplitude of the ions meet the critical value, the oscillating ions can send false signals for the opening or

closing of channels, which are voltage-gated. This will negatively affect the membrane's electrochemical balance and consequently impact the function of the whole cell [60].

In conclusion, it has been shown that biological matter exposed to pulsed electromagnetic fields has more response and more drastic effects than when it is exposed to continuous electromagnetic fields where the EM pulses are constant. This is due to the fact that repetitive EM pulses increase the effects on biological samples because of repetitive exposure [60].

Chapter 4: Simulation and Experimental Configuration

In this chapter, research related to characterizing the response of blood with high glucose concentration to 850 and 900 MHz electromagnetic radiation is presented. The simulation of the GTEM cell and its design are presented in section 4.1. The experimental setup of the GTEM cell, including its construction and calibration, as well as the experiments related to blood preparation and experimental procedures are discussed in section 4.2. This chapter also presents another GTEM cell designed through simulation (but not constructed), which show an improvement in the testing area and well as in field uniformity.

4.1 Simulation Configuration

4.1.1 GTEM Cell Characteristics

In this section, the simulation results for the GTEM cell design is presented. The objective of this study is to construct a GTEM cell which provides a shielded environment with a uniform EM field for the testing of small biological objects in a frequency range from DC to at least 4 GHz. The voltage standing wave ratio (VSWR) should be less than 2 to ensure no existence of field non-uniformity, field distortion, and undesirable effects from the resonance inside the GTEM cell.

The GTEM cell in this study was designed using CST Microwave Studio software [1]. This software enables 3D electromagnetic analysis in the microwave frequency

range, where the simulation is based on perfect boundary approximation (PBA) and finite integration technique (FIT) method [1].

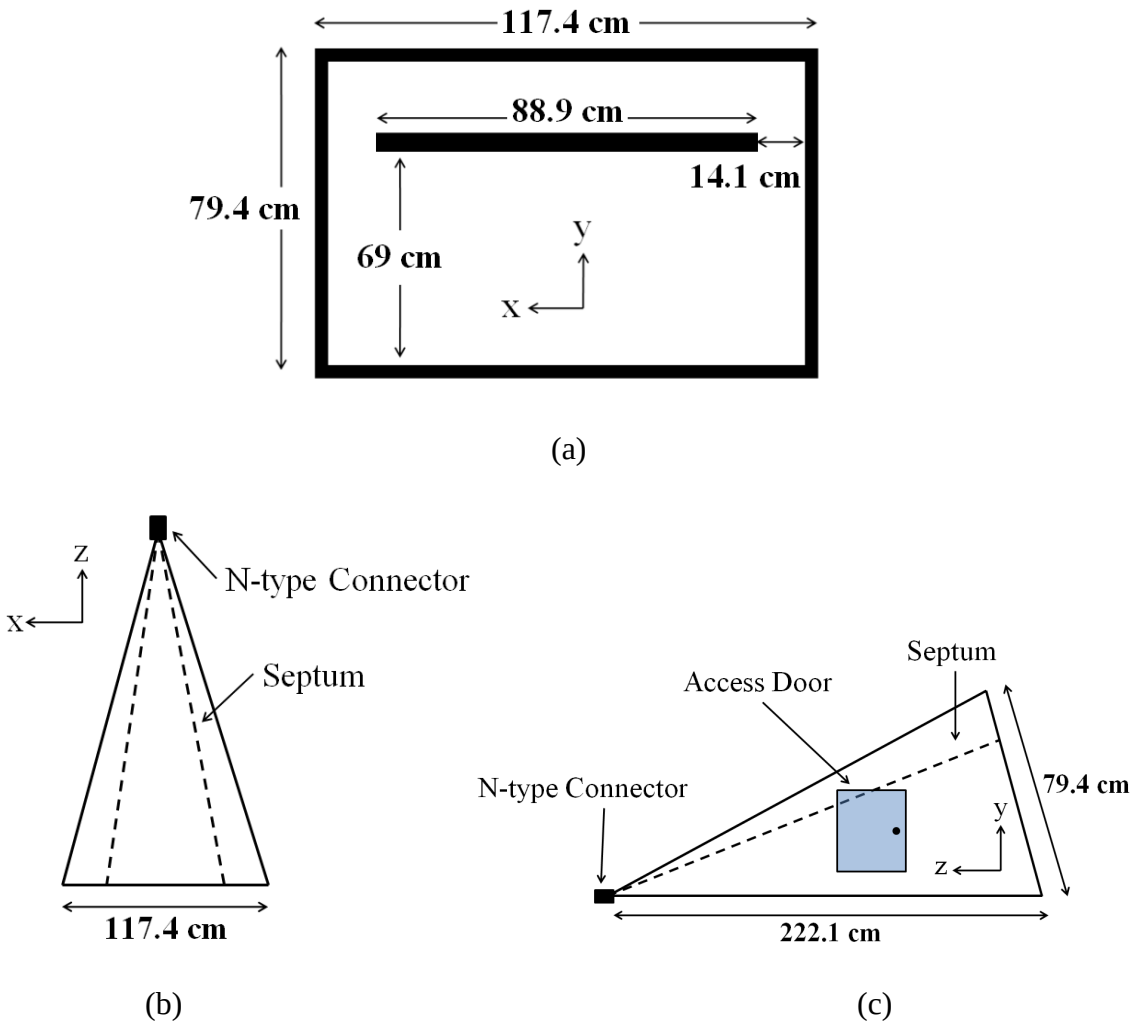

Figure 4 - 1 Dimension parameters of the GTEM cell: (a) cross-sectional view, (b) top view, and (c) side view.

The GTEM cell parameters were obtained by using equation 3.1.1. All input parameters used in the simulation are shown in Fig. 4-1. The length of the GTEM cell was 222.1 cm. The width of the GTEM cell was 117.4 cm. The height of the GTEM cell was 79.4 cm. The width of the septum was 88.9 cm. The height of the septum was 69 cm.

The material of the GTEM cell was assumed to be a perfect electric conductor (PEC) with the thickness of 0.2 cm.

The GTEM cell was designed horizontally, which means the electric field vector was oriented in the y-direction, and the electromagnetic wave propagates in the z-direction, as shown in Fig. 4-2.

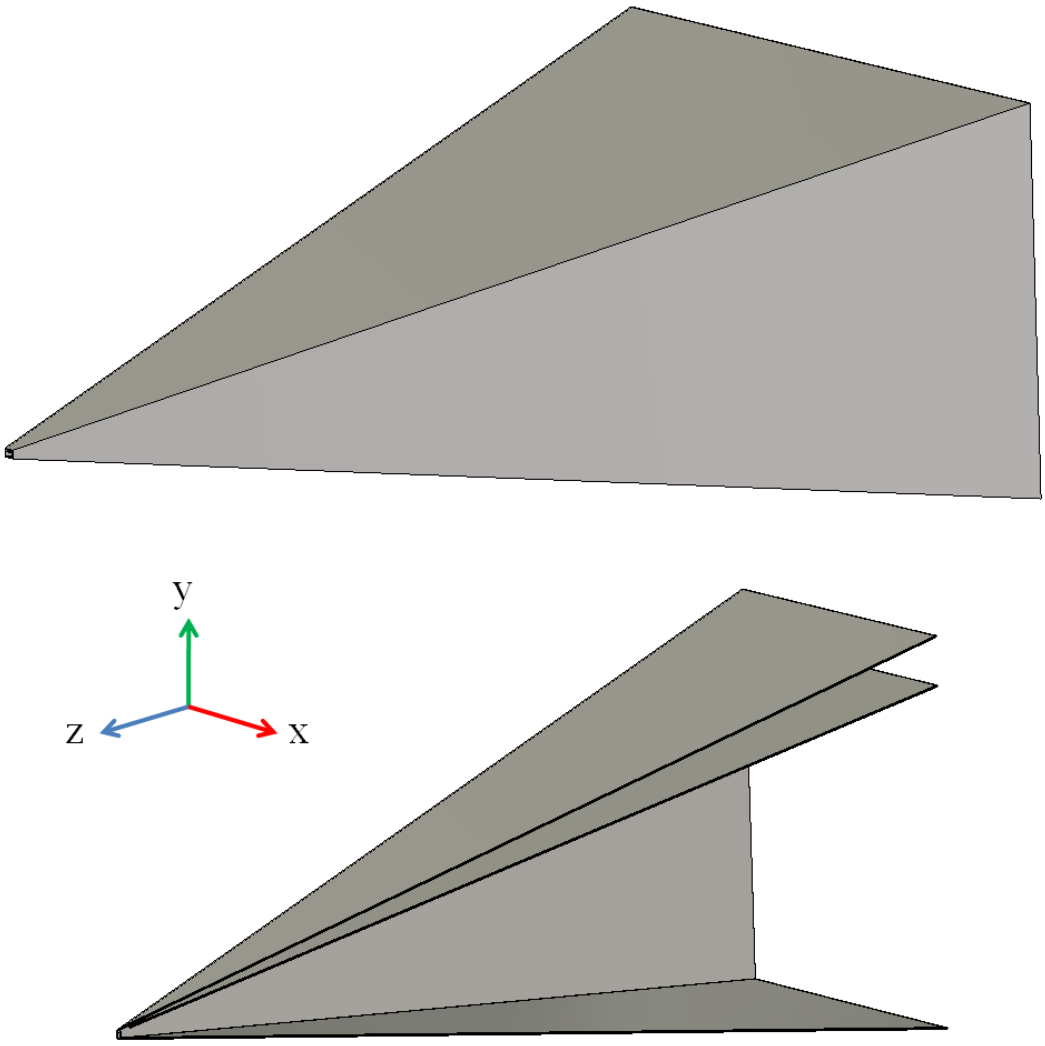

Figure 4 - 2 The CST model of the GTEM cell: outside view (top) and inside view (bottom).

The waveguide ports were used to apply an input signal into the opened-end port and to terminate the EM field at the other end of the GTEM cell, as shown in Fig. 4-3 (top and bottom, respectively). Also, for the excitation signal a Gaussian pulse was applied at the waveguide input port.

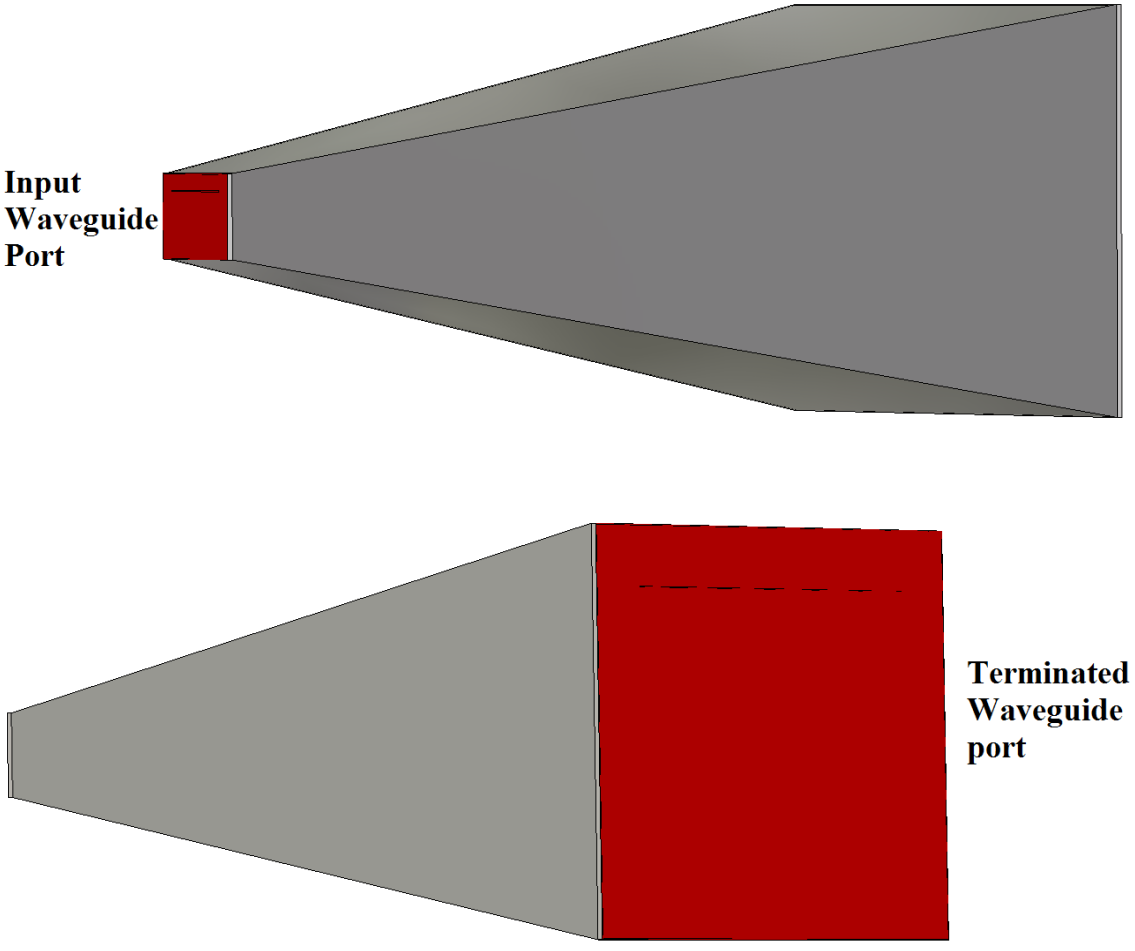

Figure 4 - 3 Input signal port (top) and terminated signal port (bottom).

Fig. 4-4 shows the boundary condition of the simulation, which was defined as open space condition. This simulation setup provided the results of electromagnetic fields, VSWR, and return loss.

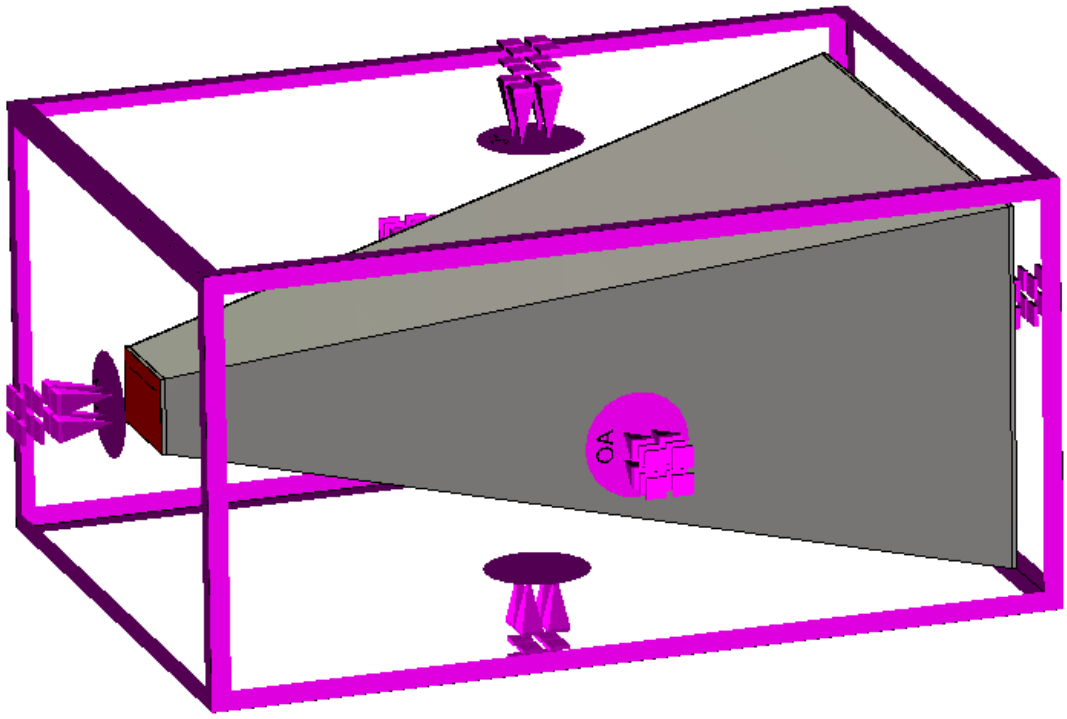

Figure 4 - 4 Boundary condition of GTEM cell.

4.1.2 Improvement of Testing Area and Field uniformity

To improve a testing area, a simple option is to build a bigger GTEM cell. However, the usage of the frequency range will decrease because the frequency range depends on the GTEM cell's size, according to the waveguide concept. Moreover, the construction cost is higher for a bigger GTEM cell because the bigger GTEM cell requires more aluminum sheets as well as more RF absorbers for the EM field termination. In addition, it is not convenient to move or carry such a GTEM cell to other

laboratories. Finally, a bigger GTEM cell is not effective for biological experiments because most of the treated biological samples have a small size.

The GTEM cell developed for this project was designed horizontally, which means the electric field vector is oriented in the y-direction, and the electromagnetic wave propagates in the z-direction, as shown in Fig. 4-5.

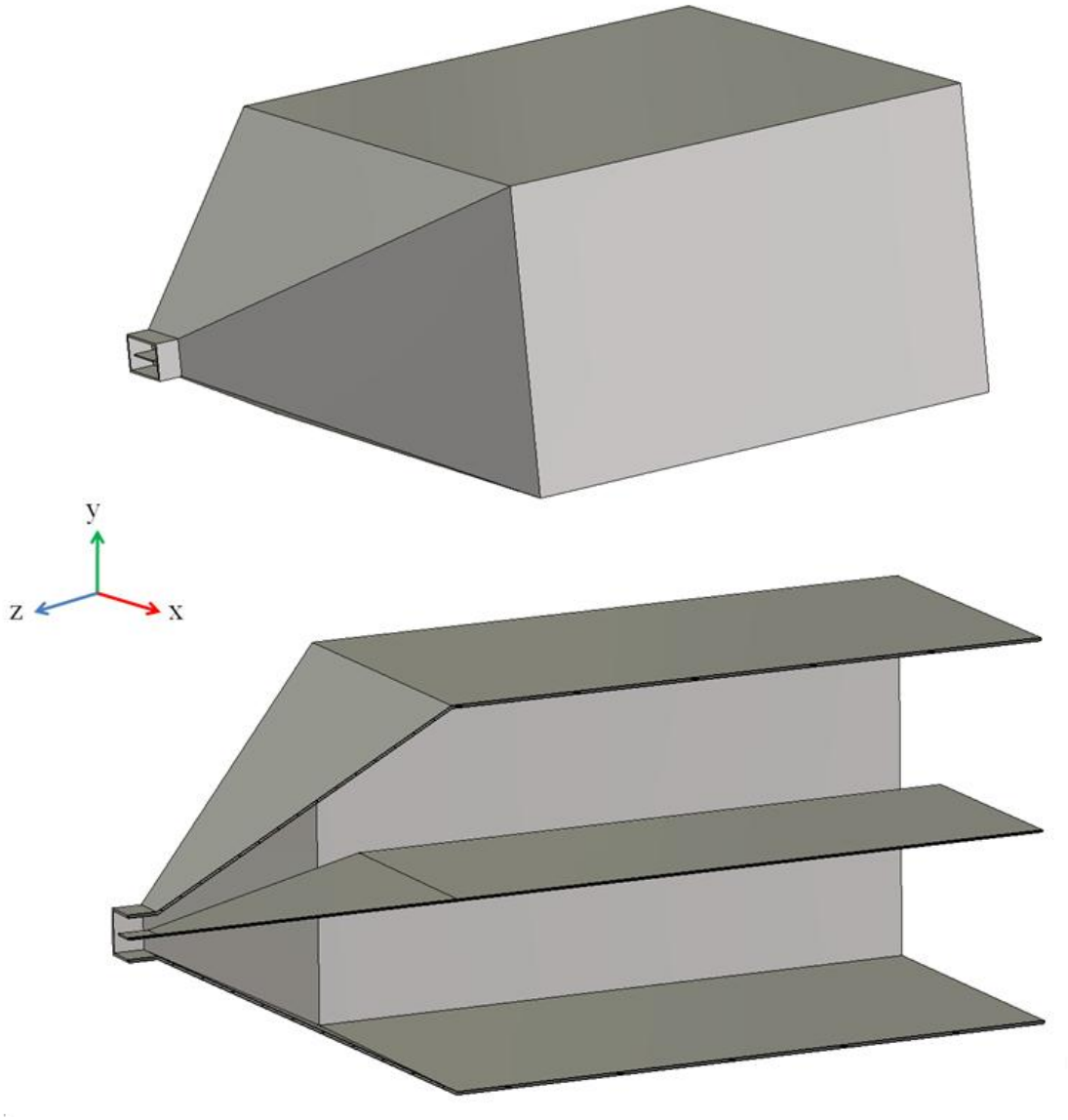

Figure 4 - 5 Developed GTEM cell: outside view (top) and inside view (bottom).

The designed GTEM cell, as shown in Fig. 4-5, is more than twice as small as the original GTEM cell and can be comfortably moved and carried anywhere. Its construction cost is also lowered due to its smaller size and use of less RF absorbers. In addition, the designed GTEM cell provides more usage of the frequency range. The testing area of the designed GTEM cell is more than double when compared to the original GTEM cell. Therefore, it allows more samples, especially blood samples, to be tested (or analyzed) in the biological experiments. The testing area of the developed GTEM cell will be shown and discussed more in the next chapter.

The dimension parameters of the GTEM cell are shown in Fig. 4-6. The length of the GTEM cell is 78 cm. The width of the developed GTEM cell is 50.4 cm. The height of the GTEM cell is 30.3 cm. The width of the septum is 36.05 cm. The height of the septum is 15.15 cm. The material of the GTEM cell is assumed to be a perfect electric conductor (PEC) with a thickness of 0.127 cm.

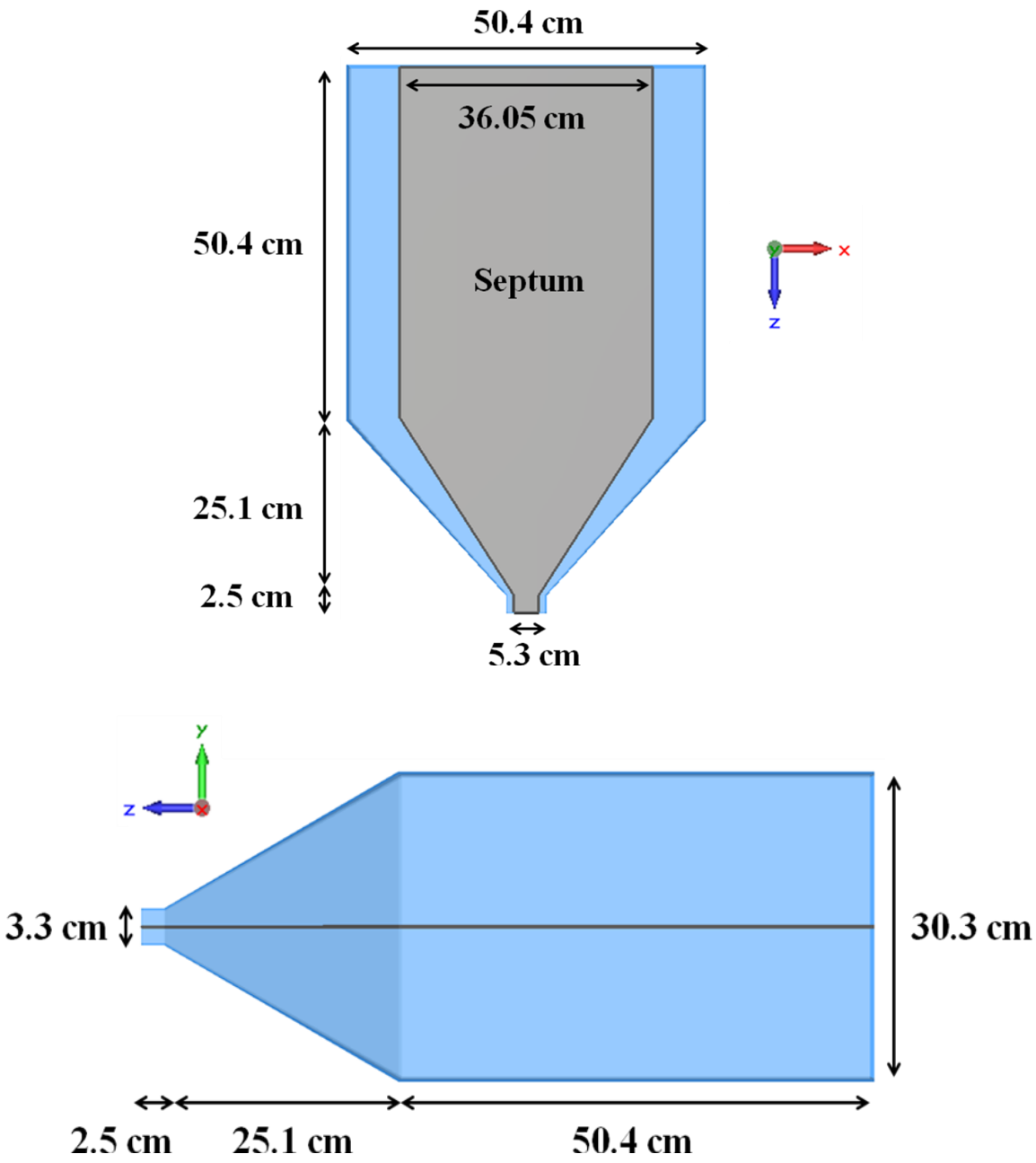

Figure 4 - 6 Dimension parameters of the developed GTEM cell: top view (top) and side view (bottom).

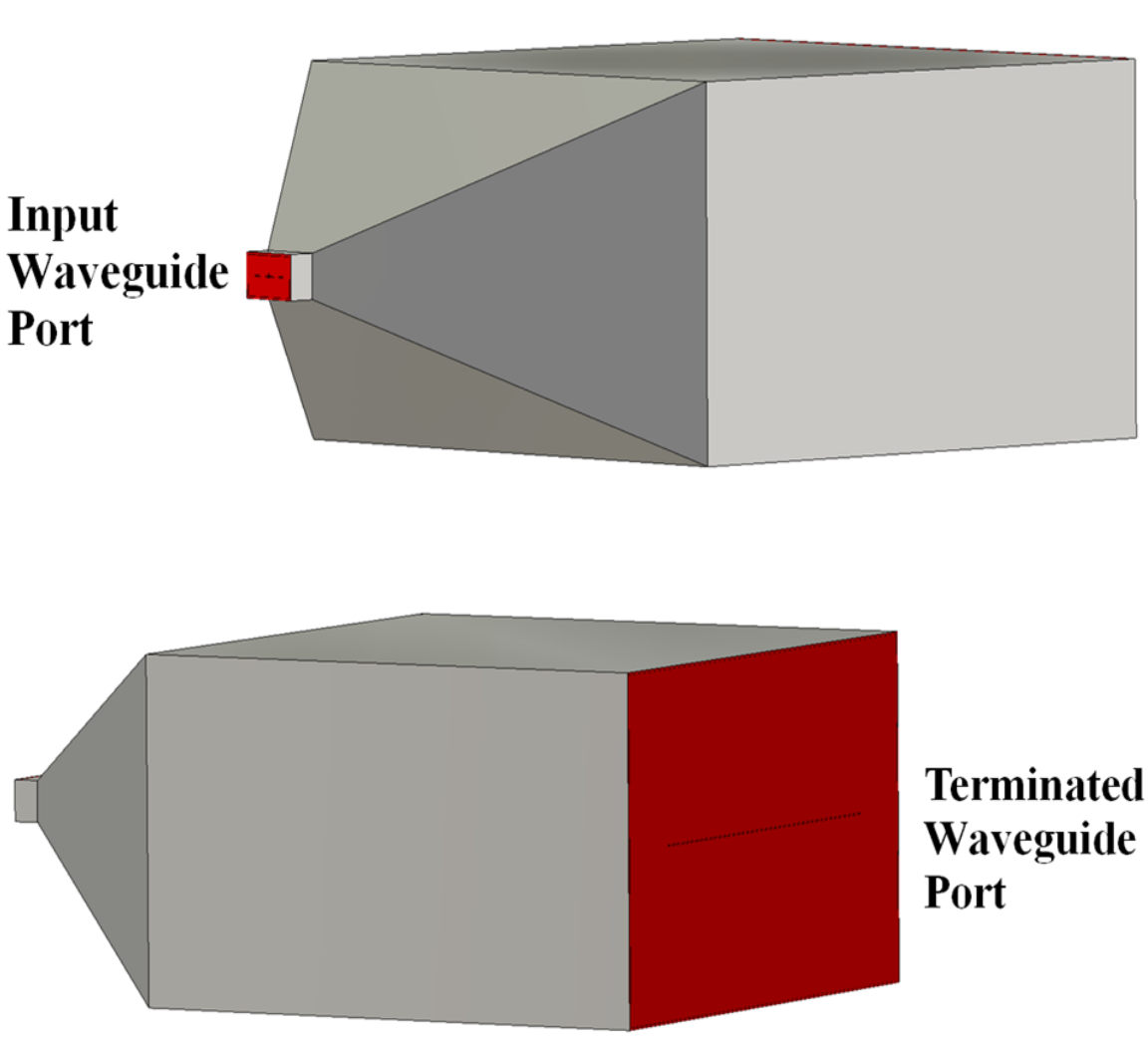

Figure 4 - 7 Input signal port (top) and terminated signal port (bottom).

The waveguide ports were used to apply an input signal into the opened-end port and to terminate the EM field at the other end of the GTEM cell, as shown in Fig. 4-7 (top and bottom, respectively).

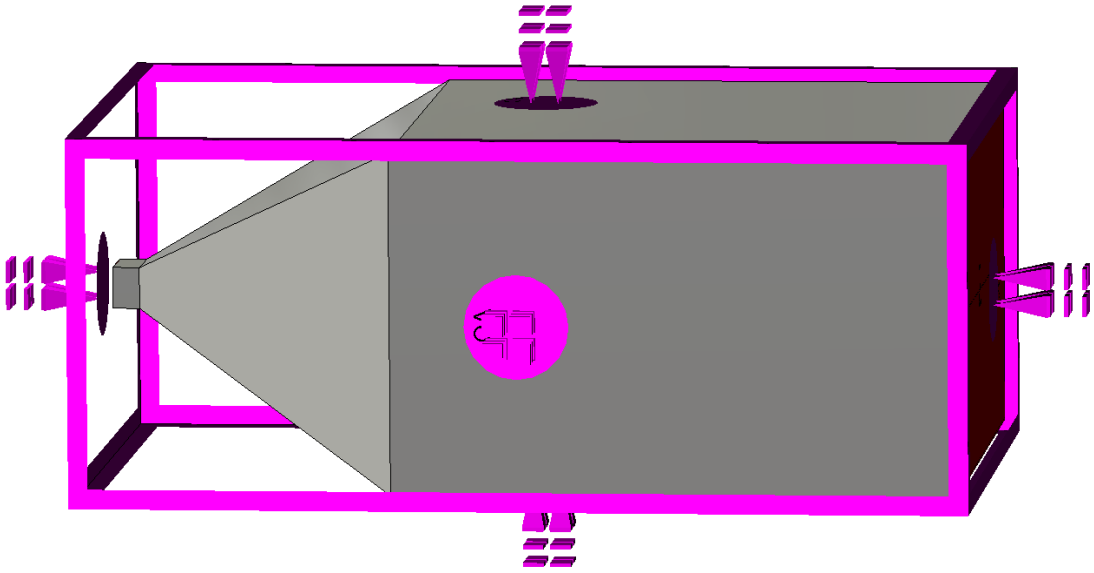

Figure 4 - 8 Boundary condition of the developed GTEM cell.

In addition, for the excitation signal a Gaussian pulse was applied at the waveguide input port. Fig. 4-8 shows the boundary condition of the simulation, which was defined as open space condition. This simulation setup provided the results of electromagnetic fields, VSWR and return loss.

4.2 Experimental Configuration

4.2.1 Construction of GTEM Cell

To conduct this experiment, a shielded environment is required. The GTEM cell was built to generate an electric field and to provide a shielded environment. The dimensions of the laboratory constructed GTEM cell are shown in Fig. 4-1. First, I started with building the septum, as shown in Fig. 4-9.

Figure 4 - 9 The constructed septum.

Fig. 4-10 shows the tapered transmission section of the GTEM cell, which was fabricated second.

Figure 4 - 10 The constructed tapered transmission section.

To terminate the EM fields, the pyramidal EMC-24PCL microwave absorbers (200 V/m, 80-250 MHz: 6 dB absorption, >250 MHz: 10 dB absorption, ETS-Lindgren L.P., Cedar Park, TX, USA) shown in Fig. 3-4 were placed inside the GTEM cell. The absorber dimensions are shown in Fig 4-11. The absorber footprint is 61 cm by 61 cm. The pyramid height of the absorbers is 45.7 cm. The overall absorber height is 61 cm. The pyramid base dimension is 20.3 cm by 20.3 cm. There are 9 pyramids per absorber. The absorber weight is 4.6 kg.

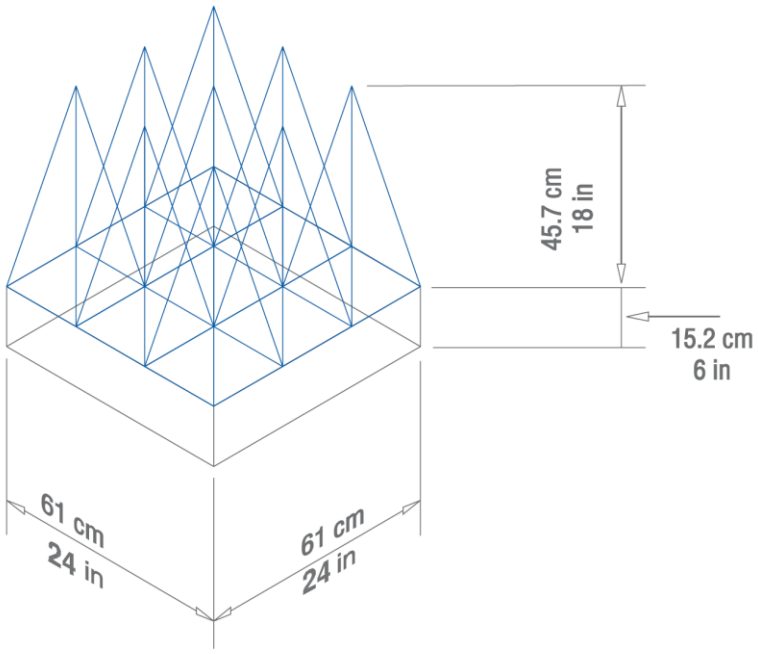

Figure 4 - 11 Dimensions of EMC-24PCL microwave absorbers by ETS-Lindgren L.P. [61].

To terminate the current, four SXR7-200 smoothwound resistors (200 Ω, 2.3 amps, 1050 watts, 600 V_{AC}, Powerohm Resistors, Inc., Katy, TX, USA),shown in Fig. 4-12, were used. The resistors were connected in parallel and connected between the inner and outer conductors at the rear wall. The resistor dimensions are shown in Fig 4-13. The completed GTEM cell is shown in Fig. 4-14.

Figure 4 - 12 SXR smoothwound resistor by Powerohm Resistors, Inc [62].

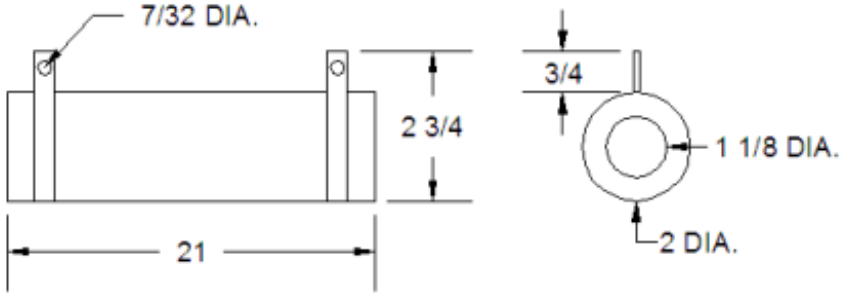

Figure 4 - 13 Dimensions (in inches) of SXR smoothwound resistor by Powerohm Resistors, Inc [54].

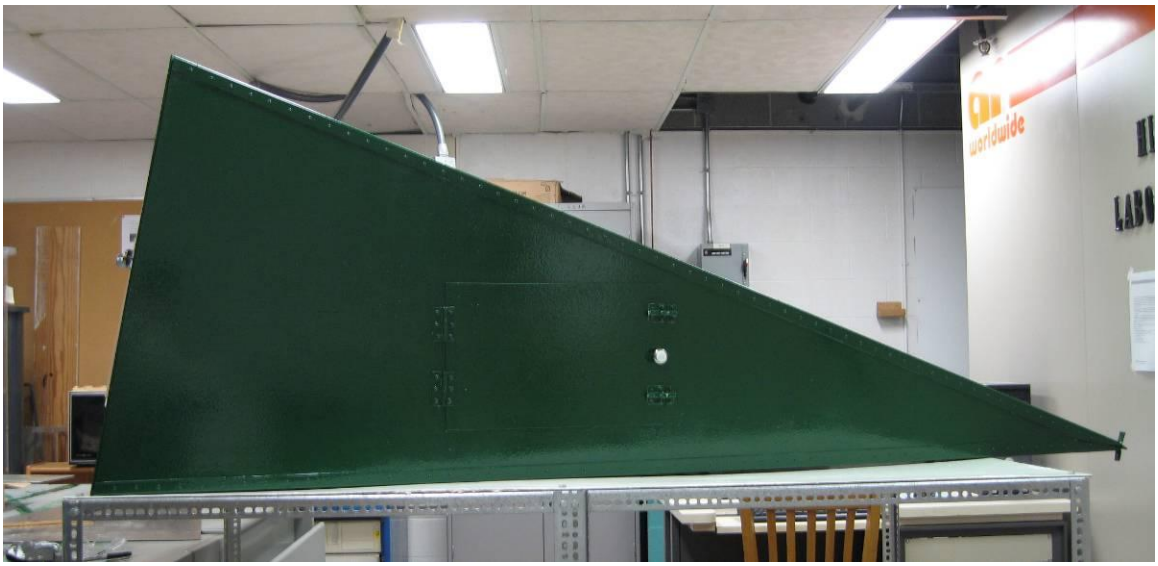

Figure 4 - 14 The completed GTEM cell.

4.2.2 GTEM Calibration Procedures

In this dissertation, I performed two experiments. The first experiment was checking the return loss and VSWR measurements of the GTEM cell to make sure that my constructed GTEM cell worked appropriately and as designed. To do this, a HP 8719A network analyzer (Agilent Technologies, Inc., Sanata Clara, CA, USA) was needed in the experimental setup. The network analyzer, which has the capability of broadband measurement from 130 MHz to 13.5 GHz, was used to measure VSWR. The VSWR was measured, and then the VSWR results were converted to return loss results by calculation. For the experimental setup, I connected the network analyzer to the end of the GTEM cell, as show in Fig. 4-15.

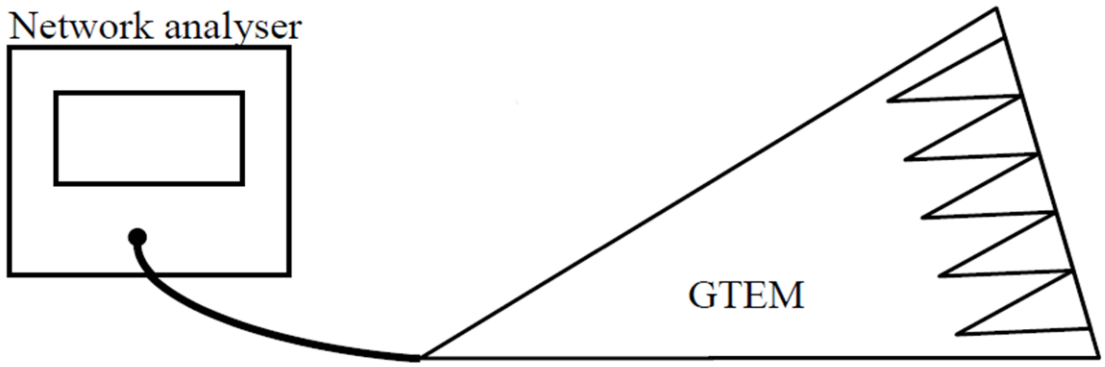

Figure 4 - 15 Experimental setup for return loss and VSWR measurements.

The second experiment was characterizing the electric field of the GTEM cell as well as the testing area. The AR FL7004 electric field probe (100 kHz to 4.2 GHz, 0.5 – 300 V/m, Amplifier Research, Souderton, PA, USA) was used to measure the electric field. I measured the electric field in the testing area between the septum and the floor inside the GTEM cell, as showing in Fig 4-16.

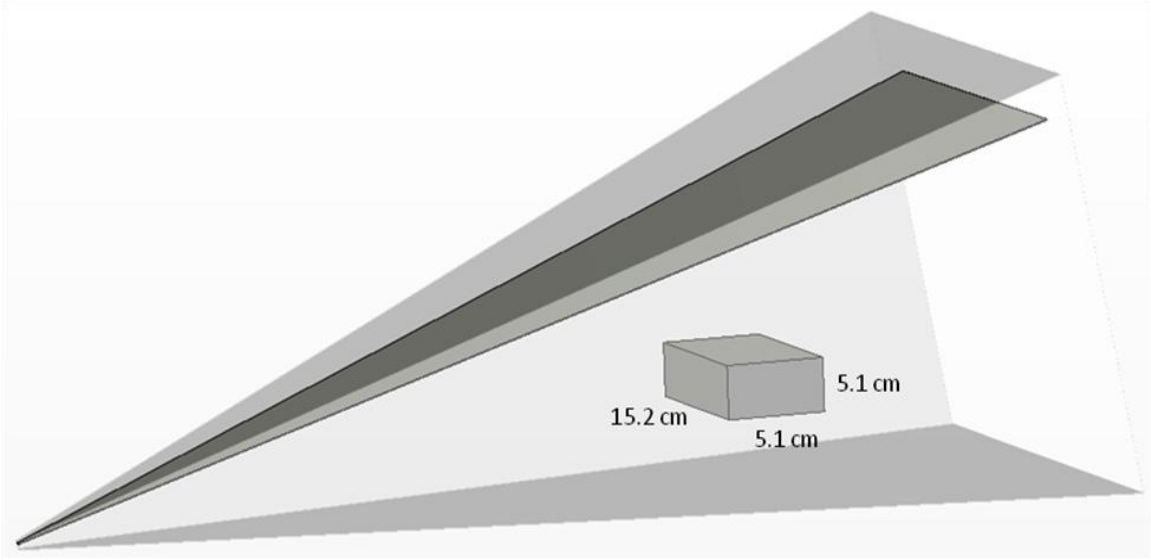

Figure 4 - 16 The dimension and testing position of the object inside the GTEM cell.

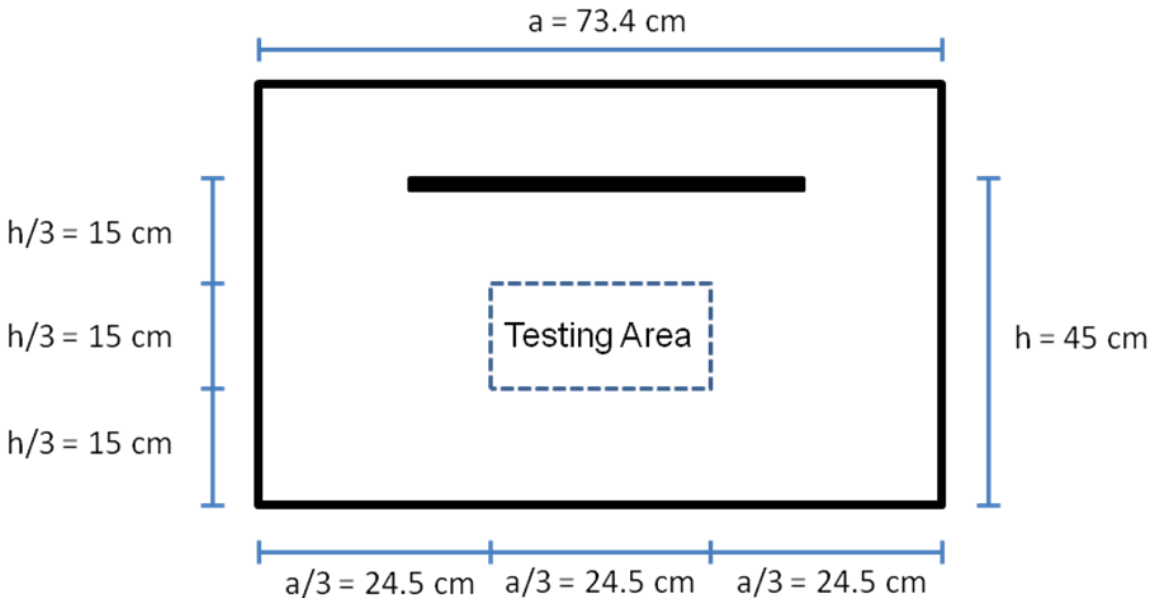

Figure 4 - 17 Cross sectional view of the testing area inside the GTEM cell.

The testing area, which was positioned centrally between the side walls of the GTEM cell, 80 cm from the back wall of the GTEM cell and 21 cm from the floor of the

GTEM cell, was 15.2 cm x 5.1 cm x 5.1 cm. The area under test, which was one-third of the volume between the septum and the bottom floor of the outer conductor, was determined from Fig 4-17. Twenty-seven field observation positions were measured at the corner and the edge on each border side of the testing area, as shown in Fig. 4-18.

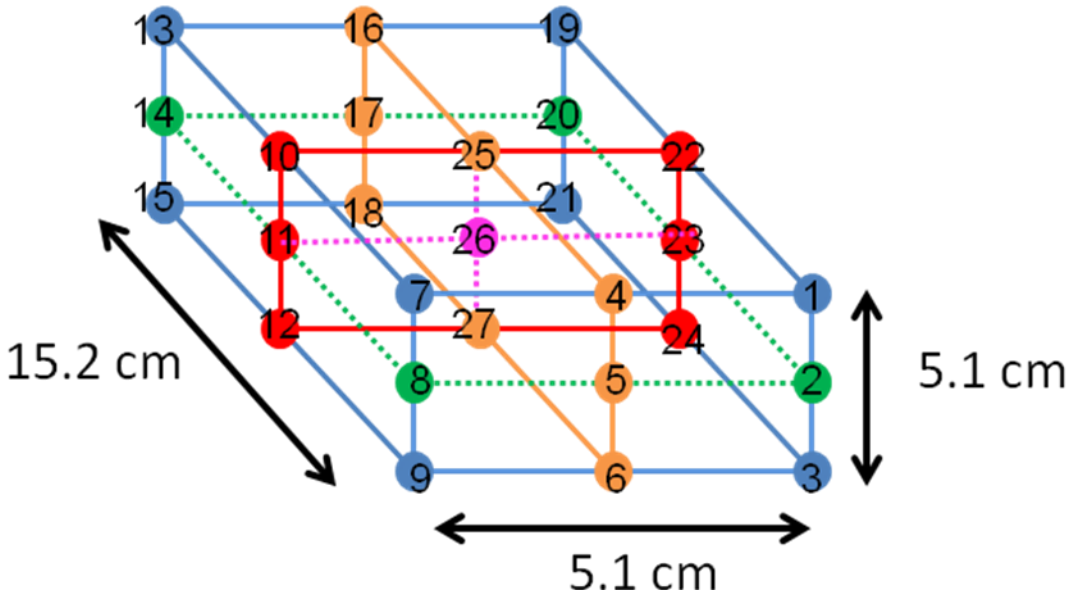

Figure 4 - 18 E-field measurement of 27 point locations in testing area.

4.2.3 Uniform Electromagnetic Field (EMF) Generator

The uniform EMF system in this work is shown in Fig. 4-19. This exposure system consists of an R&S SML01 signal generator (9 kHz to 1.1 GHz, Rohde & Schwarz GmbH & Co. KG, Munich, Germany), AR 150W10000M3 amplifier (150 watts, 80 – 1000 MHz, Amplifier Research, Souderton, PA, USA), dielectric supporter, and the lab designed GTEM cell.

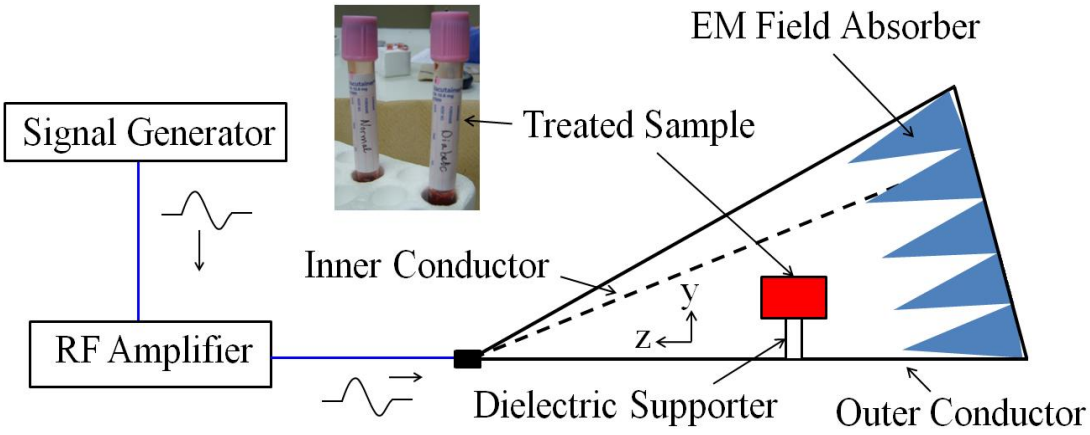

Figure 4 - 19 Configuration of the uniform EMF system, consisting of the signal generator, RF amplifier, dielectric supporter, and GTEM cell.

4.2.3 Blood Preparation

The normal blood (NB) samples, as shown in Fig. 4-20 (left), were drawn from non-diabetic volunteers (healthy). The high glucose concentration (HGB) samples, as shown in Fig. 4-20 (right), were prepared by adding alpha-D-glucose (96%) to the normal blood. All the samples were filled in dielectric blood collection tubes with 0.5 ml of blood. The treated samples were exposed to electromagnetic radiation in the testing area inside the GTEM cell, while the untreated samples, called controls, were placed in room conditions.

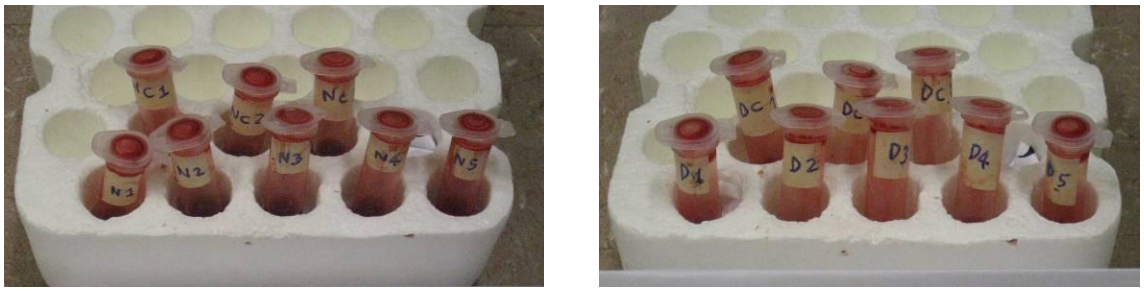

Figure 4 - 20 Blood samples: normal blood (left) and high glucose concentration (right).

The glucose levels for the treated samples and controls were monitored through an ACCU-CHEK Advantage blood glucose meter (Roche Diagnostics, Indianapolis, IN, USA), as shown in Fig. 4-21.

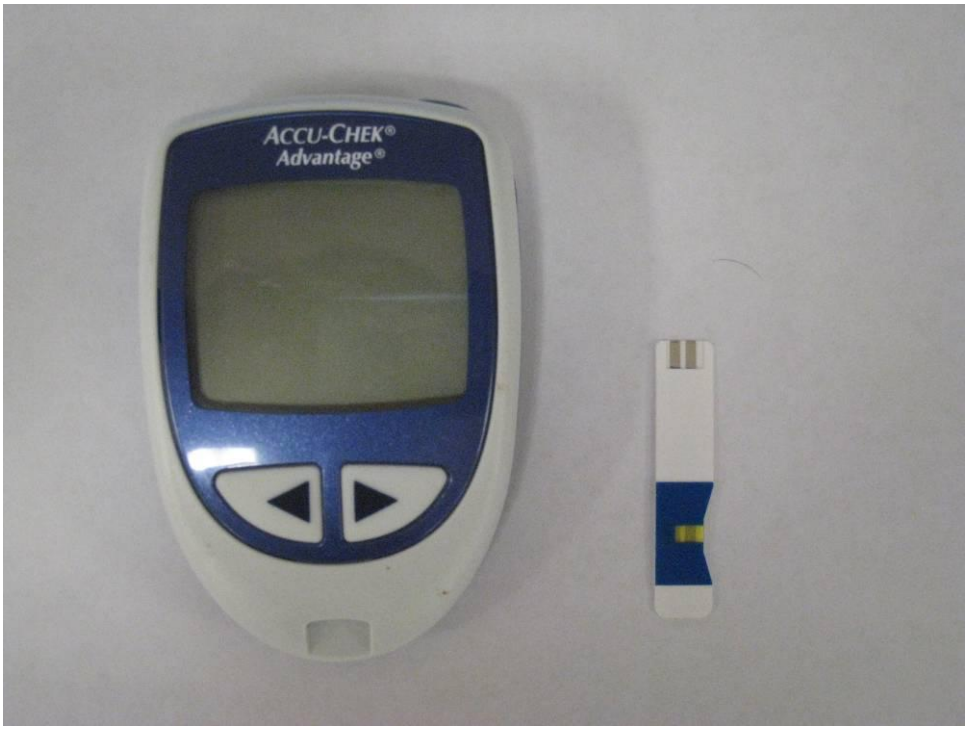

Figure 4 - 21 ACCU-CHEK Advantage blood glucose meter and strip.

4.2.4 Experimental Procedures of 850 MHz Exposure

The measured electric field was carried out by AR FL7004 electric field probe (100 kHz to 4.2 GHz, 0.5 – 300 V/m, Amplifier Research, Souderton, PA, USA). The measured E-fields were 18.68 and 58.91 V/m at the operating power of 2 and 60 W, respectively.

96 samples of NB and HGB were prepared for 6 tests. The NB and HGB samples were placed on the dielectric supporter in the usable area inside the GTEM cell for 10,

30, and 60 minutes. The treated samples were subjected to EM radiation at 850 MHz frequency for two power levels (2 and 60 watts). The glucose levels of the treated samples were measured and compared with the controls before and after treatment. The RBC and WBC of the treated samples were counted immediately after treatment and compared with controls.

4.2.5 Experimental Procedures of 900 MHz Exposure

The electric field measurement was again carried out through an AR FL7004 electric field probe (100 kHz to 4.2 GHz, 0.5 – 300 V/m, Amplifier Research, Souderton, PA, USA). At the operating power of 2 W, the E-field was 26.34 V/m, and at the operating power of 60 W, the E-field was 73.43 V/m.

The exposure procedure was the same as for the 850 MHz exposure. There were 6 tests, and 96 samples of NB and HGB were used. The NB and HGB samples were exposed to the electromagnetic radiation for 10, 30, and 60 minutes in the testing area inside the GTEM cell. Exposure levels of 2 and 60 watts at 900 MHz were generated. The glucose levels of the NB and HGB samples were monitored and compared with the controls before and after treatment. The RBC and WBC of the treated samples and control were counted and compared immediately after treatment.

Chapter 5: Simulation and Experimental Results

In this chapter, the simulated and experimental results related to this work are presented. Section 5.1 discusses the results of the GTEM cell characterization, including return loss, VSWR, electric field, the design parameter optimization, and the exposure dosimetry in the usable area inside the cell. In section 5.2, the experimental results are presented, including the GTEM cell characterization measurements and the sugar-laden blood's changes in glucose levels, cell viability, and other responses after 850 and 900 MHz electromagnetic exposure.

5.1 Simulation Results

5.1.1 GTEM Cell Characterization

As mentioned in chapter 4, all simulations in this study were carried out using the CST Microwave Studio 2011 software [1]. Fig. 5-1 shows the time domain reflectometer (TDR) results. The TDR results represent the characteristic impedance of the GTEM cell. The characteristic impedance of the GTEM cell is about 52.625 Ω, which is within the acceptable limits and are close to the theoretical characteristic impedance of the GTEM cell (50 Ω). The results also show that there are no reflections at any transmission section of the GTEM cell.

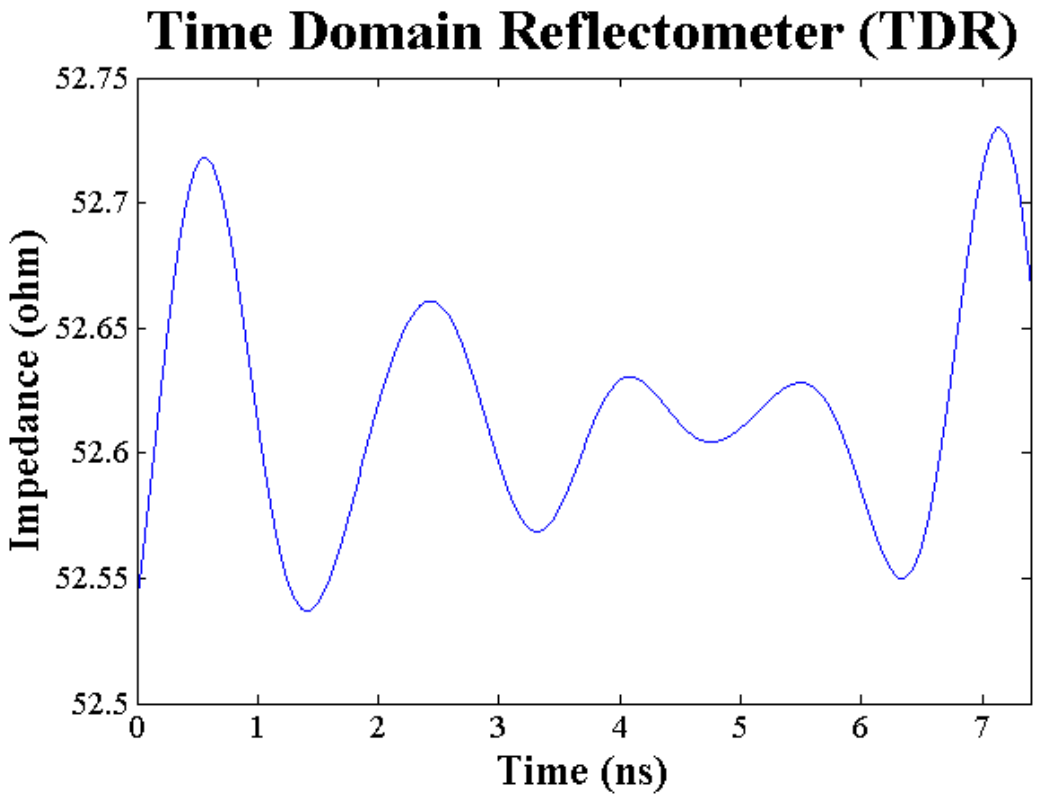

Figure 5 - 1 TDR results represented the characteristic impedance of the GTEM cell.

To ensure that the GTEM cell could provide a uniform electromagnetic field, the return loss and voltage standing wave ratio (VSWR) were analyzed.

The simulated return loss and the VSWR values cell from 0 to 4.0 GHz for the GTEM are shown in Fig. 5-2 and Fig. 5-3, respectively. Due to the wideband matching of the GTEM cell, the return loss, as shown in Fig. 5-2, is better than 10 dB. In addition, the VSWR, is lower than 2, as is shown in Fig. 5-3. These results thus ensure that there is no field non-uniformity or undesirable effects from the resonances inside the cavity, thus providing the perfect conditions for EM field exposures of experimental subjects.

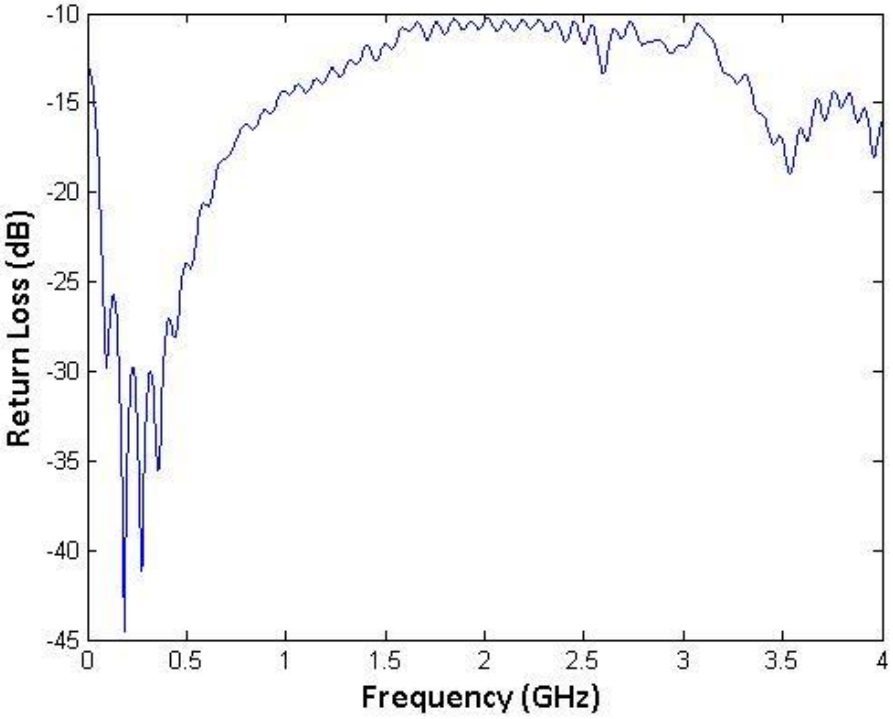

Figure 5 - 2 Simulated result of return loss.

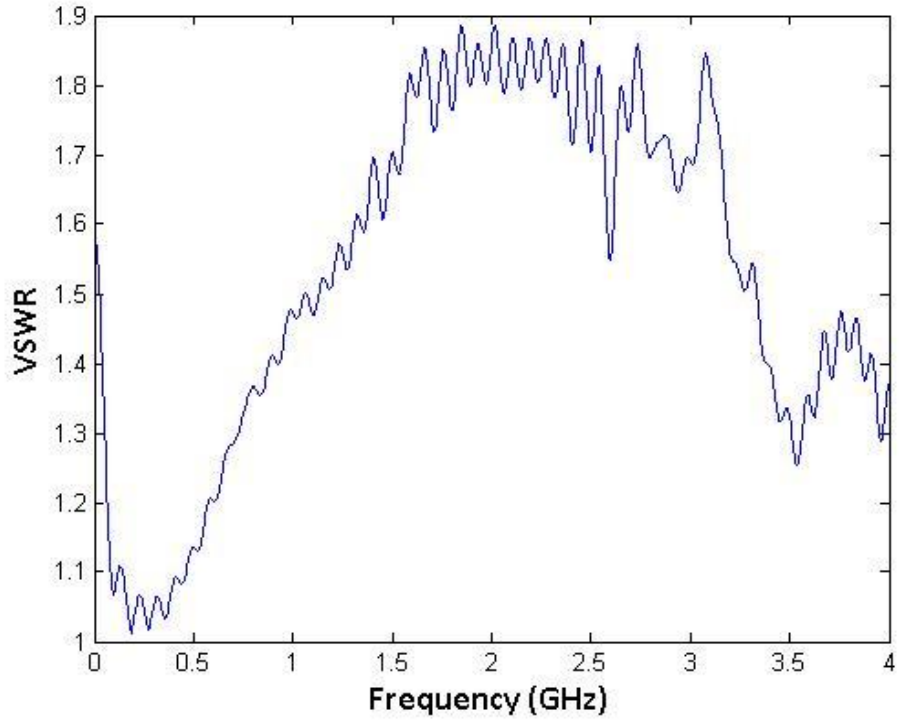

Figure 5 - 3 Simulated result of voltage standing wave ratio (VSWR).

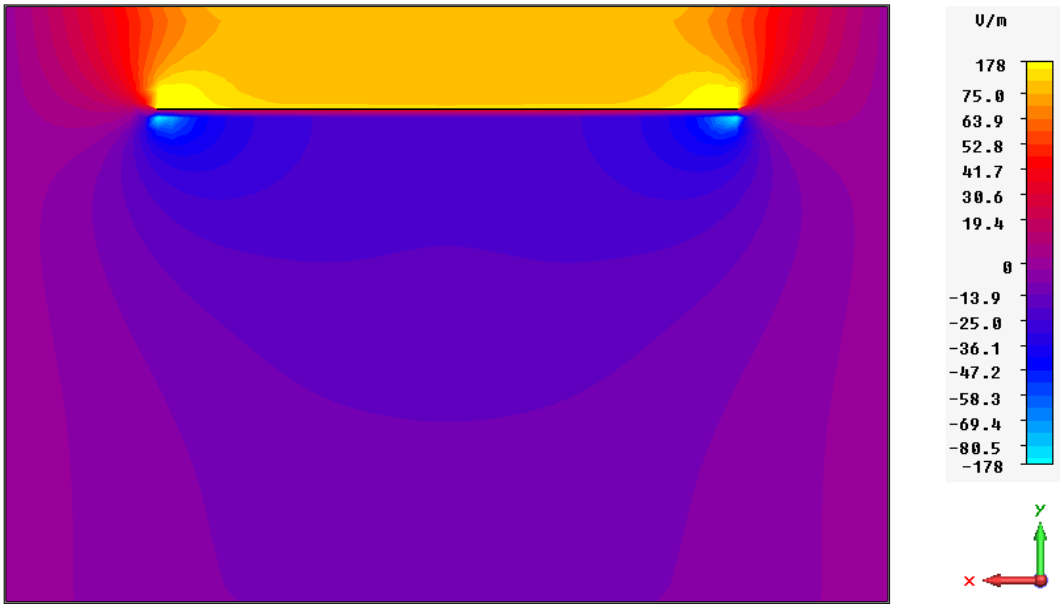

Figure 5 - 4 Simulation of E-field distribution at 100 MHz, position at 90 cm from terminated wall.

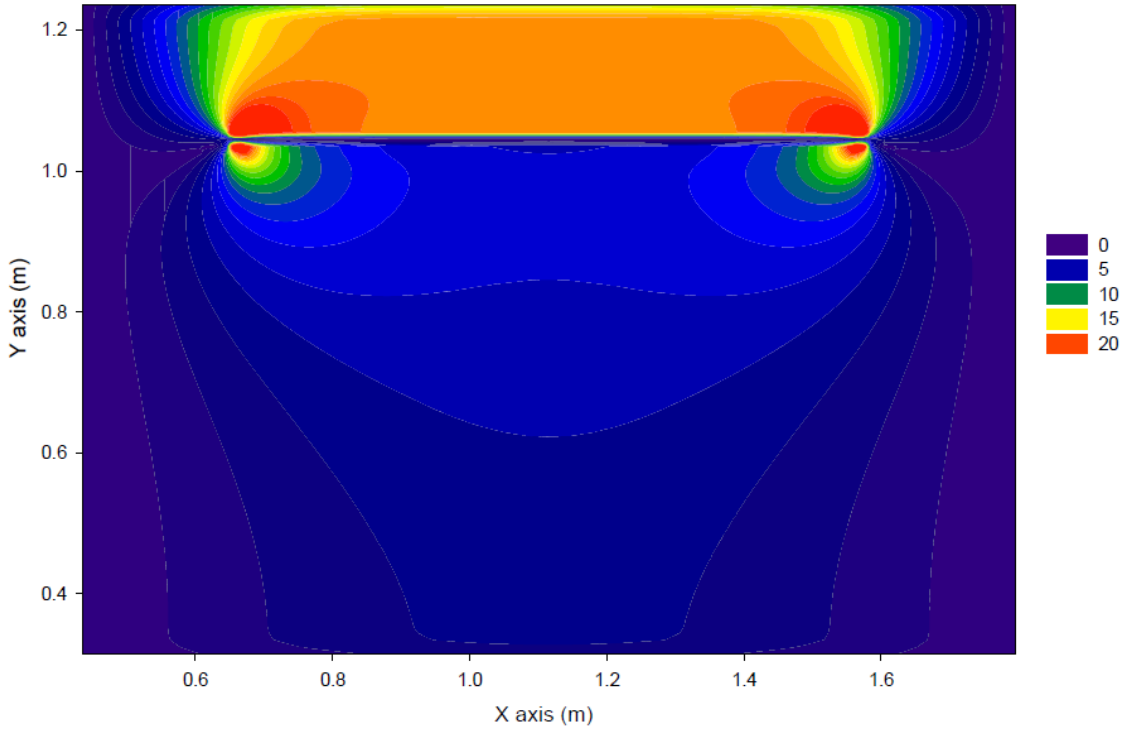

Figure 5 - 5 Theoretical E-field distribution at 100MHz by X. T. I. Ngu [63].

Fig. 5-4 shows a cross sectional view of the simulated electric field contour at 100 MHz inside the GTEM cell. The contour shows a uniform electric field, which covers one-third of the GTEM cell's volume. This is in agreement with K. Malaric, A. Sarolic, V. Roje, J. Bartolic, and B. Modlic's paper [36] and with X. T. I. Ngu's results, as shown in Fig. 5-5 [63].

Figs. 5-1 to 5-4 suggest that the design of the GTEM cell is correct and in agreement with the desired results, which categorically states that the VSWR should be less than 2 and the areas under test, or the uniformity areas, should be one-third of the GTEM cell volume.

5.1.2 Improvement of Testing Area and Field Uniformity

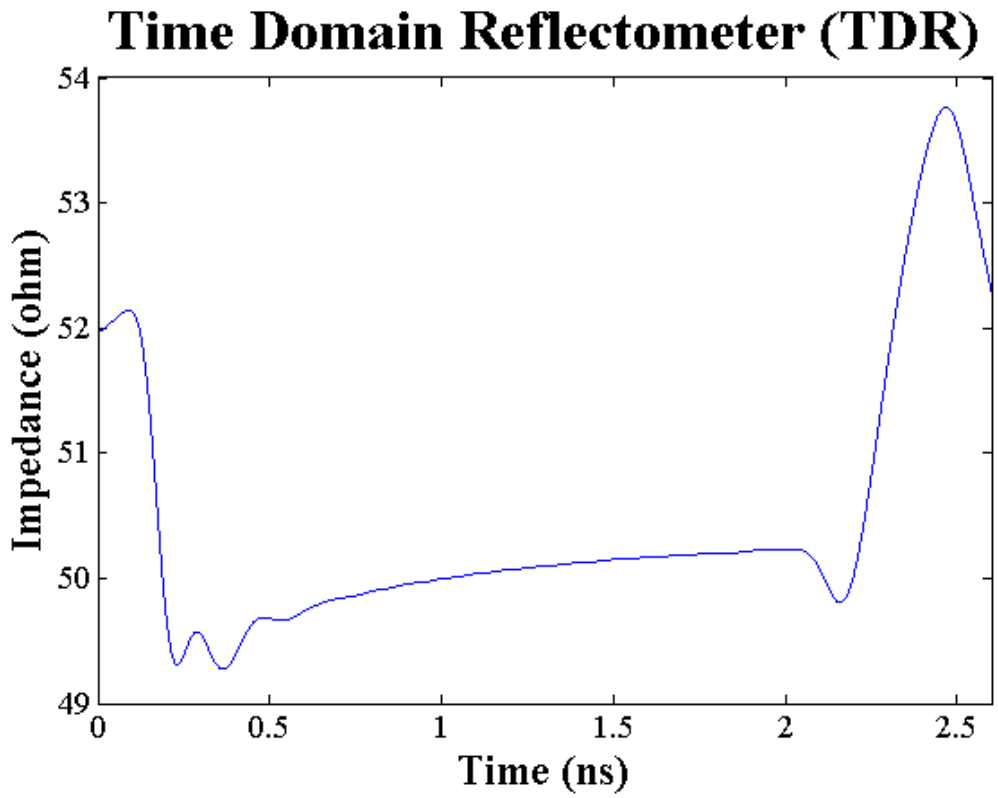

Figure 5 - 6 TDR result representing the characteristic impedance of the developed GTEM cell.

As mentioned in the previous chapter, the GTEM cell was developed in an attempt to further improve the testing area and the uniformity of the field distribution in a GTEM cell and was designed with the parameters shown in Fig. 4-6. The dimension parameters of the developed GTEM cell are more than twice as small as the original GTEM cell. In this experiment, the developed GTEM cell's established frequency range was from 0 to 12.5 GHz. The cell impedance, as shown in Fig. 5-6, is about 50.48 ohms, which is acceptable and close to the theoretical characteristic impedance of a GTEM cell (50 Ω).

Again, to ensure that the improved GTEM cell could provide the uniform electromagnetic field, the return loss and voltage standing wave ratio (VSWR) were analyzed.

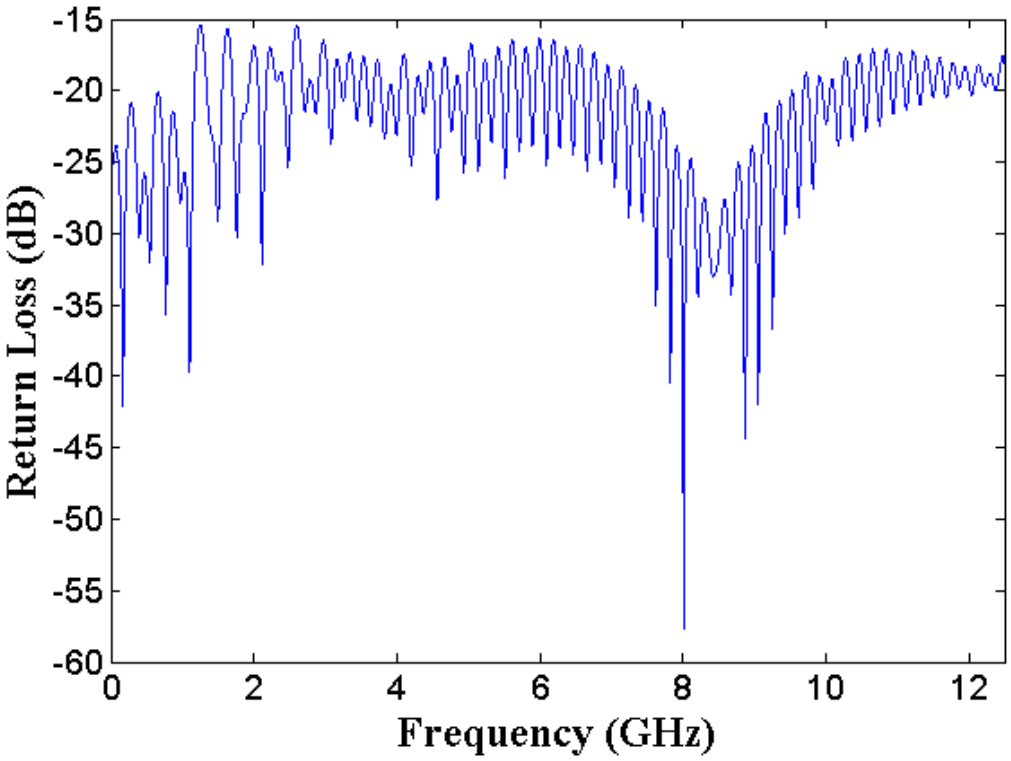

Figure 5 - 7 Simulated return loss result of the developed GTEM cell.

The simulated return loss and VSWR results of the developed GTEM cell from 0 to 12.5 GHz are shown in Fig. 5-7 and Fig. 5-8, respectively. Due to the wideband matching of the GTEM cell, the return loss, as shown in Fig. 5-7, is better than 15 dB, which is better than the return loss of the original GTEM cell. The VSWR of the developed GTEM cell, as shown in Fig. 5-8, is lower than 1.45, which is also better than that of the original GTEM cell. Both these results indicate that the developed GTEM cell improves the field uniformity as compared to the original GTEM cell. In addition, the results ensure that there are no field non-uniformity or undesirable effects from the resonance inside the cavity, providing the perfect conditions for EM field exposure experiments.

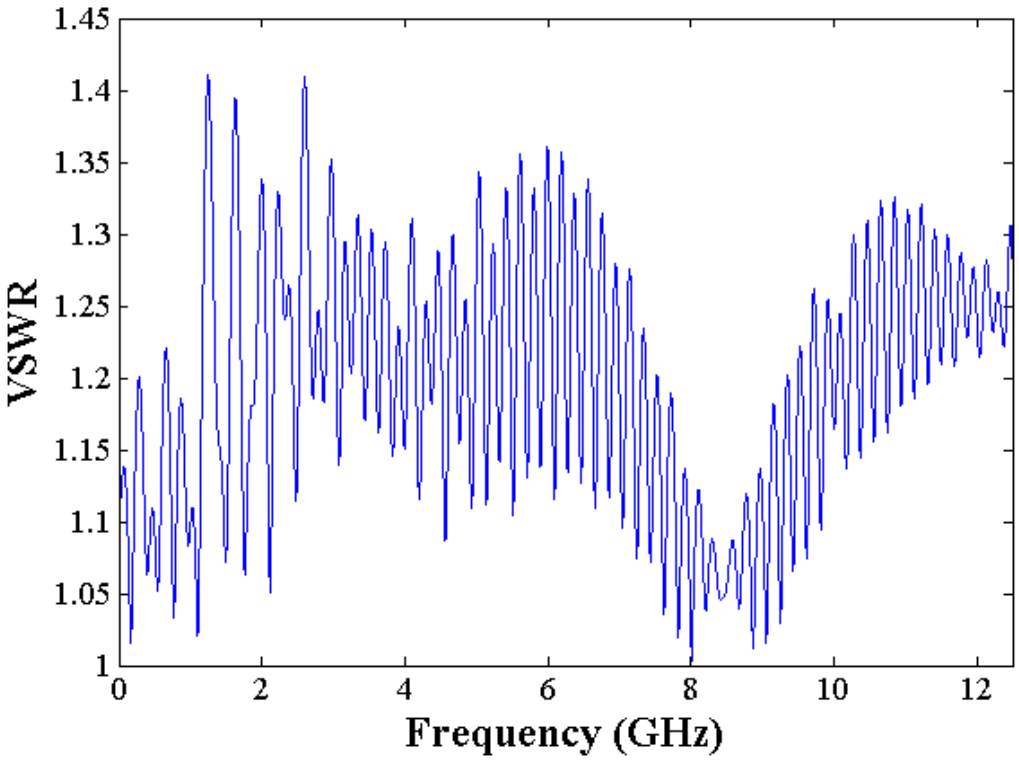

Figure 5 - 8 Simulated voltage standing wave ratio (VSWR) results of the developed GTEM cell.

Fig. 5-9 shows a cross sectional of the electric field contour inside the developed GTEM cell, simulated at 100 MHz. The contour shows the uniform electric field, which is one-third of the GTEM cell's volume both above and below the septum. This is good agreement with the theoretical electric field strength inside the TEM cell in Fig. 5-10, presented in *A Handbook for EMC Testing and Measurement* by David Morgan [17].

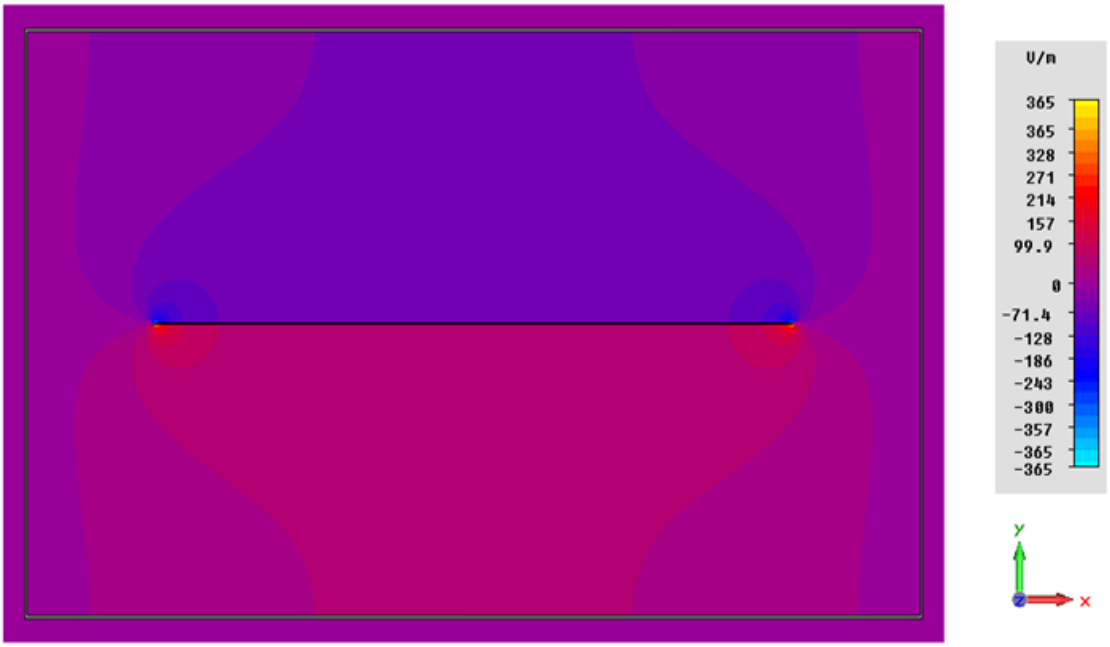

Figure 5 - 9 Simulated E-field distribution of the developed GTEM cell at 100 MHz. Position at 30 cm from termination.

The ideal field strength for a particular experiment may lie at different heights above and below the septum. While different levels in the GTEM cell show different field strength results, field strengths at the same levels on either side of the septum have the same values. In addition, because of this symmetrical design, identical positions on the side walls (left and right) have identical electric field strengths. In Figure 5-10, level 1 which is the furthest from the septum, has the least strength electric field. Level 2 is the

middle level between level 1 and 3. Level 3 is the nearest to the septum, so its electric field has the highest strength. Therefore, in Figure 5-10, the higher the level, the stronger the electric field [20].

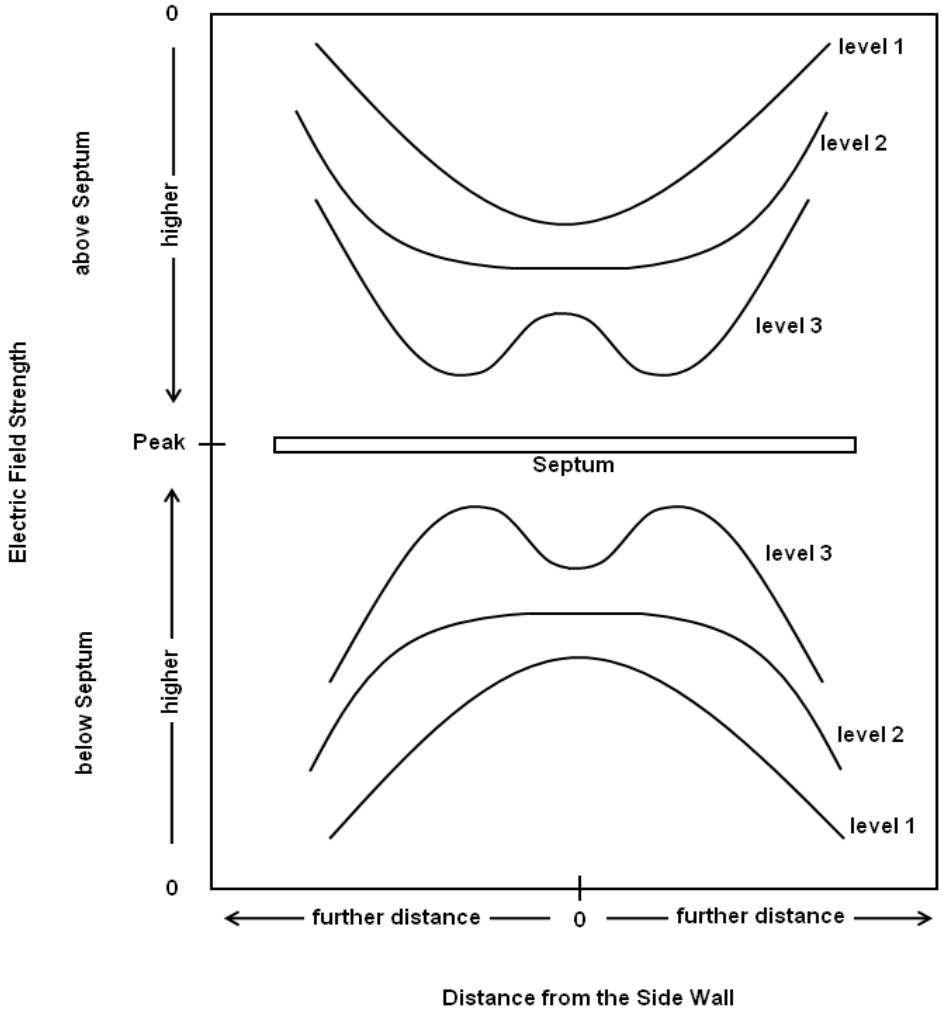

Figure 5 - 10 Ideal field strength plots with various heights above and below the septum [20].

Fig. 5-11 shows the testing area, which has increased twice in size thus allowing for more samples during biological experiments. As previously mentioned, the electromagnetic fields inside the developed GTEM cell are symmetric systems (top-

bottom and left-right). Therefore, the developed GTEM cell has two testing areas: the testing area above the septum, which is one-third of the volume between the septum and the top ceiling, and the testing area under the septum, which is one-third of the volume between the septum and the bottom floor.

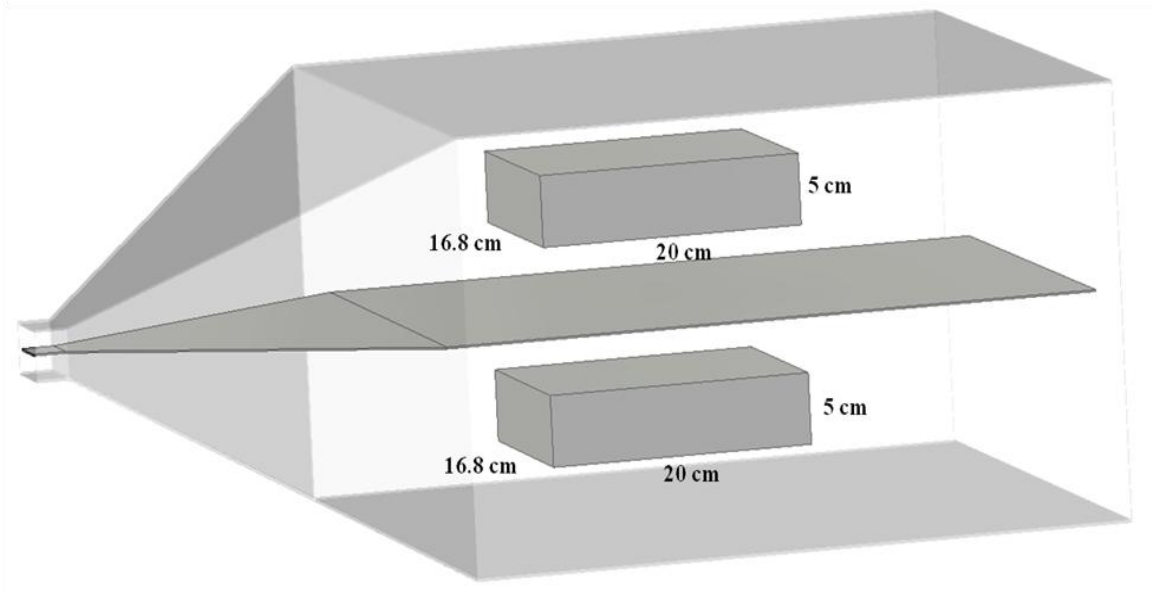

Figure 5 - 11 Objects under test dimensions and positions inside the developed GTEM cell.

For the testing area above the septum, the testing position is at the center, between the side and back wall of the developed GTEM cell: 20 cm from the back wall, 5 cm from the septum, and 5 cm from the ceiling. The dimensions of the testing area was found to be 16.8 cm x 20 cm x 5 cm.

For the testing area under the septum, the testing position is at the center, between the center and back wall of the developed GTEM cell: 20 cm from the back wall, 5 cm from the septum, and 5 cm from the floor. The dimensions of the testing area are 16.8 cm x 20 cm x 5 cm.

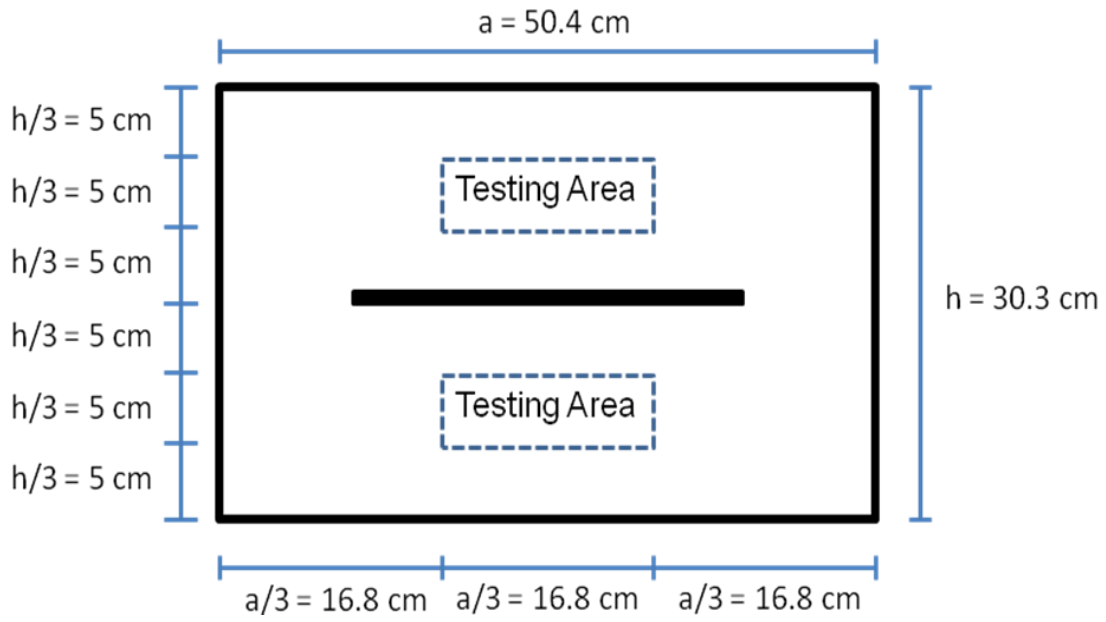

Figure 5 - 12 Cross sectional view of the testing areas inside the developed GTEM cell.

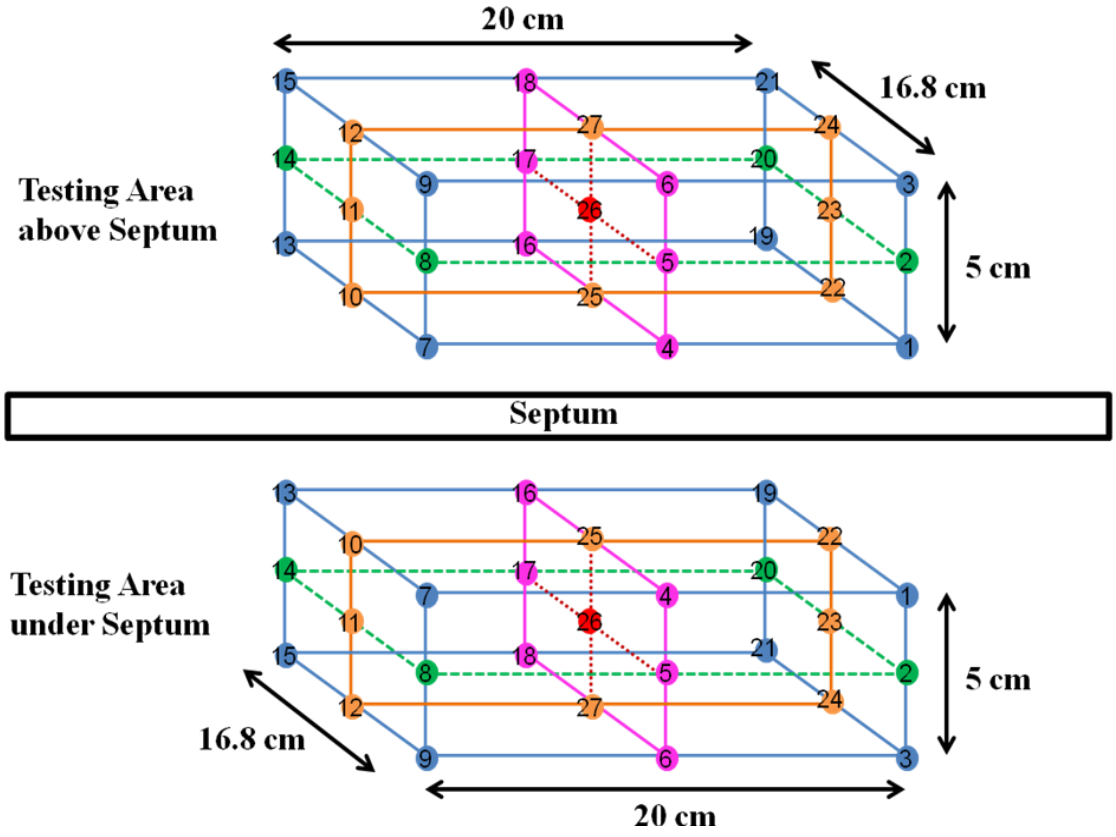

Figure 5 - 13 Cross sectional view of testing area inside the developed GTEM cell.

The testing areas in Fig. 5-11 can be determined from Fig 5-12 based on the fact that the testing areas are one- third of the volume between the septum and the upper and lower outer walls.

In these testing areas, 54 field observation positions above and below the septum (27 positions each) were measured at the corners and edges of all sides of the testing area, as shown in Fig. 5-13.

The simulated results of the twenty-seven field observation positions above and below the septum are also shown in Table 1. The electric field strength in the testing region above the septum of the developed GTEM cell was between 52.17744 V/m and 45.58318 V/m. The highest E-field strength above the septum was at point 1, while the lowest E-field strength above the septum was at point 6. The electric fields in the testing area were ±1.173563 dB difference, which is less than ±3 dB difference. This indicates that the electromagnetic fields in the testing area are uniform.

The electric fields in the testing region below the septum of the developed GTEM cell were between 52.17749 V/m and 45.58362 V/m. The highest E-field strength under the septum was also at point 1, while the lowest E-field strength under the septum was at point 6. The electric fields in the testing area were ±1.173487 dB difference, which is also less than ±3 dB difference. This suggests that the electromagnetic fields in the testing area under the septum are uniform as well.

TABLE 1

ELECTRIC FIELD RESULTS OF 27 POINTS AROUND SAMPLES ABOVE AND UNDER THE SEPTUM OF THE DEVELOPED GTEM CELL

Point	E-field (V/m)	
	Testing Area above Septum	Testing Area under Septum
1	52.17744	52.17749
2	49.23538	49.2354
3	46.78919	46.78936
4	50.65564	50.65611
5	47.89361	47.8935
6	45.58318	45.58362
7	51.35237	51.35307
8	50.36648	50.36612
9	47.44074	47.4412
10	47.63217	47.59184
11	47.11387	47.11211
12	47.95205	47.95254
13	51.33788	51.3525
14	50.36445	50.36471
15	47.44087	47.4405
16	50.65353	50.64051
17	47.8932	47.89275
18	45.59325	45.59358
19	52.17299	52.16812
20	49.23524	49.23469
21	46.79324	46.79267
22	50.73412	50.75595
23	50.33578	50.33597
24	48.77878	48.77861
25	49.61951	49.62416
26	49.50365	49.50299
27	49.74162	49.74061

For both results, the highest E-field of both testing areas was at point 1, and the lowest E-field of both testing areas was at point 6. This is because the electromagnetic fields inside the developed GTEM cell are symmetric systems. In addition, the electric field difference between both testing areas was ±1.173571 dB, which is also less than ±3 dB difference. This means that the electromagnetic fields in both testing areas are uniform and there is no resonance inside the developed GTEM cell. Therefore, the biological samples used for biological experiments can be placed in any of the two testing areas.

Table 1 and Figs. 5-6 to 5-9 suggest that the design of the GTEM cell is correct and agrees with standard theory, which mentions that the VSWR should be less than 2 and the areas under test, or the uniformity areas, should be one-third of the GTEM cell volume. In fact, the developed GTEM cell, which has a smaller size than the original GTEM cell, provides a larger testing area and better electromagnetic field uniformity.

5.1.3 Exposure Dosimetry

In order to ascertain whether the treated blood samples absorbed the electromagnetic energy, the specific absorption rate (SAR) level at 850 and 900 MHz was simulated using CST Microwave Studio 2011 software [1]. A dielectric tube (thickness = 0.1 cm, height = 4 cm, $\varepsilon_{r\ polystyrene} = 2.55$) filled with 0.5 ml of blood (height = 0.8 cm, $\varepsilon_{r\ nucleoplasm} = 120$, $\sigma_{nucleoplasm} = 0.31$ S/m, blood density = 1049 kg/m^3) [39]-[40] was designed and placed in the testing area inside the GTEM cell. The SAR uniformity at 850 MHz is shown in Fig. 5-14. The average SAR levels were 0.109 W/kg at 2 W and 1.308 W/kg at 60 W. The highest SAR levels were found on the top layer of the tested blood because the top layer was nearest to the inner conductor (the source of the

electromagnetic radiation). With the power level increased to 60 W (maintaining the field frequency at 850 MHz), the same SAR uniformity was obtained due to the uniformity of the electromagnetic field inside the GTEM cell. The SAR results would ensure that observations made later in the cell counts and glucose level in blood following electromagnetic radiation at 850 MHz are due to absorption of electromagnetic energy.

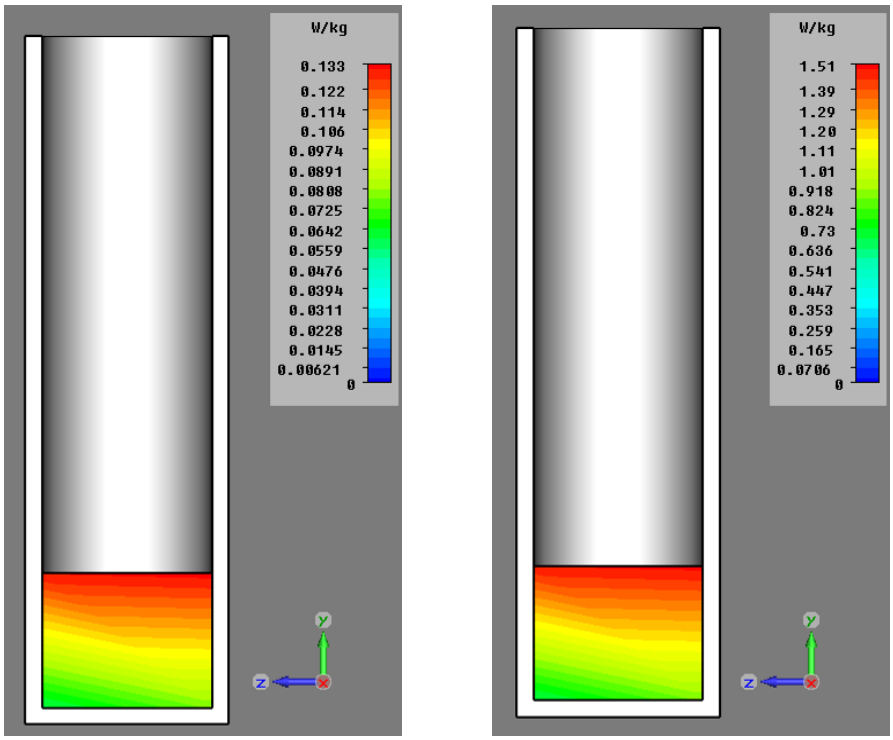

(a) at 2 W (b) at 60 W

Figure 5 - 14 Cross sectional view of simulated SAR uniformity at 850 MHz.

In addition, the SAR level at 900 MHz, as shown in Fig. 5-15, was analyzed in order to ensure that the treated samples were absorbing the electromagnetic energy as well. The average SAR levels were 0.142W/kg at 2 W and 1.260 W/kg at 60 W. The highest and lowest SAR levels were between points 1 and 2, respectively. Again, as seen in Fig, 5-15, the highest SAR value was also on the top layer of the tested blood due to

the top layer's position near the radiation source or septum. With the power level increased to 60 W (maintaining the field frequency at 900MHz), the same SAR uniformity was obtained due to the uniformity of the electromagnetic field inside the GTEM cell. The results suggest that the treated blood samples also absorbed the electromagnetic energy at 900 MHz.

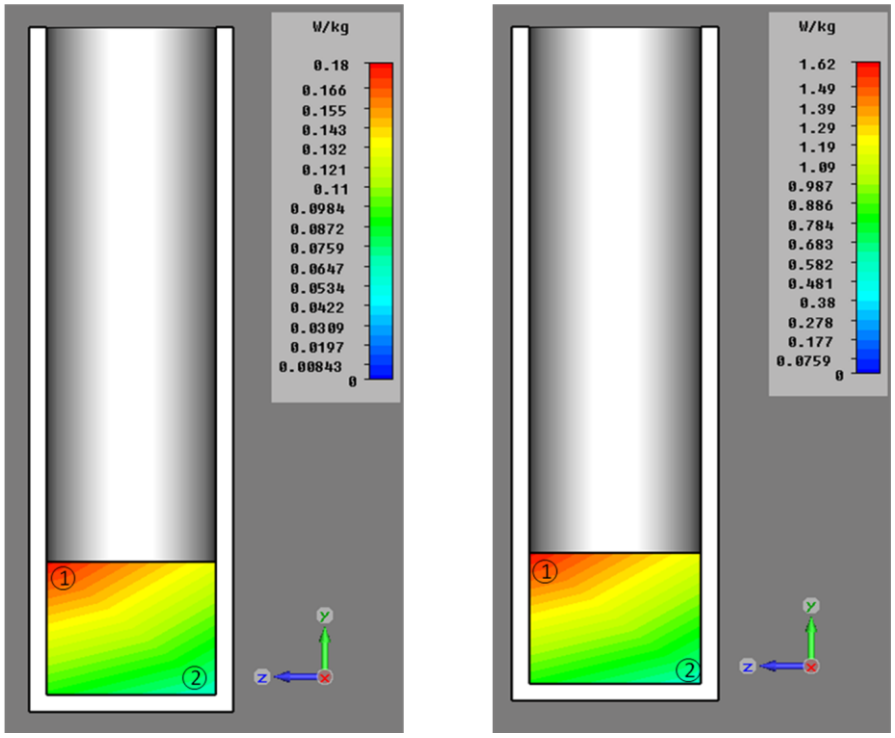

(a) at 2 W (b) at 60 W

Figure 5 - 15 Cross sectional view of simulated SAR uniformity at 900 MHz.

5.2 Experimental Results

5.2.1 GTEM Cell Characterization

To characterize the GTEM cell, the return loss and voltage standing wave ratio (VSWR) were monitored through an HP 8719A network analyzer (Agilent Technologies,

Inc., Sanata Clara, CA, USA). The return loss and VSWR was measured from 0-6 GHz. The return loss, as shown in Fig. 5-14, was better than 10 dB in the 0-6 GHz range. The VSWR in Fig. 5-15 is less than 2 in the same wideband range. These results ensure that the GTEM cell can provide a uniform electric field and that there is no resonance inside the GTEM cell, ensuring good conditions for biological exposure experiments in this study.

The measured return loss and VSWR showed good agreement with the simulated results. As seen from Fig. 5-16 and 5-17, the usable frequency of the constructed GTEM cell is up to 6 GHz, which is better than that of the simulated design (up to 4 GHz). This means the constructed GTEM cell provides 2 GHz higher frequency usage than the simulated design.

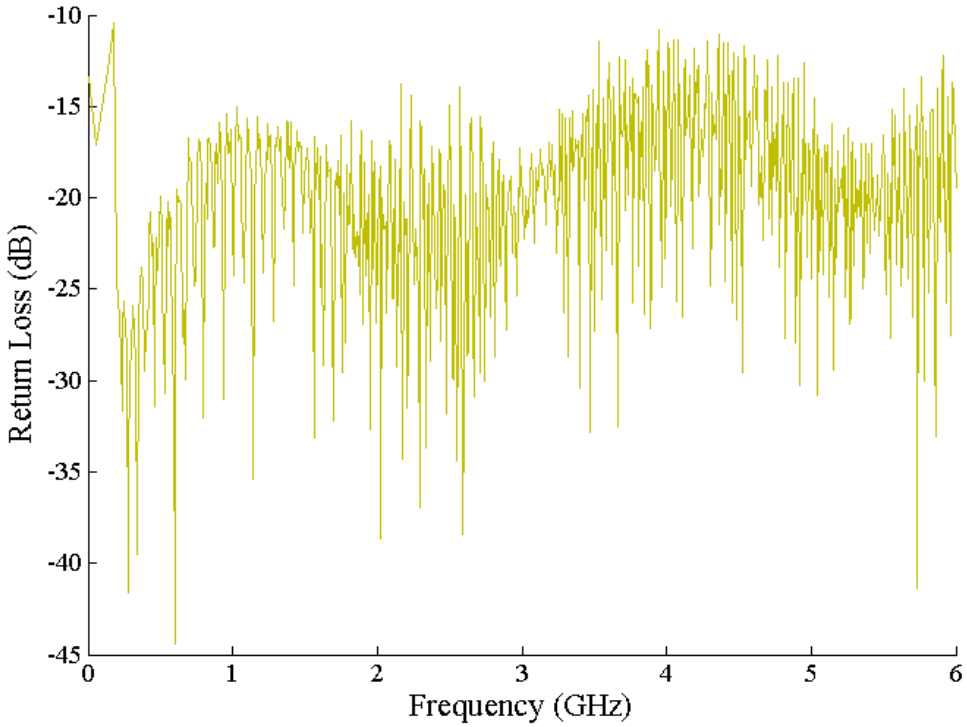

Figure 5 - 16 Result of the return loss measurement.

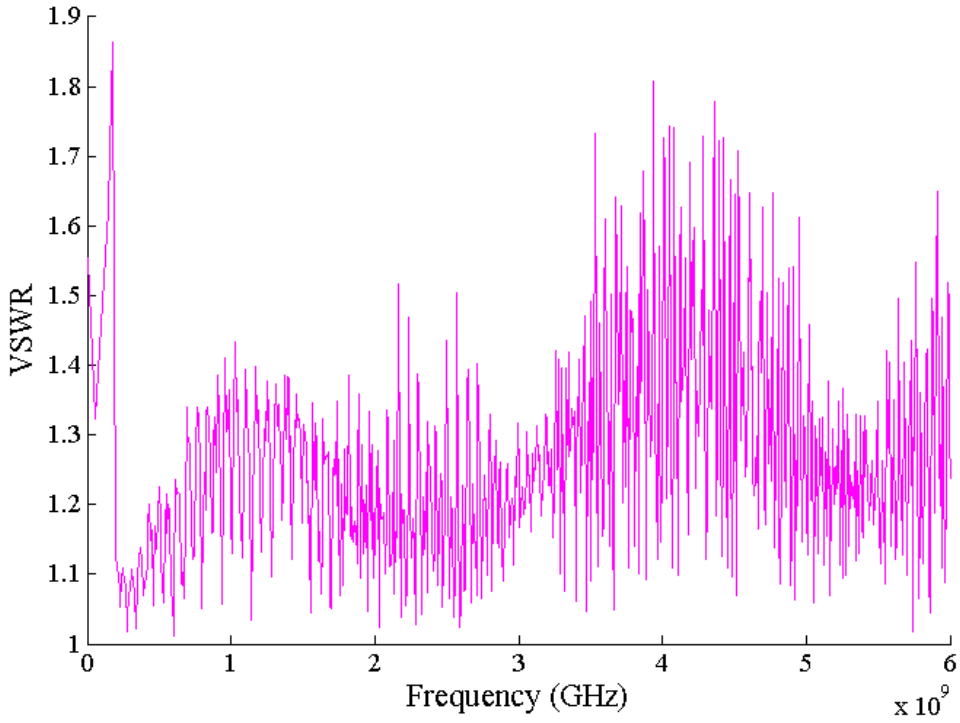

Figure 5 - 17 Result of the VSWR measurement.

As previously mentioned in section 4.2.2, the electric field was also measured with an AR FL7004 electric field probe (100 kHz to 4.2 GHz, 0.5 – 300 V/m, Amplifier Research, Souderton, PA, USA) to ensure that the E-field in the testing area was uniform. Twenty-seven E-field observation positions in the testing area inside the GTEM cell between the septum and the floor, as showing in Fig 4-18, were investigated at an operating power of 2 W and at 850 MHz.

The results of the electric field measurements of the GTEM cell are shown in Table 2. The electric field was between 18.13 and 23.67 V/m. The lowest E-field, 18.13 V/m, was at testing point 22, while the highest E-field, 23.67 V/m, was at testing point 4. The E-field difference between the lowest and highest values in the test region was ±2.3 dB, which is less than ±3 dB difference. Therefore, the results confirm the uniformity of

the electric field in the testing area, and the GTEM cell can be used for studies on biological exposure to electromagnetic radiation.

TABLE 2

ELECTRIC FIELD RESULTS OF 27 POINTS AROUND SAMPLES AT 2 OPERATING POWERS AND AT 850 MHZ

Point	E-field (V/m)	Point	E-field (V/m)	Point	E-field (V/m)
1	21.18	11	18.43	21	19.81
2	23.51	12	18.77	22	18.13 *(lowest)*
3	23.62	13	23.62	23	23.15
4	23.67 *(highest)*	14	18.58	24	21.88
5	21.85	15	19.68	25	18.62
6	18.23	16	20.44	26	19.64
7	23.05	17	19.63	27	19.17
8	19.53	18	18.29	**Note**: E-fields between 18.13 – 23.67 V/m, which is ±2.3dB difference.	
9	19.54	19	23.22		
10	18.98	20	23.65		

5.2.2 Blood Response to 850 MHz Exposure

Three blood samples, including normal blood (NB), high glucose blood (HGB), and control blood (CB), were investigated. The red blood cell (RBC) and white blood cell (WBC) counts were monitored immediately after exposure to electromagnetic radiation. The glucose levels in these samples were also measured immediately before and after treatment. The pre and post treated cell survivability and glucose levels for the samples are shown in Tables 3 to 4.

TABLE 3

GLUCOSE AND BLOOD CELL LEVELS FOR NORMAL SAMPLES EXPOSED TO 850 MHZ ELECTROMAGNETIC FIELDS AT 2 AND 60 W

Source	Samples	Glucose Level (mg/dL)						Viability (cell/mL)	
		Before Treatment			After Treatment				
		1st time	2nd time	3rd time	1st time	2nd time	3rd time	RBC	WBC
2 W, 10 min	1	95	98	97	91	91	94	5.70E+09	4.90E+06
	2	94	95	93	97	95	94	5.60E+09	4.10E+06
	3	94	92	93	95	95	96	5.10E+09	5.00E+06
	4	93	97	96	95	95	96	6.00E+09	4.80E+06
	5	97	96	96	97	96	93	5.50E+09	4.70E+06
	Control 1	91	95	96	97	97	97	5.10E+09	4.80E+06
	Control 2	97	98	94	95	93	93	5.80E+09	5.00E+06
	Control 3	97	96	98	94	93	93	5.60E+09	5.10E+06
2 W, 30 min	1	89	87	88	78	73	77	4.20E+09	4.20E+06
	2	87	90	89	73	76	73	4.30E+09	5.40E+06
	3	85	90	89	75	73	75	4.40E+09	5.40E+06
	4	86	86	88	75	75	74	3.90E+09	5.70E+06
	5	89	85	87	74	73	77	3.80E+09	5.10E+06
	Control 1	85	87	87	72	73	71	4.00E+09	5.10E+06
	Control 2	88	85	86	70	71	72	4.10E+09	5.40E+06
	Control 3	85	86	86	73	73	73	4.10E+09	5.20E+06
2 W, 60 min	1	96	98	101	74	79	79	4.20E+09	5.10E+06
	2	98	95	98	76	78	79	3.90E+09	4.80E+06
	3	97	95	101	75	76	76	3.90E+09	4.80E+06
	4	97	97	99	79	78	77	4.40E+09	5.50E+06
	5	97	95	95	70	71	76	4.40E+09	5.40E+06
	Control 1	94	93	95	81	82	84	3.80E+09	4.60E+06
	Control 2	93	94	94	80	81	82	4.40E+09	4.50E+06
	Control 3	94	93	95	83	83	83	4.40E+09	4.80E+06
60 W, 10 min	1	101	100	103	93	93	95	5.50E+09	5.40E+06
	2	98	99	103	93	93	95	5.50E+09	5.50E+06
	3	99	97	103	93	91	92	5.50E+09	5.30E+06
	4	100	104	104	94	95	93	4.80E+09	5.50E+06
	5	99	102	101	96	90	93	5.00E+09	5.40E+06
	Control 1	101	100	104	93	94	94	4.60E+09	5.20E+06
	Control 2	103	99	98	90	94	93	4.70E+09	5.30E+06
	Control 3	97	97	100	88	85	87	5.50E+09	4.70E+06
60 W, 30 min	1	96	93	97	91	90	93	6.00E+09	5.50E+06
	2	94	94	93	90	92	91	4.20E+09	5.80E+06
	3	95	97	95	90	91	91	4.70E+09	5.60E+06
	4	93	96	97	91	90	90	4.70E+09	5.70E+06
	5	94	93	93	93	93	92	4.20E+09	5.60E+06
	Control 1	94	98	95	83	84	82	4.20E+09	5.00E+06
	Control 2	95	92	96	86	85	84	4.20E+09	5.10E+06
	Control 3	92	92	98	85	82	85	4.60E+09	5.30E+06
60 W, 60 min	1	106	102	106	96	94	96	4.00E+09	4.10E+06
	2	102	107	103	93	95	97	4.10E+09	5.00E+06
	3	100	103	104	95	92	96	3.90E+09	4.80E+06
	4	103	103	104	90	93	95	4.60E+09	5.10E+06
	5	101	100	103	92	95	95	5.00E+09	5.30E+06
	Control 1	103	100	103	92	94	93	4.00E+09	4.80E+06
	Control 2	104	103	102	93	93	95	4.70E+09	4.10E+06
	Control 3	102	108	105	92	91	92	4.40E+09	4.80E+06

TABLE 4

GLUCOSE AND BLOOD CELL LEVELS FOR HIGH GLUCOSE BLOOD SAMPLES EXPOSED TO 850 MHZ ELECTROMAGNETIC FIELDS AT 2 AND 60 W

Source	Samples	Glucose Level (mg/dL)						Viability (cell/mL)	
		Before Treatment			After Treatment				
		1st time	2nd time	3rd time	1st time	2nd time	3rd time	RBC	WBC
2 W, 10 min	1	183	188	182	175	170	172	5.10E+09	4.10E+06
	2	181	182	185	170	172	172	5.30E+09	5.10E+06
	3	188	186	183	166	166	168	5.50E+09	4.80E+06
	4	181	188	186	172	171	171	5.40E+09	4.80E+06
	5	187	183	184	172	172	172	5.10E+09	4.70E+06
	Control 1	183	188	182	170	173	170	5.00E+09	4.80E+06
	Control 2	184	181	181	172	172	170	5.10E+09	4.90E+06
	Control 3	182	181	184	175	177	175	5.80E+09	4.70E+06
2 W, 30 min	1	210	213	214	203	200	201	4.10E+09	5.60E+06
	2	212	213	212	201	205	204	3.60E+09	5.30E+06
	3	209	212	210	201	202	203	4.20E+09	5.10E+06
	4	212	209	210	203	204	204	4.40E+09	4.90E+06
	5	209	213	211	207	204	206	4.00E+09	5.50E+06
	Control 1	209	214	211	206	202	202	4.10E+09	5.00E+06
	Control 2	209	214	213	205	206	207	4.00E+09	5.30E+06
	Control 3	214	214	212	202	202	207	3.90E+09	5.10E+06
2 W, 60 min	1	181	184	183	170	166	175	3.80E+09	5.20E+06
	2	186	186	186	166	176	168	4.20E+09	4.80E+06
	3	187	187	188	174	177	180	4.00E+09	5.80E+06
	4	188	179	180	166	164	178	4.80E+09	5.30E+06
	5	189	183	184	170	174	174	3.80E+09	5.30E+06
	Control 1	192	190	183	174	176	176	4.20E+09	4.80E+06
	Control 2	188	191	183	171	170	174	4.20E+09	4.40E+06
	Control 3	180	183	184	163	170	181	4.50E+09	4.30E+06
60 W, 10 min	1	154	157	157	140	141	139	5.30E+09	5.30E+06
	2	159	158	159	142	142	139	5.50E+09	5.60E+06
	3	158	158	157	140	143	141	5.60E+09	5.10E+06
	4	157	157	156	142	142	142	5.50E+09	5.20E+06
	5	155	158	159	142	142	139	5.10E+09	5.00E+06
	Control 1	159	159	159	142	142	142	4.10E+09	5.00E+06
	Control 2	154	154	159	140	142	142	5.20E+09	5.00E+06
	Control 3	157	154	159	142	142	142	4.80E+09	5.00E+06
60 W, 30 min	1	133	137	137	134	131	137	3.80E+09	5.30E+06
	2	135	141	141	134	131	134	3.90E+09	5.10E+06
	3	138	131	135	131	131	132	3.70E+09	5.50E+06
	4	138	138	135	138	135	133	4.00E+09	4.10E+06
	5	134	138	131	132	130	137	3.50E+09	4.40E+06
	Control 1	134	137	139	134	132	135	3.30E+09	4.00E+06
	Control 2	136	135	137	133	132	132	3.30E+09	4.20E+06
	Control 3	135	137	136	133	136	132	3.50E+09	4.70E+06
60 W, 60 min	1	203	205	211	197	199	198	4.10E+09	5.00E+06
	2	211	205	213	204	203	203	4.20E+09	4.80E+06
	3	213	209	209	196	197	199	4.00E+09	5.30E+06
	4	203	208	205	200	201	198	5.10E+09	5.90E+06
	5	207	208	214	196	200	199	3.70E+09	5.00E+06
	Control 1	207	204	204	196	199	195	4.30E+09	4.50E+06
	Control 2	206	213	203	195	195	198	4.20E+09	4.80E+06
	Control 3	203	204	207	197	195	201	4.70E+09	4.10E+06

In general, for an average adult the normal RBC and WBC counts range from 4,300,000,000 - 6,000,000,000 cells/mL and 4,300,000 - 11,000,000 cells/mL, respectively. As seen in Tables 3 and 4, the RBC and WBC counts for the sample blood were lower than the normal values for average adults. This is because many blood cells died in the few hours outside of the body, but this was not likely to affect the experimental results since the treated and control blood samples were prepared by the same process, and the cells in all samples expired through the same process. The glucose levels and cell counts in the treated samples were compared with the controls.

For the cell viability analysis, the Restricted Maximum Likelihood (REML) Linear Mixed Model was used. The mean number of the red blood and white blood cell counts of each test was compared with that of the corresponding controls. The statistical analysis was carried out with SAS statistical analysis software, where the significant level was $\alpha = 0.05$. The comparison of the red and white blood cell counts between normal and high glucose blood samples are shown in Fig. 5-18 to 5-19, respectively.

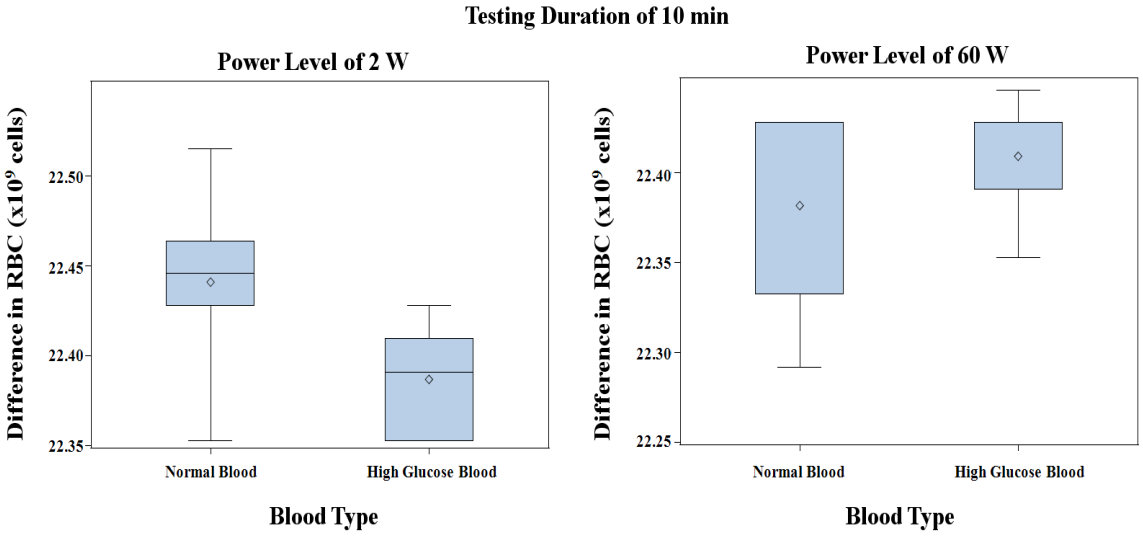

(a) 10 min Treatment

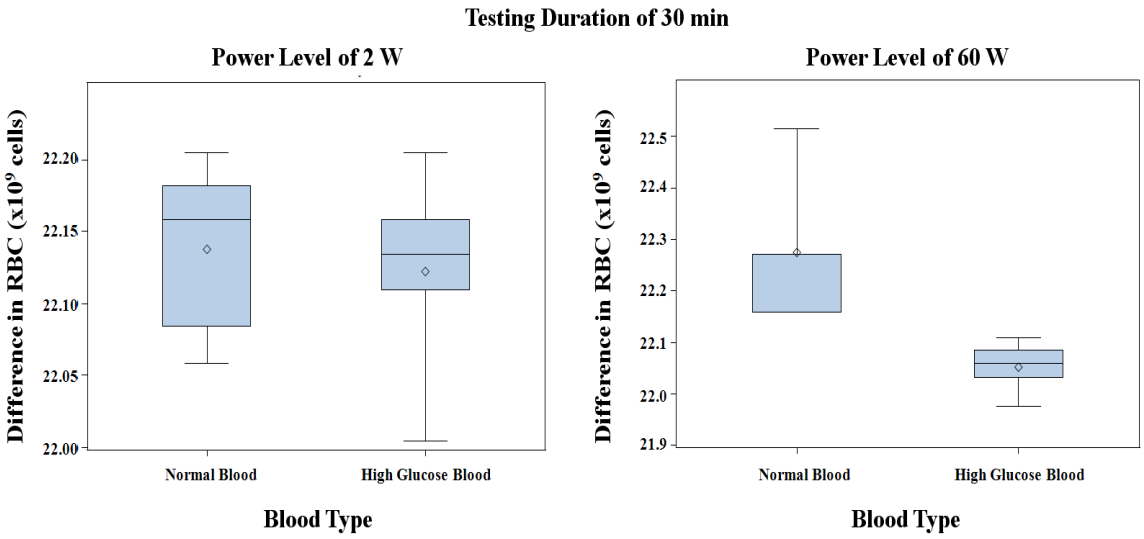

(b) 30 min Treatment

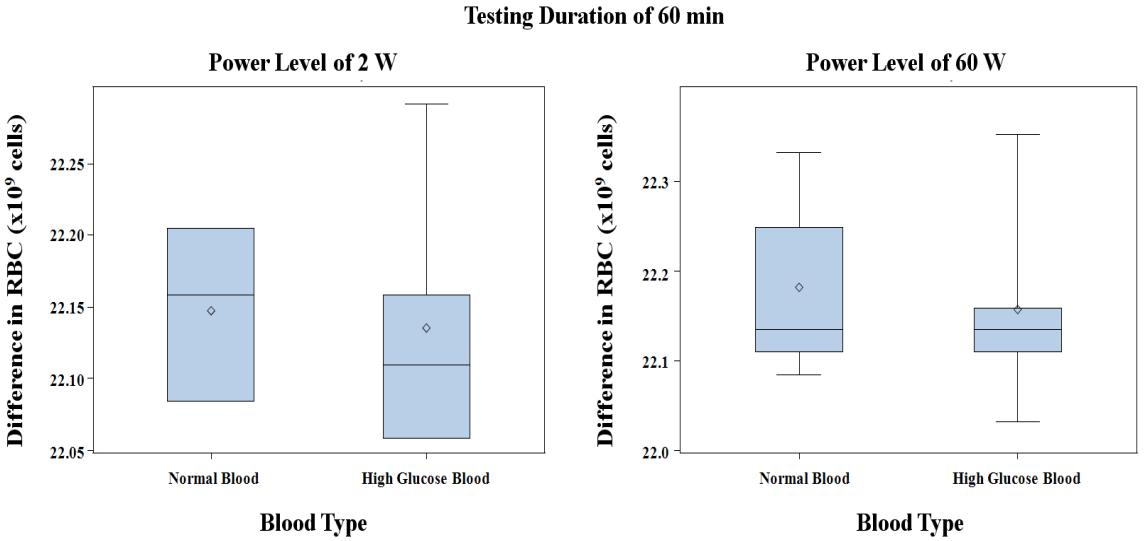

(c) 60 min Treatment

Figure 5 - 18 Comparison of red blood cell count in samples exposed to 850 MHz with power levels of 2 and 6 W: (a) 10 min, (b) 30 min, and (c) 60 min exposure durations.

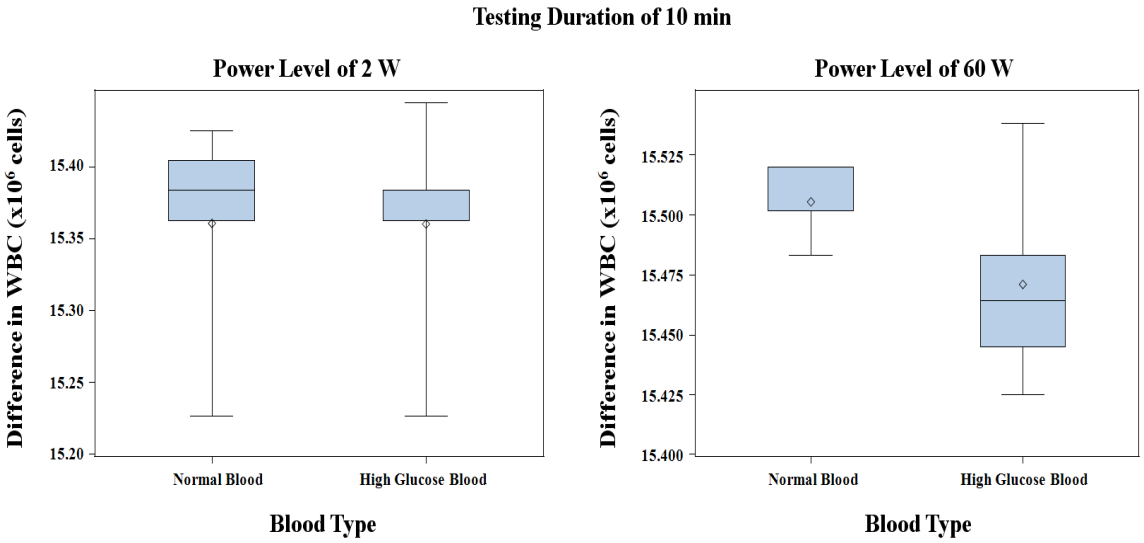

(a) 10 min Treatment

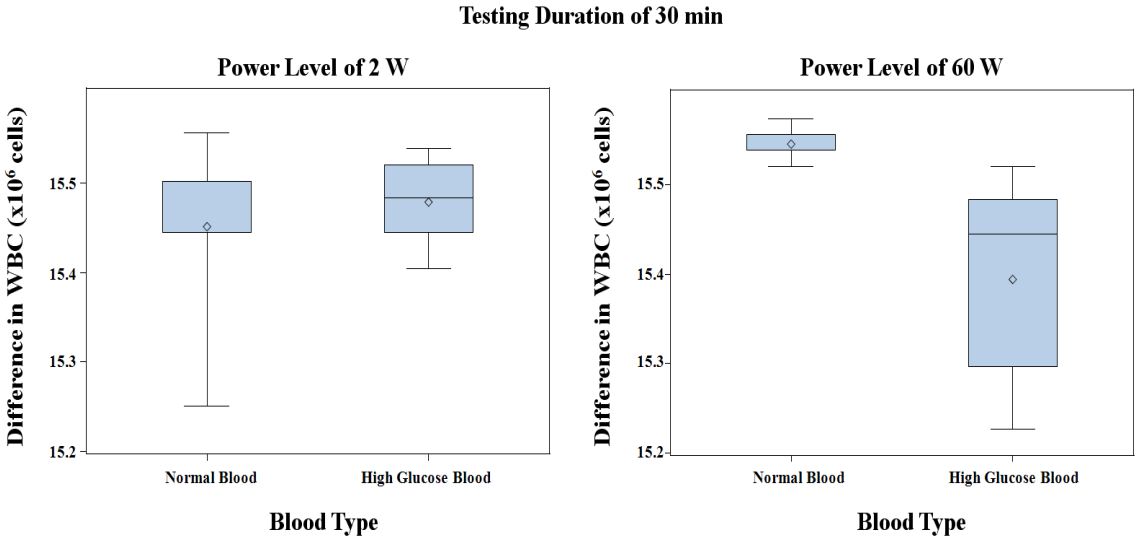

(b) 30 min Treatment

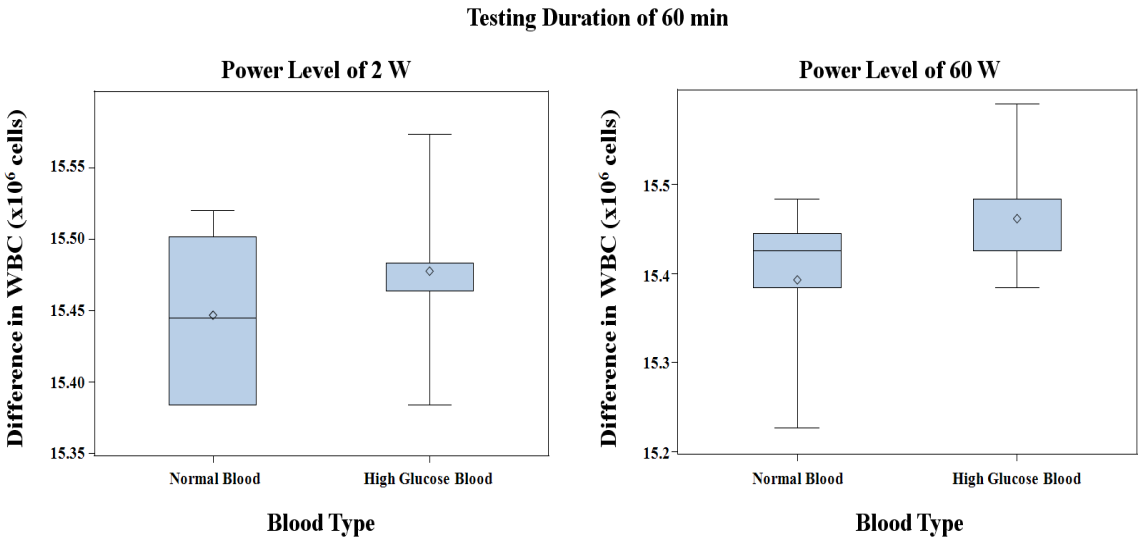

(c) 60 min Treatment

Figure 5 - 19 Comparison of white blood cell count in samples exposed to 850 MHz with power levels of 2 and 6 W: (a) 10 min, (b) 30 min, and (c) 60 min exposure durations.

The p-values in Table 5 show the comparison of RBC and WBC viability between treated samples and their respective controls. The results show that in normal blood, the survivability of the WBC at a 2W/60min treatment was significantly higher than the control. For a 60W/30min treatment of normal blood samples, both WBC and RBC counts were significantly higher than the controls. There was no change at other testing combinations.

In the high glucose blood, at 2W/30min, 2W/60min and 60W/60min tests the WBC viability was significant higher than that of the controls, while there were no changes observed in the RBC and WBC counts at other exposure combinations.

As seen from Table 5, there were not any significant changes in the red and white blood cells at a short exposure period of 10 min. This may be because of an energy (power x time) effect on white blood counts where the cell does not absorb enough sufficient energy to see any effects due to a low power level or a short testing duration.

TABLE 5

RBC AND WBC VIABILITY FOR EACH TESTING COMBINATION AGAINST THE ASSOCIATED CONTROLS FOR 850 MHZ EXPOSURE

Blood type	Radiation (W)	Test Duration (minutes)	RBC p-value	WBC p-value
NB	2	10	0.1807	0.1066
NB	2	30	0.7006	0.8134
NB	2	60	0.5844	0.0116*
NB	60	10	0.8397	0.0603
NB	60	30	0.0274*	0.0427*
NB	60	60	0.9000	0.1996
HGB	2	10	0.2386	0.3604
HGB	2	30	0.0525	0.0184*
HGB	2	60	0.2552	0.0014*
HGB	60	10	0.1074	0.1686
HGB	60	30	0.5638	0.4916
HGB	60	60	0.4812	0.0036*

'*' indicates that the cell survivability of the treated samples was significantly higher than that of its control.

To analyze the glucose levels, the Repeated Measures REML Linear Mixed Model was used. As seen in Tables 3 and 4, the glucose level in each sample was taken three times, both before and after treatment. Three glucose level measurements were used individually in the statistical analysis using SAS software, where the significant level was $\alpha = 0.05$. The null hypothesis used was that the testing procedure was not statistically different than the corresponding controls.

For this glucose analysis, the difference in the glucose levels between pre- and post-treatment were obtained by subtracting the measurements taken after testing to those taken before, so that the number of parameters influencing the analysis could be reduced. The difference in the measured glucose levels before and after treatment in the control, normal and high glucose samples for each test is shown in Fig. 5-20 to 5-22, respectively.

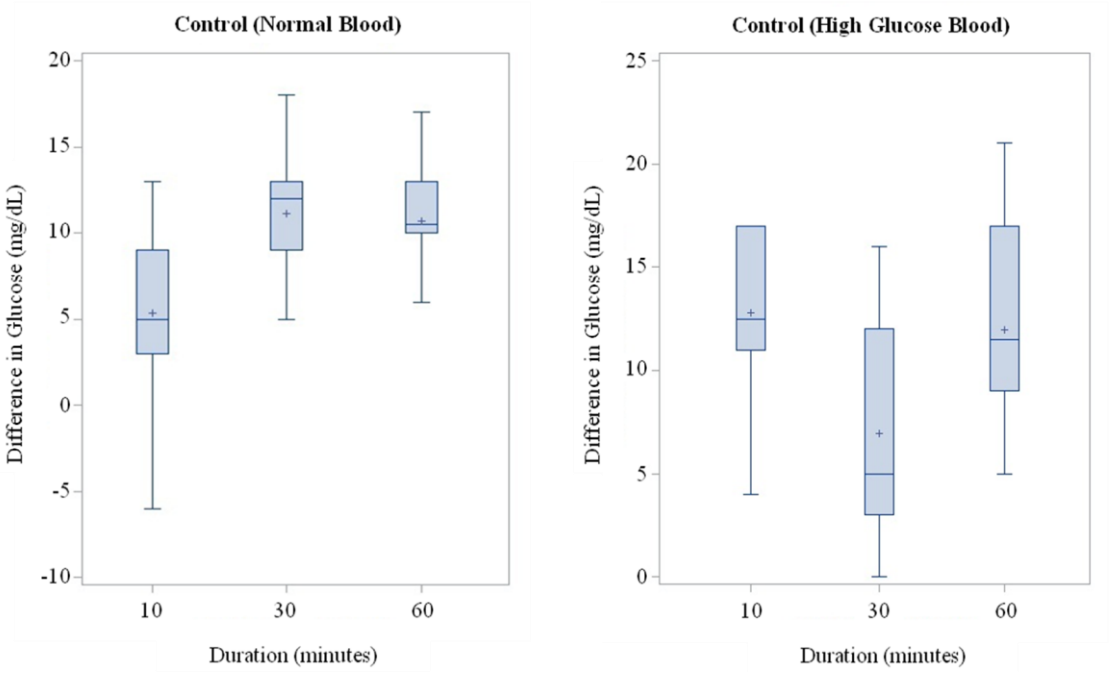

Figure 5 - 20 Comparison of glucose level differences in the control samples for 850 MHz exposure: Normal (left) and High Glucose samples (right).

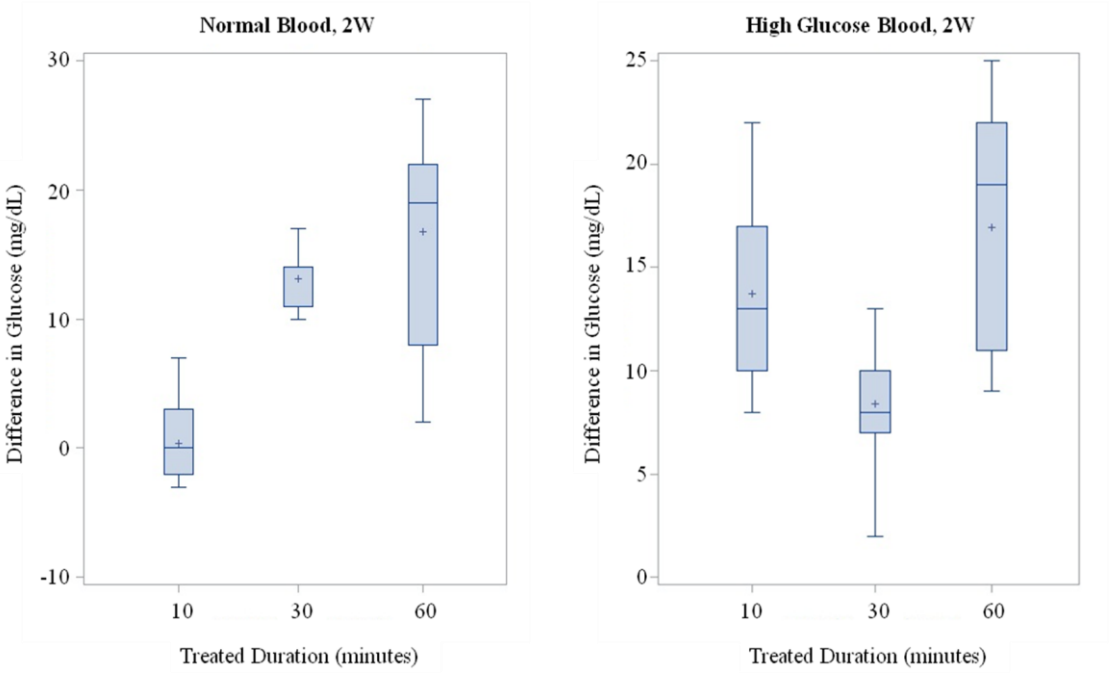

Figure 5 - 21 Comparison of glucose level differences in samples exposed to 850MHz/2W radiation: Normal (left) and High Glucose samples (right).

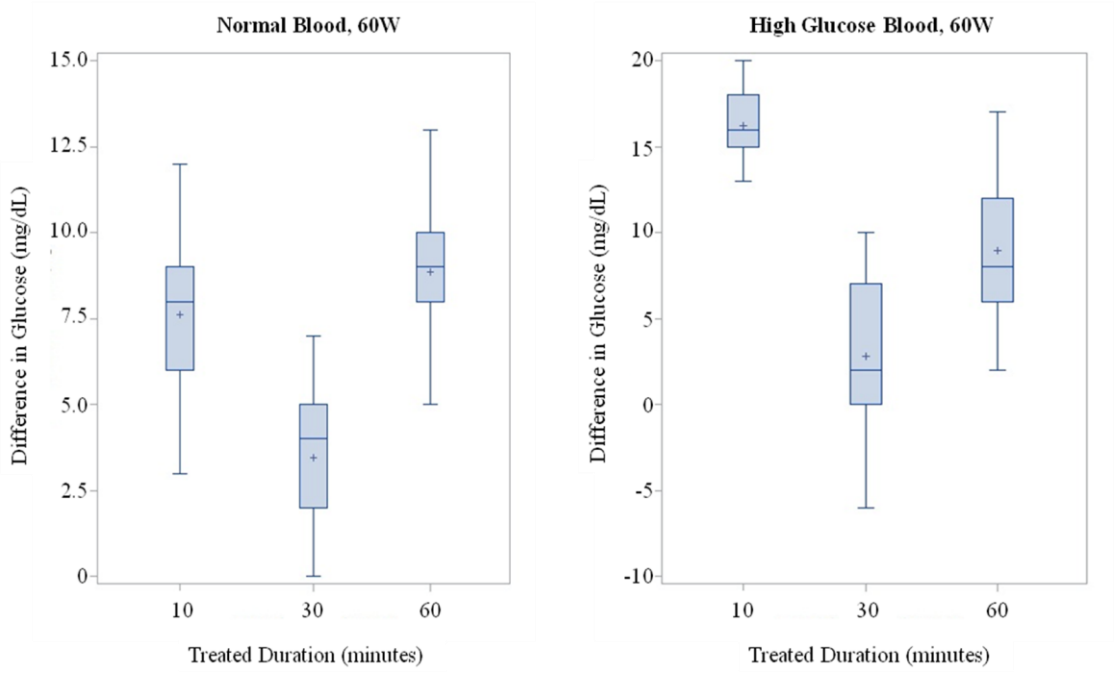

Figure 5 - 22 Comparison of glucose level differences in samples exposed to 850MHz/60W radiation: Normal (left) and High Glucose samples (right).

The plots in Figs. 5-20 to 5-22 show a primarily normal distribution with no distinct outliers, ensuring that the dataset was good for numerical hypothesis testing. This allowed the mean values and Least Squares Means differences for each testing combination against their respective controls to be calculated for the t-statistics and p-values shown in Table 6.

A comparison of the statistical significance of the glucose level in the treated samples with the controls for each testing combination is shown in Table 6. Eight of the 12 tests showed a significant difference from the control sample.

The results showed that for a 2W/10min exposure the glucose level in normal blood samples significantly decreased, while at 2W/30min and 2W/60min exposures the glucose level significantly increased compared to the controls. For 60W/30min and

60W/60min tests, the glucose level in NB samples was significantly lower when compared with the controls, while there were no changes at a 60W/10min exposure.

In the high glucose blood samples, a 2W/60min exposure resulted in a significantly higher glucose level than the controls. For a 60W/30min test, the glucose level in HGB samples significantly decreased compared to controls, while at a 60W/10min exposure the glucose level significantly increased compared with the controls.

TABLE 6

STATISTICAL ANALYSIS OF THE GLUCOSE LEVEL IN NORMAL AND HIGH GLUCOSE SAMPLES FOR EACH TESTING COMBINATION AGAINST THEIR CONTROLS FOR 850 MHZ EXPOSURE

Blood type	Radiation (W)	Test Duration (minutes)	t-value	p-value
NB	2	10	2.31	0.0234*
NB	2	30	-2.55	0.0127**
NB	2	60	-6.22	< 0.0001**
NB	60	10	-1.21	0.2289
NB	60	30	7.92	< 0.0001*
NB	60	60	2.30	0.0244*
HGB	2	10	-0.52	0.6024
HGB	2	30	-0.87	0.3887
HGB	2	60	-3.25	0.0017**
HGB	60	10	-2.41	0.0183**
HGB	60	30	2.41	0.0181*
HGB	60	60	1.60	0.1141

'*' indicates that the glucose level of the treated samples was significantly lower compared with their corresponding controls.
'' indicates that the glucose level of the treated samples was significantly higher compared with their corresponding controls.**

These results suggested that the total energy exerted (power x time) could be a factor influencing changes in glucose levels. Because of this, a significant difference in

glucose levels can be observed at an exposure level of 60 W for both short and long treatment periods.

Potential differences in glucose counts between normal blood and high glucose blood samples were also analyzed by using the Repeated Measures REML Linear Mixed Model, the same procedure used in the analysis of glucose levels in treated samples against their controls. The Least Squares Means differences for normal blood versus high glucose blood at each testing combination were calculated. Fig. 5-23 shows the comparison of the differences in glucose levels between NB and HGB samples. The t-values and p-values of NB samples against HGB samples for each testing combination were calculated and are shown in Table 7.

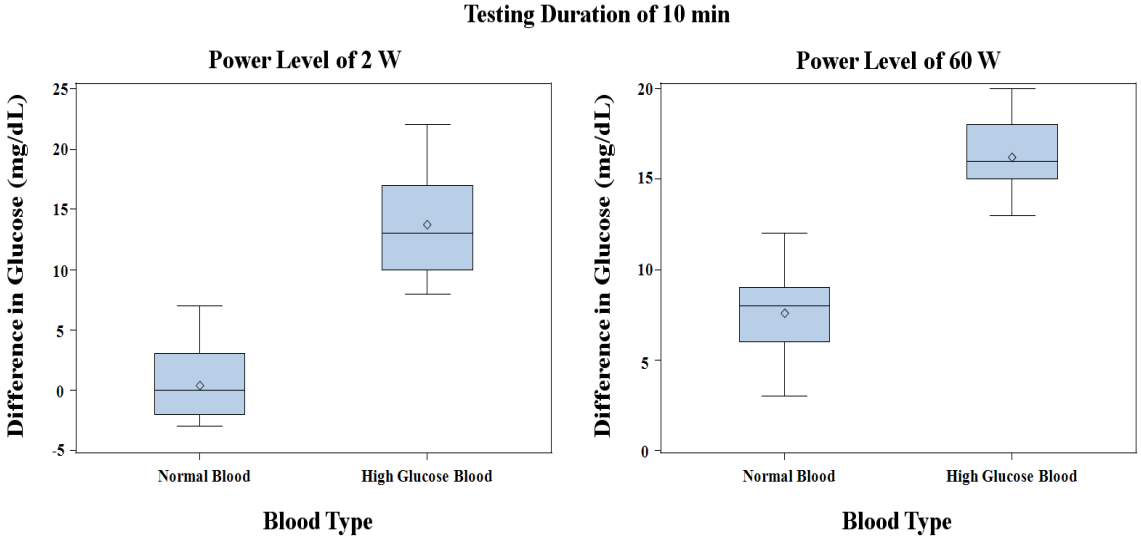

(a) 10 min Treatment

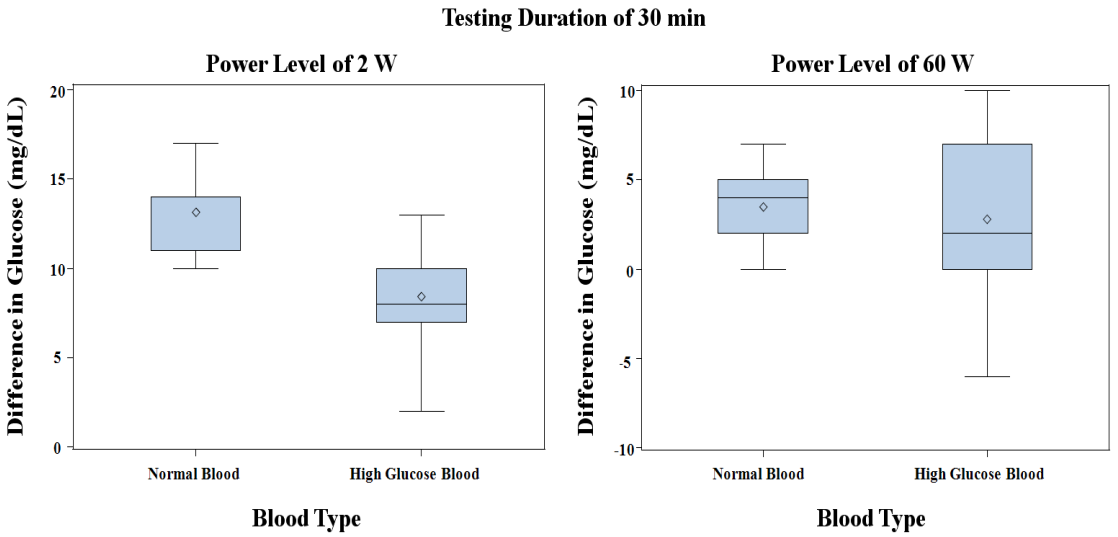

(b) 30 min Treatment

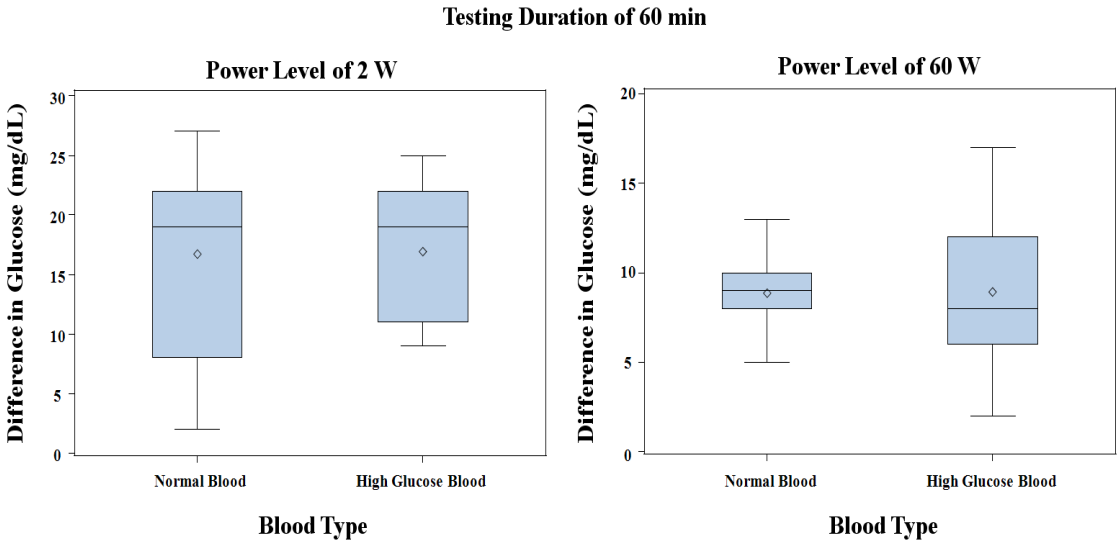

(c) 60 min Treatment

Figure 5 - 23 Comparison of differences in glucose levels in treated samples exposed to 850 MHz with exposure levels of 2 and 60 W: (a) 10 min, (b) 30 min, and (c) 60 min exposure periods.

The p-value results in Table 7 show three significant differences in glucose levels in the normal blood samples versus the high glucose blood samples.

For exposure to 2W/10min and 60W/10min radiation, the changes in the glucose levels in the HGB samples were significantly higher when compared to NB samples,

while at 2W/30min testing the glucose levels in HGB samples were significantly lower than in NB samples. As my previous assertion stated, these results also suggest that at long testing durations the total energy deposited to both NB and HGB samples ensure that there are no significant differences observed in the glucose levels.

TABLE 7

DIFFERENCES IN THE GLUCOSE LEVEL BETWEEN NORMAL BLOOD VS. HIGH GLUCOSE BLOOD FOR 850 MHZ EXPOSURE

Radiation (W)	Test Duration (minutes)	t-value	p-value
2	10	-8.15	$< 0.0001^{*}$
2	30	5.57	$< 0.0001^{**}$
2	60	-0.2	0.8429
60	10	-15.88	$< 0.0001^{*}$
60	30	0.62	0.5357
60	60	-0.05	0.9612

'*' indicates that the change in the glucose level of the HGB samples was significantly higher than that of the NB samples.
'' indicates that the change in the glucose level of the NB samples was significantly higher than that of the HGB samples.**

5.2.3 Blood Response to 900 MHz Exposure

For the study on blood response to electromagnetic radiation at 900 MHz, all the experimental procedures and conditions were the same as in the previous study of 850 MHz exposure effects on blood. Three blood types, normal blood (NB), high glucose blood (HGB) and control blood (CB), were used. The red blood cell (RBC) and white blood cell (WBC) counts and the glucose levels were observed and investigated. The viability of the RBC and WBC were monitored immediately after treatment. The glucose levels in the treated samples were also measured immediately before and after treatment and compared with their respective controls. The pre and post treated cell survivability and glucose levels for the samples were also collected and are shown in Tables 8 and 9.

TABLE 8

GLUCOSE AND BLOOD CELL LEVELS FOR NORMAL SAMPLES EXPOSED TO 900 MHZ ELECTROMAGNETIC FIELDS AT 2 AND 60 W

Source	Samples	Glucose Level (mg/dL)						Viability (cell/mL)	
		Before Treatment			After Treatment				
		1st time	2nd time	3rd time	1st time	2nd time	3rd time	RBC	WBC
2 W, 10 min	1	89	90	89	78	78	78	3.10E+09	5.00E+06
	2	89	90	91	78	79	79	3.80E+09	4.80E+06
	3	90	89	89	77	78	77	3.50E+09	5.50E+06
	4	91	91	91	78	78	78	3.30E+09	5.30E+06
	5	89	91	91	79	77	79	3.40E+09	5.10E+06
	Control 1	91	91	90	77	75	77	3.40E+09	5.10E+06
	Control 2	91	91	89	77	76	76	3.50E+09	5.30E+06
	Control 3	91	91	90	74	77	74	3.50E+09	5.30E+06
2 W, 30 min	1	80	80	82	68	69	67	3.60E+09	4.80E+06
	2	81	83	82	69	67	69	3.70E+09	5.50E+06
	3	81	81	82	66	66	67	3.30E+09	5.50E+06
	4	80	83	83	67	66	69	3.70E+09	5.30E+06
	5	80	81	80	68	68	67	3.50E+09	5.10E+06
	Control 1	80	80	82	65	66	68	3.50E+09	5.10E+06
	Control 2	80	80	80	65	67	66	3.40E+09	5.30E+06
	Control 3	80	82	82	67	67	68	3.30E+09	5.50E+06
2 W, 60 min	1	98	96	96	83	85	85	4.10E+09	4.40E+06
	2	99	96	98	81	83	84	4.70E+09	4.20E+06
	3	96	99	96	84	84	85	4.30E+09	4.80E+06
	4	95	96	99	84	82	83	4.10E+09	4.70E+06
	5	97	98	97	82	85	83	4.50E+09	4.70E+06
	Control 1	98	96	98	85	82	82	4.00E+09	5.00E+06
	Control 2	96	97	97	82	82	82	4.40E+09	4.80E+06
	Control 3	96	97	97	84	82	83	4.50E+09	4.50E+06
60 W, 10 min	1	82	83	85	75	72	72	4.40E+09	6.60E+06
	2	82	83	84	70	73	72	4.10E+09	6.10E+06
	3	81	83	82	71	75	71	4.20E+09	6.20E+06
	4	82	82	83	71	71	75	4.40E+09	6.40E+06
	5	81	81	83	74	74	75	4.50E+09	6.00E+06
	Control 1	82	84	82	75	72	73	4.00E+09	6.00E+06
	Control 2	81	81	81	73	73	73	4.10E+09	6.20E+06
	Control 3	84	82	81	70	70	70	4.20E+09	6.50E+06
60 W, 30 min	1	95	98	95	85	88	90	4.50E+09	6.10E+06
	2	93	96	94	89	87	85	4.20E+09	6.10E+06
	3	92	93	93	87	88	90	4.60E+09	6.60E+06
	4	92	92	92	85	86	86	4.70E+09	6.50E+06
	5	96	93	95	85	89	87	4.20E+09	6.20E+06
	Control 1	92	91	95	79	80	82	4.80E+09	6.00E+06
	Control 2	93	95	97	80	83	83	4.70E+09	6.10E+06
	Control 3	92	93	94	83	82	84	4.00E+09	6.20E+06
60 W, 60 min	1	87	85	85	74	73	75	3.50E+09	4.80E+06
	2	85	85	88	74	73	72	3.40E+09	5.30E+06
	3	88	85	85	73	70	71	3.30E+09	5.10E+06
	4	86	90	90	72	72	71	3.30E+09	5.00E+06
	5	87	85	90	72	73	73	3.50E+09	4.90E+06
	Control 1	86	90	88	73	70	75	3.00E+09	5.50E+06
	Control 2	87	87	85	72	72	71	3.50E+09	5.40E+06
	Control 3	85	85	86	71	70	72	3.20E+09	5.00E+06

TABLE 9

GLUCOSE AND BLOOD CELL LEVELS FOR HIGH GLUCOSE BLOOD SAMPLES EXPOSED TO 900 MHZ ELECTROMAGNETIC FIELDS AT 2 AND 60 W

Source	Samples	Glucose Level (mg/dL)						Viability (cell/mL)	
		Before Treatment			After Treatment				
		1st time	2nd time	3rd time	1st time	2nd time	3rd time	RBC	WBC
2 W, 10 min	1	135	135	135	128	126	127	3.20E+09	5.10E+06
	2	135	133	133	126	126	129	3.40E+09	5.00E+06
	3	135	134	134	126	127	129	3.70E+09	5.00E+06
	4	135	133	135	126	129	129	3.10E+09	5.00E+06
	5	135	135	134	126	129	129	3.40E+09	4.80E+06
	Control 1	135	133	134	131	133	134	3.50E+09	4.80E+06
	Control 2	133	135	133	131	131	133	3.10E+09	5.00E+06
	Control 3	135	133	135	134	131	131	3.40E+09	4.90E+06
2 W, 30 min	1	186	189	189	176	179	177	3.40E+09	5.20E+06
	2	189	187	188	178	177	177	3.50E+09	5.30E+06
	3	188	186	188	179	179	179	3.60E+09	5.30E+06
	4	187	186	187	176	176	179	3.30E+09	5.80E+06
	5	188	186	189	179	179	179	3.80E+09	5.20E+06
	Control 1	186	186	186	184	181	183	3.80E+09	5.10E+06
	Control 2	186	186	189	181	180	181	3.30E+09	5.40E+06
	Control 3	187	186	189	184	180	184	3.70E+09	5.50E+06
2 W, 60 min	1	263	264	266	245	245	244	4.00E+09	4.10E+06
	2	266	266	266	245	243	245	4.40E+09	4.20E+06
	3	264	264	265	244	243	243	4.30E+09	5.00E+06
	4	266	267	265	243	243	246	4.20E+09	5.00E+06
	5	266	265	264	245	246	246	4.40E+09	4.80E+06
	Control 1	265	264	266	245	248	247	3.90E+09	4.20E+06
	Control 2	263	264	264	245	249	247	4.40E+09	4.80E+06
	Control 3	264	265	265	245	249	245	4.70E+09	5.00E+06
60 W, 10 min	1	209	205	209	198	198	202	4.60E+09	5.30E+06
	2	208	208	209	200	199	202	4.10E+09	5.20E+06
	3	206	208	208	202	199	200	4.30E+09	5.00E+06
	4	206	206	206	202	202	201	4.40E+09	4.90E+06
	5	209	206	207	203	198	199	4.10E+09	5.50E+06
	Control 1	208	205	209	202	203	202	4.50E+09	5.00E+06
	Control 2	205	206	206	201	201	200	4.10E+09	5.20E+06
	Control 3	207	208	205	199	201	202	4.30E+09	5.30E+06
60 W, 30 min	1	161	163	162	142	144	142	4.60E+09	6.00E+06
	2	158	155	157	145	148	146	4.30E+09	6.50E+06
	3	152	150	155	148	144	147	4.00E+09	6.40E+06
	4	151	154	154	144	146	147	4.60E+09	6.30E+06
	5	160	161	163	147	143	144	4.70E+09	6.00E+06
	Control 1	157	158	158	147	145	145	4.80E+09	6.20E+06
	Control 2	158	157	155	144	145	144	4.50E+09	6.30E+06
	Control 3	162	166	163	150	148	150	4.20E+09	6.10E+06
60 W, 60 min	1	182	187	185	170	173	169	3.50E+09	6.10E+06
	2	184	187	183	169	174	171	3.30E+09	6.20E+06
	3	190	188	190	171	168	170	3.10E+09	6.30E+06
	4	188	192	190	174	168	172	3.00E+09	6.60E+06
	5	188	185	186	171	171	168	3.20E+09	6.10E+06
	Control 1	191	190	190	169	170	171	3.50E+09	6.10E+06
	Control 2	185	182	183	173	172	170	3.20E+09	6.50E+06
	Control 3	189	192	190	172	174	171	3.30E+09	6.70E+06

As seen in Tables 8 and 9, the RBC and WBC levels were also lower than the normal values for average adults, where normal RBC and WBC counts are about 4,300,000,000 - 6,000,000,000 cells/mL and 4,300,000 - 11,000,000 cells/mL, respectively. This difference was due to a large amount of blood cells dying in their few hours outside of the body. However, this did not have an effect on the experimental results because the treated and control blood samples were prepared using the same process. Therefore, the cells in both the treated and control blood died through the same process. In addition, all results were also compared to the controls.

The statistical analysis for each of the tests done at 900MHz was performed using the same methods as for the study of the blood response to 850 MHz exposure. For the cell viability analysis, again the REML Linear Mixed Model was used and carried out through SAS statistical analysis software. Again, the level of significance was $\alpha = 0.05$. The comparison of the viability of the red and white blood cell between normal and high glucose blood samples is shown in Figs. 5-24 to 5-25, respectively.

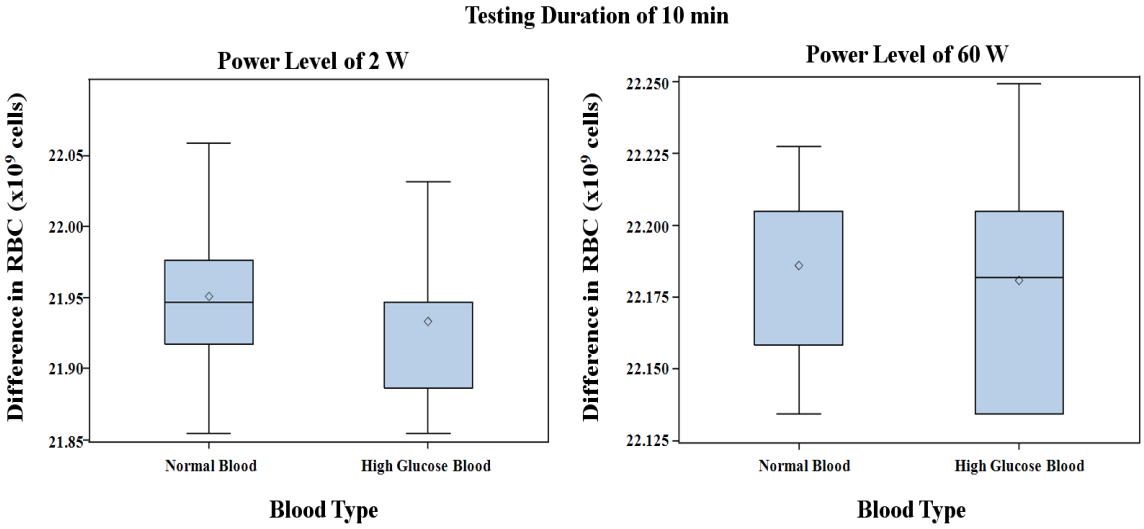

(a) 10 min Treatment

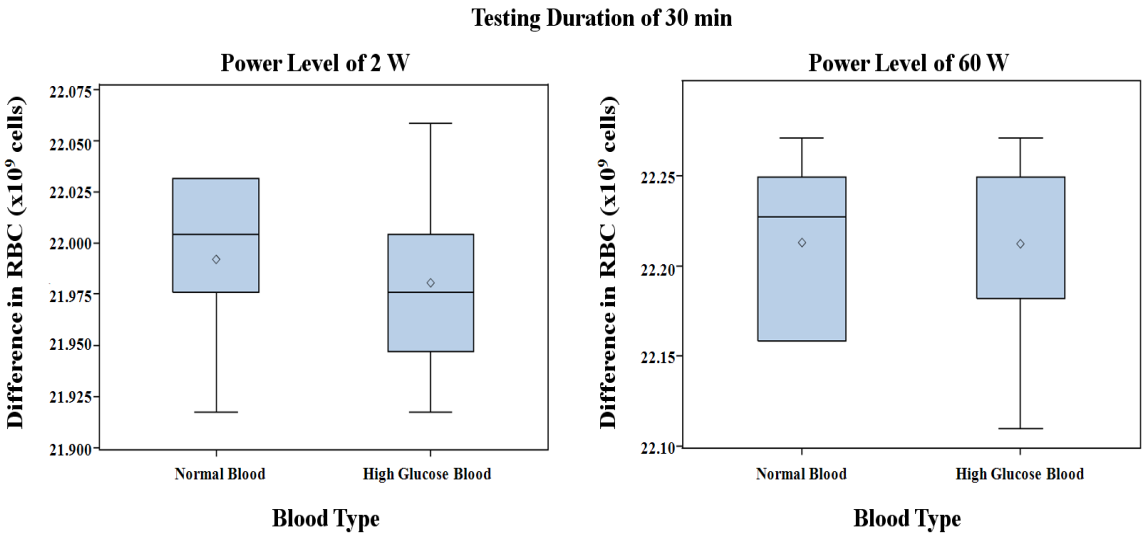

(b) 30 min Treatment

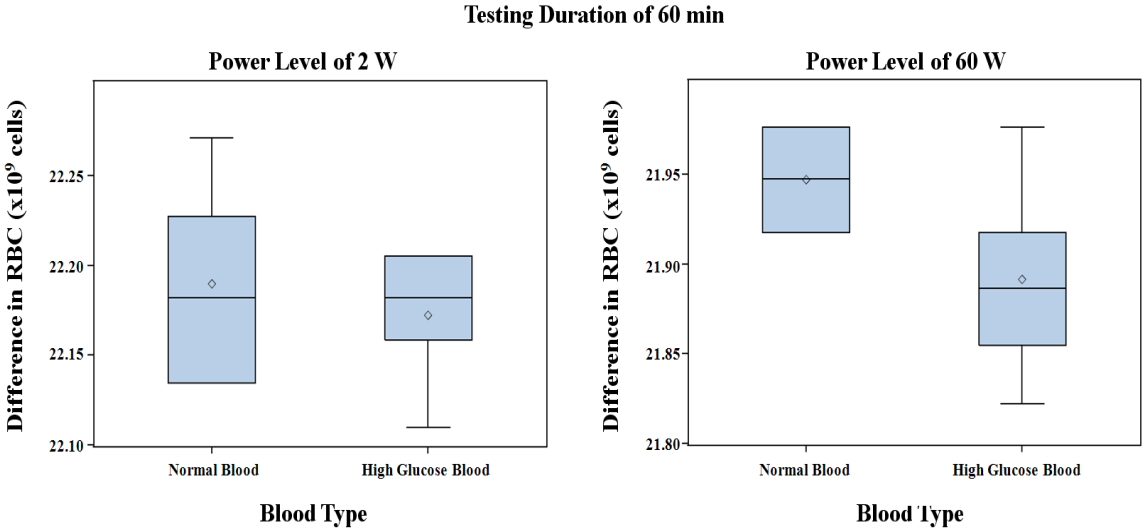

(c) 60 min Treatment

Figure 5 - 24 Comparison of red blood cell count in samples exposed to 900 MHz with power levels of 2 and 6 W: (a) 10 min, (b) 30 min, and (c) 60 min exposure durations.

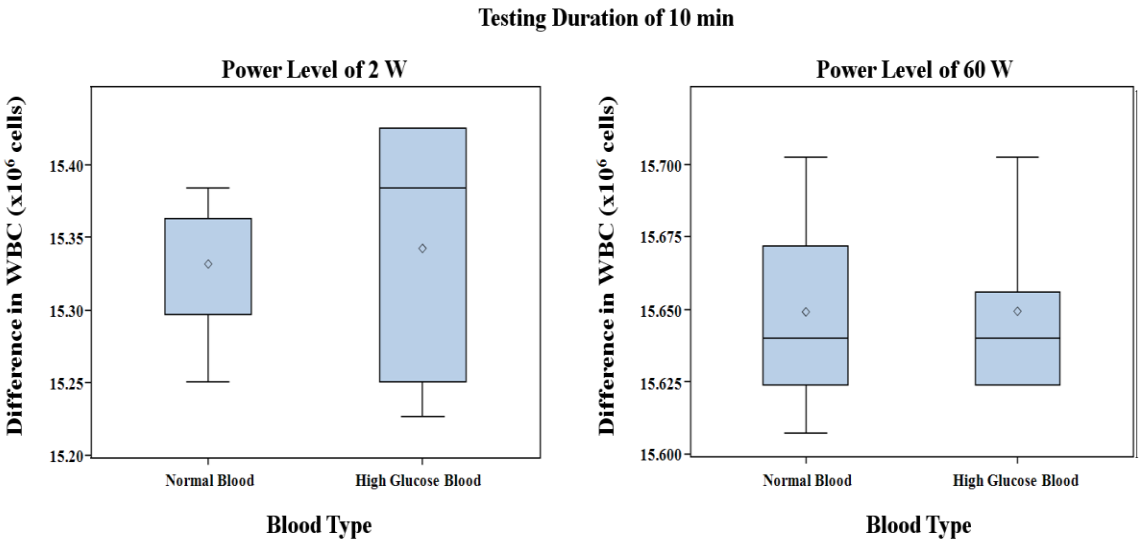

(a) 10 min Treatment

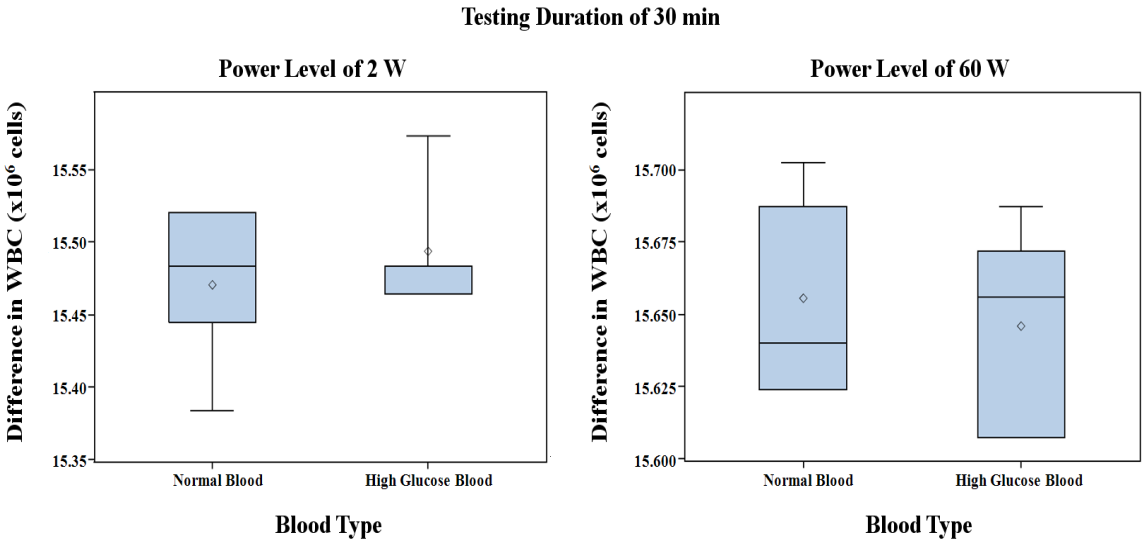

(b) 30 min Treatment

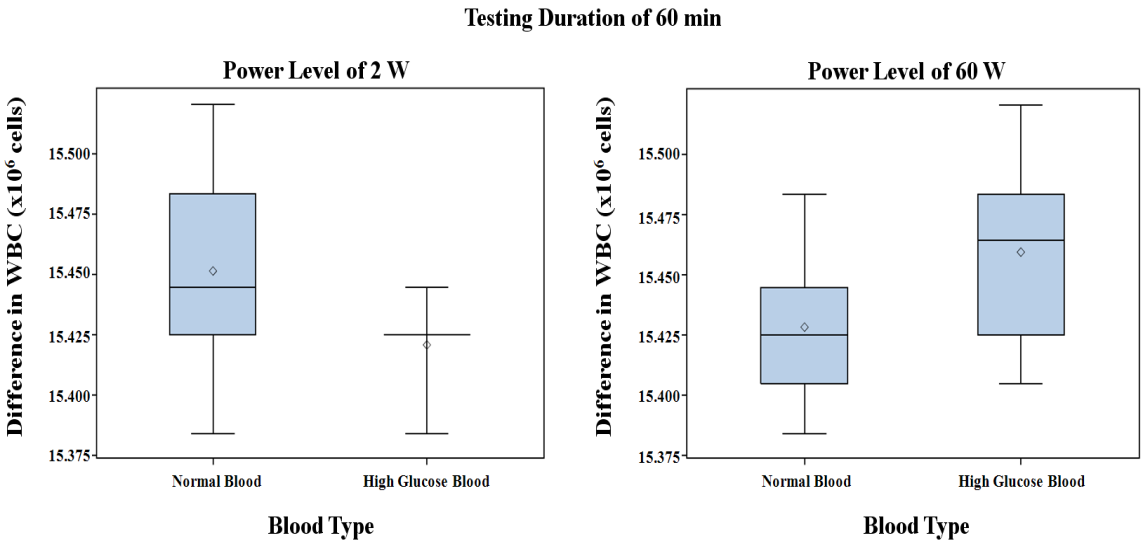

(c) 60 min Treatment

Figure 5 - 25 Comparison of white blood cell count in samples exposed to 900 MHz with power levels of 2 and 6 W: (a) 10 min, (b) 30 min, and (c) 60 min exposure durations.

Table 10 shows the p-values of the RBC and WBC counts in the treated samples compared with the controls. The results showed a significant difference in 6 of the 12 p-values of RBC count and 5 of the 12 p-values of WBC count.

In the normal blood samples, the RBC viability at the 2W/60min, 60W/10min, and 60W/30min treatments was significantly higher than the control. For exposure to 2W/60min radiation, the WBC count in normal blood was significantly lower than the control, while at 60W/10min and 60W/30min treatments the WBC level was significantly higher. There were no changes at other exposures.

In high glucose blood samples, the RBC level at the 2W/30min and 60W/60min treatments was significantly lower compared with the controls, while at a 60W/10min exposure the RBC count was significantly higher than the controls. The WBC viability in the HGB samples at 2W/60min was significantly lower compared to the controls, while at

60W/60min WBC levels were significantly higher. There was no change at other testing combinations.

As seen in Table 10, the results show that EM exposure is not likely to affect red and white blood cell counts for a short exposure period (10 min) at both 2 and 60 W power levels, with one exception. Again, as previously explained, this could be because of an energy (power x time) effect on blood cells.

TABLE 10

RBC AND WBC VIABILITY FOR EACH TESTING COMBINATION AGAINST THE ASSOCIATED CONTROLS FOR 900 MHZ EXPOSURE

Blood type	Radiation (W)	Test Duration (minutes)	RBC p-value	WBC p-value
NB	2	10	0.1709	0.5786
NB	2	30	0.1311	0.0706
NB	2	60	0.0162*	0.0003**
NB	60	10	0.0306*	0.0035*
NB	60	30	0.0417*	0.0269*
NB	60	60	0.1407	0.2870
HGB	2	10	0.0591	0.8444
HGB	2	30	0.0369**	0.1812
HGB	2	60	0.0697	0.0020**
HGB	60	10	0.0461*	0.5878
HGB	60	30	0.1207	0.1255
HGB	60	60	0.0109**	0.0136*

'*' indicates that the cell survivability of the treated samples was significantly higher than that of its control.
'' indicates that the cell survivability of the treated samples was significantly lower than that of its control.**

A glucose level analysis was taken based on the Repeated Measures REML Linear Mixed Model using SAS software. Again, each of the three measured glucose levels were analyzed individually for the statistical analysis. The significant level was also set at $\alpha = 0.05$. The null hypothesis assumed the treated blood was not statistically

different from their associated controls. To reduce the parameters influencing the analysis, the measurements taken after the tests were subtracted from those taken before, resulting in a glucose level difference. The comparison of the glucose difference before and after treatment in the control, normal, and high glucose samples at each testing combination is shown in Fig. 5-26 to 5-28, respectively.

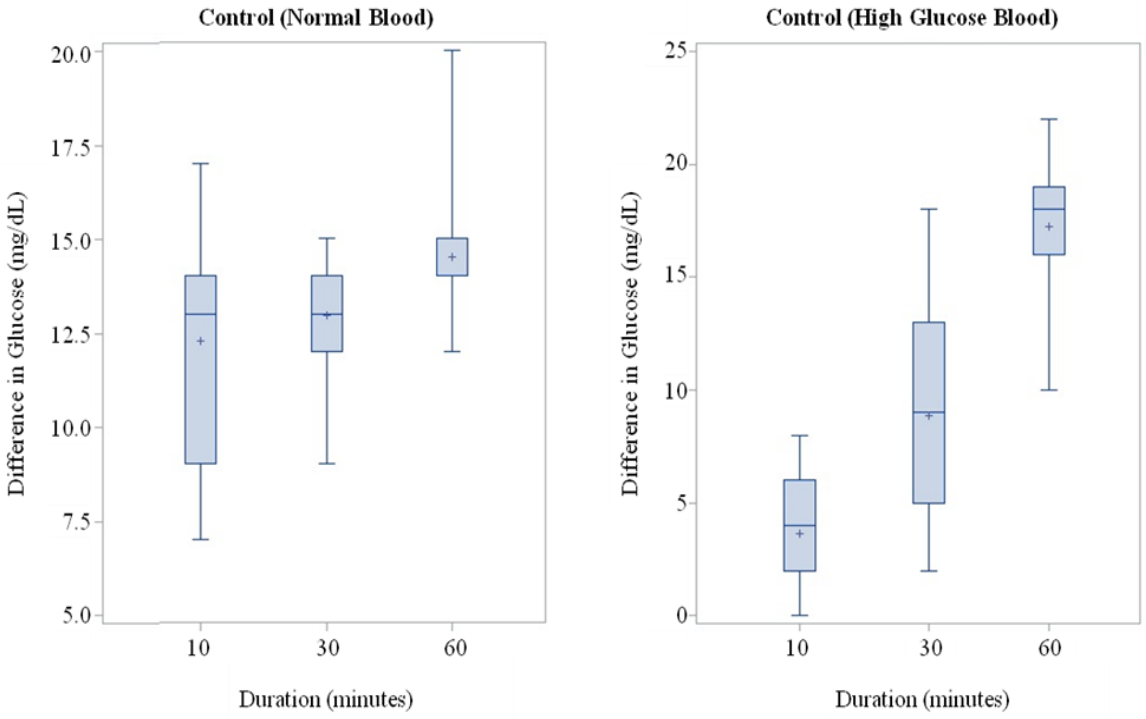

Figure 5 - 26 Comparison of glucose level differences in the control samples for 900 MHz exposure: Normal (left) and High Glucose samples (right).

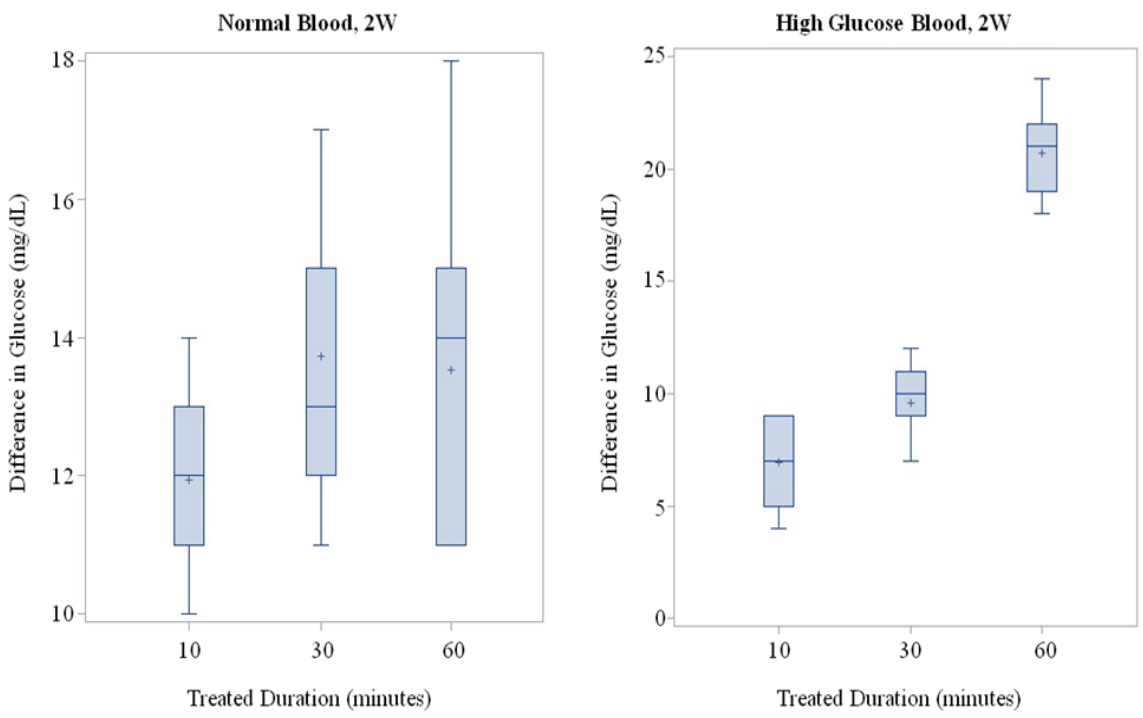

Figure 5 - 27 Comparison of glucose level differences in the samples exposed to 900MHz/2W radiation: Normal (left) and High Glucose samples (right).

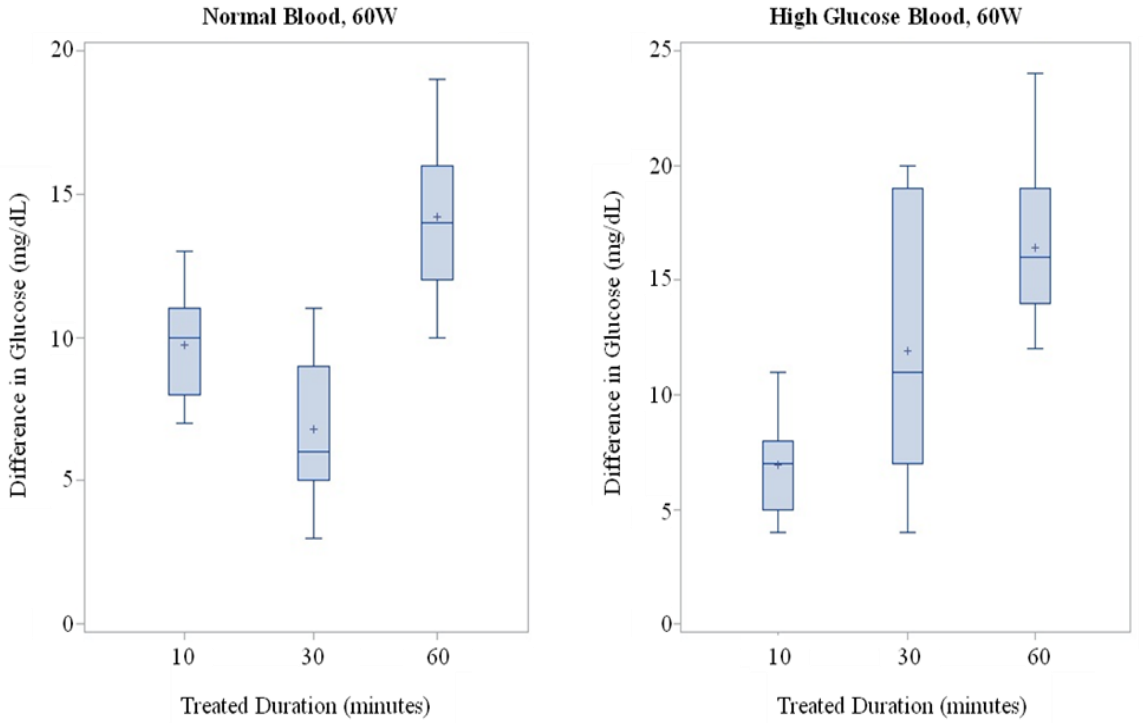

Figure 5 - 28 Comparison of glucose level differences in the samples exposed to 900MHz/60W radiation: Normal (left) and High Glucose samples (right).

Fig. 5-26 to 5-28 ensure that there are not any blatant errors in the data set, which would throw off the numerical hypothesis testing. Then, the statistical analysis for the glucose levels for each testing combination against their respective controls were calculated based on the mean values and the Least Squares Means differences and are shown in Table 11.

TABLE 11

STATISTICAL ANALYSIS OF THE GLUCOSE LEVELS IN NORMAL AND HIGH GLUCOSE SAMPLES FOR EACH TESTING COMBINATION AGAINST THEIR CONTROLS FOR 900 MHZ EXPOSURE

Blood type	Radiation (W)	Test Duration (minutes)	t-value	p-value
NB	2	10	0.30	0.7671
NB	2	30	-1.06	0.2938
NB	2	60	2.04	0.0448*
NB	60	10	4.63	< 0.0001*
NB	60	30	4.48	< 0.0001*
NB	60	60	-12.05	< 0.0001**
HGB	2	10	-4.31	< 0.0001**
HGB	2	30	-0.43	0.6667
HGB	2	60	-2.92	0.0046**
HGB	60	10	-3.49	0.0008**
HGB	60	30	-1.07	0.2881
HGB	60	60	0.52	0.6016

'*' indicates that the glucose level of the treated samples was significantly lower compared with their corresponding controls.
'' indicates that the glucose level of the treated samples was significantly higher compared with their corresponding controls.**

A statistically significant difference from the control samples were detected in 7 out of 12 tests. In NB samples, the 2W/60min, 60W/10min, and 60W/30 treatments showed a significant decrease in glucose levels compared to the controls, while at a 60W/60min exposure the glucose level in the NB samples significantly increased compared to the controls. There was no significant change in the other treatments.

In the HGB samples, the 2W/10min, 2W/60min, and 60W/10min exposure showed significantly higher glucose levels than controls, while there was no significant difference found for other testing combinations.

These results show agreement with the previous findings from the study of blood response to 850 MHz radiation: at long testing durations (60 min) both 2 and 60 W exposure levels influence changes in the glucose levels of the NB and HGB samples, with one exception. The results also affirm that the effects on glucose levels could be due to the total energy deposited rather than only due to the power level or treated duration of the EM field.

Finally, the changes in the glucose levels between NB and HGB samples were compared and are shown in Fig. 5-29 and Table 12. The analysis was based on the Repeated Measures REML Linear Mixed Model. The Least Squares Means differences for normal blood versus its high glucose blood counterpart at each testing combination generated the t-values and p-values.

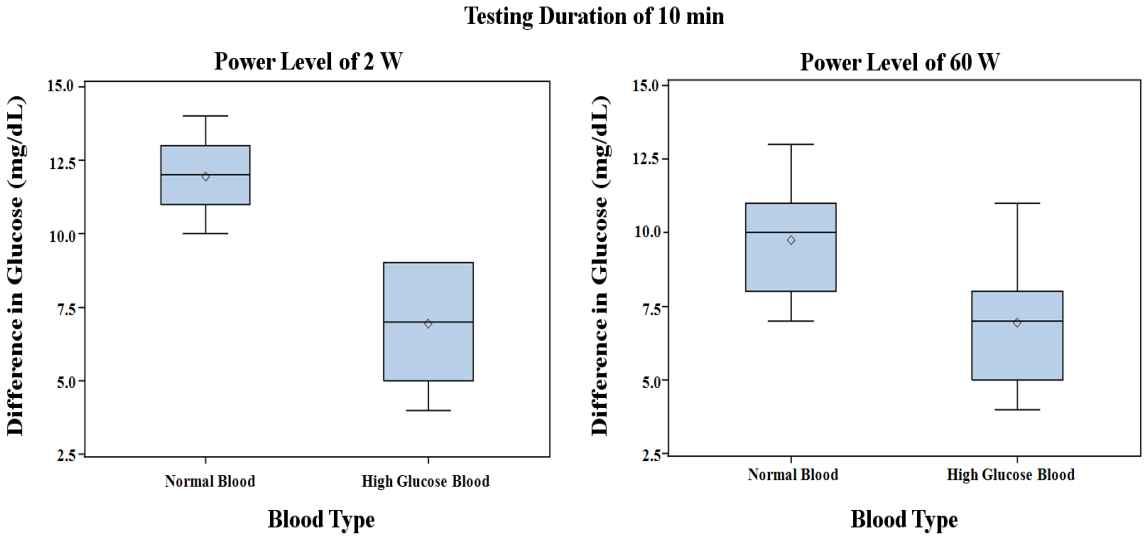

(a) 10 min Treatment

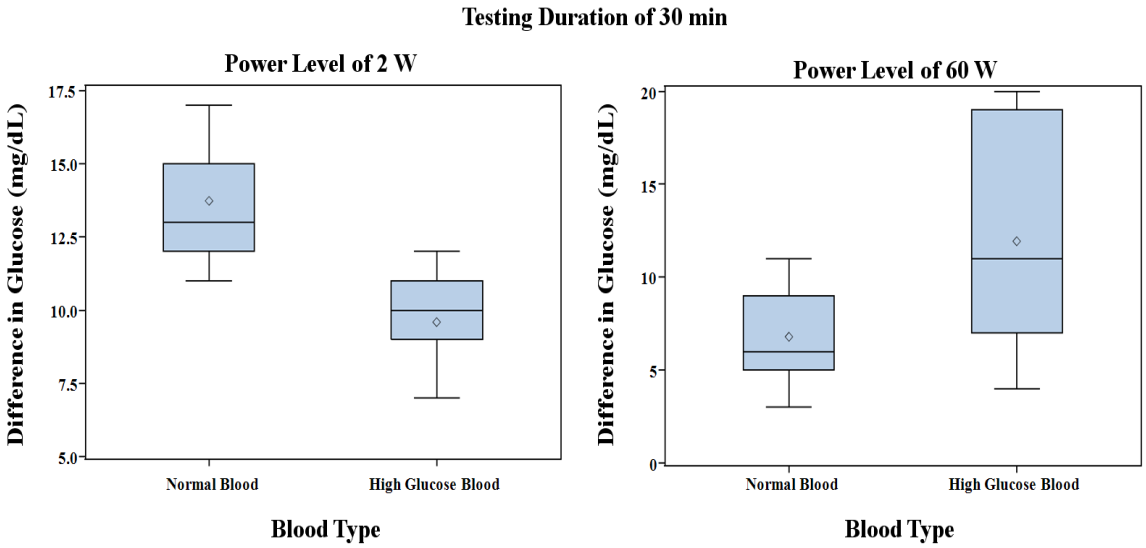

(b) 30 min Treatment

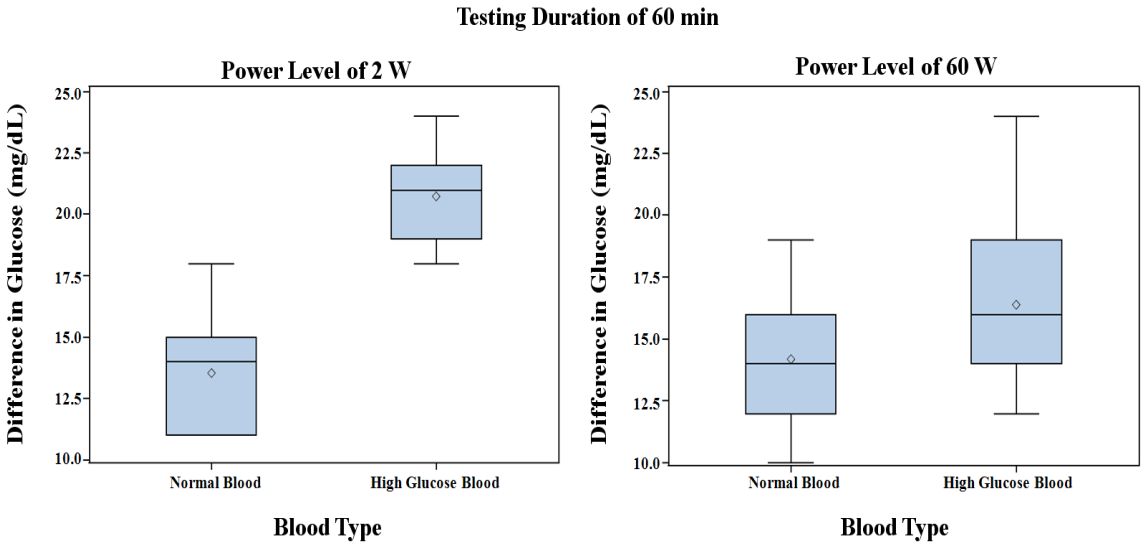

(c) 60 min Treatment

Figure 5 - 29 Comparison of differences in glucose levels in treated samples exposed to 900 MHz with exposure levels of 2 and 60 W: (a) 10 min, (b) 30 min, and (c) 60 min exposure periods.

The p-value results in Table 12 show five statistically significant changes in the glucose levels in the NB samples versus the HGB samples. The 2W/10min, 2W/30min, and 60W/10min treatments led to more changes in the glucose levels of the HGB samples compared with NB samples, while at 2W/60min and 60W/30min exposures less glucose

changes in the HGB samples compared to the NB samples was detected. These results suggest that electromagnetic radiation influenced changes in the glucose levels in each sample in a different way. At a power level of 2 W most of the significant changes were observed in the HGB samples, but not in the NB samples. At the 60 W exposure level most of the significant changes were found in the NB samples, but not in the HGB samples. For this reason, the majority of the results in Table 12 show a significant difference in the glucose levels between both samples.

TABLE 12

DIFFERENCE IN THE GLUCOSE LEVEL BETWEEN NORMAL BLOOD VS. HIGH GLUCOSE BLOOD FOR 900 MHZ EXPOSURE

Radiation (W)	Test Duration (minutes)	t-value	p-value
2	10	-13.34	<0.0001*
2	30	-6.7	<0.0001*
2	60	11.26	<0.0001**
60	10	-3.28	0.0015*
60	30	2.13	0.0367**
60	60	1.6	0.1131

'*' indicates that the change in the glucose level of the HGB samples was significantly higher than that of the NB samples.
'' indicates that the change in the glucose level of the NB samples was significantly higher than that of the HGB samples.**

Chapter 6: Discussion and Conclusion

This dissertation characterizes the response of normal and high glucose concentration blood to uniform electromagnetic fields at the cellular phone frequency. A GTEM cell was designed and constructed to provide the uniform electromagnetic fields with a shielded environment in order to study electromagnetic radiation susceptibility and the biological effects of electromagnetic radiation. The developed GTEM cell's design achieved better field uniformity and doubled both the testing frequency and usable area inside the GTEM cell, compared to the standard and smaller sized GTEM cell. The developed GTEM cell ensures that there is no signal interference when the exposure system is used for biological effect studies, and its uniform electromagnetic fields are generated in the testing region where the test samples are stimulated.

Three blood samples, including normal blood, high glucose blood, and control blood were used in this study. The blood samples were exposed to electromagnetic radiation at power levels of 2 and 60 W and at frequencies of 850 and 900 MHz for testing durations of 10, 30, and 60 minutes. The 850 and 900 MHz testing frequencies represented the GSM-850 and GSM-900 cellular phone frequencies, respectively. The 2 W and 60 W exposure power levels represented the expected radiation of a cell phone and from a cell phone tower, respectively. The cell viability and glucose level in the treated samples were investigated and compared with controls. A statistical analysis was performed on the data to define significant changes in the cells and changes in the glucose levels of the blood samples from before and after treatment.

The results of this study are inconclusive at best. Variations in results are more or less stochastic. There can be two reasons for this. First, not much research effort has been dedicated in this topic area in the past. As a result there were not many data sets available for meaningful comparison. This research effort therefore can be classified as an additional source of set of data generated for possible comparison with future research work. Secondly, because of the fact that there were too many parameters involved in the experiments, such as frequency, power, and exposure duration etc., it was difficult to isolate which parameter variation affected the results. In order to isolate whether the variations are frequency dependent, or time of exposure dependent, or any other cause a lot many experiments involving minor changes in the values of the parameter are needed. This was not possible for the time allotted to the project. Some of the significant results are summarized as follows

At 850 MHz exposure, the statistical results on blood cell viability showed that there was only one significant change in red blood cell viability compared to the control, while there were five significant changes in the white blood cell viability. These significant changes were found in both the normal and high glucose blood samples. In addition, significant changes were also detected at 2 W and 60 W power levels (as stated earlier, these power levels represent power due to cell phone radiation and cell phone tower radiation, respectively). However, significant differences in glucose levels compared to the controls were found in the 30 and 60 minute treatments (long testing durations) but not in the 10 minute treatments (short testing duration). No significant variation could be due to the short testing duration, and as a result the blood cells did not absorb sufficient energy to show any effects.

At 900 MHz exposure, the statistical results on the blood cell viability showed a significant difference in red blood cell viability when compared with the control samples. These changes could be because of a greater absorption of energy by the cells at higher frequency. However, the statistical analysis on blood cell viability at 900 MHz exposure showed the same trend as the analysis on the 850 MHz exposure did. That is, significant differences in blood cell viability were found in experiments with long durations of testing or at a high power exposure, which again, could be attributed to higher energy absorption by the blood cell.

For the glucose level experiments at 850 MHz, eight of the tests showed significant changes in their glucose level compared to the controls. Most of the significant changes were found in the normal blood samples. This could be due to the fact that the permittivity of normal blood is higher than that of blood with high glucose levels. Therefore, the normal blood sample was able to respond more to the electromagnetic radiation. In addition, the analysis also supported our earlier assertion that for long testing duration and high power levels, significant differences in the glucose level could be observed.

Like exposure at 850 MHz, at 900 MHz exposure, most significant differences in the glucose level compared with the controls were detected in the normal blood samples. Significant changes were found at long testing durations and at the high exposure levels. However, statistical analysis at 900 MHz exposure was more or less random. This discrepancy in results may have been caused by the small sample size tested, possibly resulting in errors.

For the analysis of the difference in the glucose levels between the normal and high glucose blood samples at the 850 MHz frequency there were three tests that showed a significant difference in the glucose level between both the normal and high glucose blood samples. Most of the significant changes in the glucose levels were found at the short testing duration because at the long testing duration both the normal and high glucose blood samples could respond to the electromagnetic fields. The pattern of the changes in the glucose levels in the normal and high glucose blood samples were the same. Therefore, there were no significant changes in the glucose level between the normal and high glucose blood samples at a long testing duration.

At 900 MHz frequency, all testing combinations showed significant changes in glucose levels between normal and high glucose blood samples, with one exception. The analysis suggested that at high testing durations the normal blood samples showed higher significant changes in glucose levels than compared to the high glucose blood samples. This variation is due to the permittivity of high glucose blood being less than that of normal blood. Therefore, the high glucose blood sample responded less to the electromagnetic radiation.

Statistical analysis and the resulting p-value showed enough significance to suggest that radiation from a cell phone (850/900 MHz, 2/60 W uniform electromagnetic field) resulted in both an increase and decrease in the blood cell counts and glucose levels of the normal blood and high concentration glucose blood, dependent on each test combination. It would be of interest to carry out further research with larger sample sizes and fewer varying parameters. From the limited data, one can only conclude that non-ionizing electromagnetic radiation can influence a cell membrane's permeability and can

also exert an oscillating force on the free ions on the cell's plasma membrane. It is well known that the gating channels of the cell membrane are electrically sensitive. A false signal from oscillating ions can cause disordering in the gating channels and then affect the electrochemical balance of the plasma membrane, consequently affecting the whole cell function [60].

The permittivity of a cell membrane also depends on the electric charges on the cell's plasma membrane, which can exert an oscillating force [60, 64]. For this reason, electric charges can cause the oscillation of red blood cells in blood samples subjected to EM radiation, resulting in changes in the glucose concentration as well as in the dielectric and electrical properties of the blood [65, 66]. One can thus conclude that the higher the concentration of glucose in the blood, the lower the permittivity of the blood and the lower is the permittivity of the blood, the lower the electromagnetic response. Other factors that influenced changes in the blood properties were changes in the frequency, power level, and testing duration. Finally, it should be noted that the discrepancies could also have been due to the blood type. The blood samples used in each treatment were prepared from different volunteers whose reaction mechanisms were different, resulting in different responses to the electromagnetic radiation by the tested blood samples.

For future work, as explored in this experiment it is known that electromagnetic fields are likely to affect blood sugar properties, but it is difficult to pinpoint the exact power level, testing duration, and frequency where the sugar levels rise or fall. Therefore, more studies are needed to analyze the definitive power level, testing duration, and frequency that cause such changes. Such a test could be carried out with a larger sample size for better accuracy, and the GTEM cell developed in this experiment could

be used to test a large number of samples at a time and support testing frequencies higher than 6 GHz. It is highly recommended that any future analysis related to this work should not be based only on operating frequency but should be based on a combination of power level, testing duration, and frequency. Only through more comprehensive testing can we better understand the biological effects of the electromagnetic radiation so prevalent in our modern lives, particularly from cell phones and cell phone towers.

BIBLIOGRAPHY

1. *CST MICROWAVE STUDIO Educational Version, 2011.* CST Computer Simulation Technology.

2. D. Sleper, M. S. Pathan, B. Camp-Raga, S. Tantong, P. Kirawanich, J. E. Thompson, and N. E. Islam, *Optimization of Soybeans as a Biofuel Resource through Germination Studies under Electromagnetic Fields.* Proceedings of 18th International Zurich Symposium on Electromagnetic Compatibility, Munich 2007, 2007: p. 297-300.

3. T. Saunders, *Health Hazards and Electromagnetic Fields.* Complementary Therapies in Nursing and Midwifery, Nov. 2003. **9**(4): p. 191-197.

4. P. Vecchia, R. Matthes, G. Ziegelberger, J. Lin, R. Saunders, and A. Swerdlow, *Exposure to High Frequency Electromagnetic Fields, Biological Effects and Health Consequences (100 kHz – 300 GHz).* ICNIRP, 2009.

5. WHO/International Agency for Research on Cancer (IARC), *IARC classifies radiofrequency electromagnetic fields as possibly carcinogenic to humans*. 31 May 2011.

6. S. Braune, C. Wrocklage, J. Raczek, T. Gailus, and C. H. Lucking, *Resting blood pressure increase during exposure to a radio-frequency electromagnetic field.* The Lancet, Jun. 1998. **351**(9119): p. 1857-1858.

7. O. Erogul, E. Oztas, I. Yildirim, T. Kir, E. Aydur, G. Komesli, H. C. Irkilata, M. K. Irmak, and A. F. Peker, *Effects of electromagnetic radiation from a cellular phone on human sperm motility: An In Vitro stydy.* Archives of Medical Research, 2006. **37**: p. 840-843.

8. J. Hannig, and R. C. Lee, *Structural changes in cell membranes after ionizing electromagnetic field exposure.* IEEE Transactions on plasma science, 2000. **28**(1): p. 97-101.

9. L. Hardell, and C. Sage, *Biological effects from electromagnetic field exposure and public exposure standards.* Biomedicine & Pharmacotherapy, 2008. **62**: p. 104-109.

10. J. C. Lin, *Cell Phone Testing and Fundamental Scientific Research.* IEEE Antennas and Propagation Magazine, Aug. 2001. **43**(4): p. 156-158.

11. J. C. Lin, *Health Effects of Cell-Phone Research Outcomes and Source of Funding.* IEEE Antennas and Propagation Magazine, Apr. 2007. **49**(2): p. 154-155.

12. K. R. Foster, L. S. Erdreich, and J. E. Moulder, *Weak Electromagnetic Fields and Cancer in the Context of Risk Assessment.* Proceedings of IEEE, May 1997. **85**(5): p. 733-746.

13. I. Nair, and G. Morgan, *Electromagnetic Fields: the Jury's still out. 1. Biological Effects.* IEEE Spectrum, Aug. 1990. **27**(8): p. 23-27.

14. M. Havas, *Dirty Electricity Elevates Blood Sugar Among Electrically Sensitive Diabetics and May Explain Brittle Diabetes.* Electromagnetic Biology and Medicine, 2008. **27**(2): p. 135-146.

15. M. Havas, and D. Stetzer, *Dirty Electricity and Electrical Hypersensitivity: Five Case Studies.* World Health organization Workshop on Electrical Hypersensitivity, 2004: p. 1-13.

16. N. Boriraksantikul, P. Kirawanich, and N. E. Islam, *Electromagnetic radiation study of commercial cellular phones with a TEM cell for biological applications.* 2008 IEEE Region 5 Conference, 2008: p. 1-4.

17. David Morgan, *A Handbook for EMC Testing and Measurement*. c1994, Stevenage: Peter Peregrinus Ltd.

18. M. L. Crawford, *Measurement of EM Radiation from Electronic Equipment Using TEM Transmission Cells.* NBS international report, 1973: p. 73-303.

19. M. L. Crawford, *Generation of Standard EM Fields Using TEM Transmission Cells.* IEEE Transactions on Electromagnetic Compatibility, Nov. 1974. **EMC-16**(4): p. 189-195.

20. Nattaphong Boriraksantikul, *A TEM cell design to study electromagnetic radiation exposure from cellular phones*, in *Department of Electrical and Computer Engineering*. 2008, University of Missouri-Columbia: Columbia, MO.

21. M. L. Crawford, J. L. Workman, and C. L. Thomas, *Expanding the Bandwidth of TEM Cells for EMC Measurements.* IEEE Transactions on Electromagnetic Compatibility, Aug. 1978. **EMC-20**(3): p. 368-375.

22. N. Boriraksantikul, P. Kirawanich, and N. E. Islam, *Near-field radiation from commercial cellular phones using a TEM cell.* Progress In Electromagnetics Research B, 2009. **11**: p. 15-28.

23. D. Konigstein, and D. Hansen, *A New Family of TEM-Cells with Enlarged Bandwidth and Optimized Working Volume.* Proceedings of the 7th International Symposium on Electromagnetic Compatibility, Zurich, Switzerland, March 1987: p. 127-132.

24. D. Hansen, P. Wilson, D. Koenigstein, and H. Schaer, *A Broadband Alternative EMC Test Chamber Based on a TEM-Cell Anechoic-Chamber Hybrid Concept* Proceedings of IEEE Symposium on Electromagnetic Compatibility, 1989. **1**: p. 133-137.

25. Y. -B. Chen, J. Tan, X. Miao, J. Li, and G. -Z. Guo, *Electromagnetic Pulse's Effects on Insulin's Bioactivity and Mechanism Study.* 5th Asia-Pacific Conference on Environment Electromagnetic, CEEM 2009, 2009: p. 217-220.

26. N. Pinpathimrat, T. Kaweeferngfu, A. Laphodom, N. E. Islam, and P. Kirawanich, *Inhibition of Culex Quinquefasciatus (Diptera: Culicidae) Viability by Nanosecond Pulsed Electric Field Radiation.* Journal of Electrostatics, Aug. 2011. **69**(4): p. 339-344.

27. Z. Zivkovic, and A. Sarolic, *Gain and Impedance Measurement of Microstrip Patch Antennas in GTEM Cell.* 2010 Conference Proceeding ICECom, 2010: p. 1-4.

28. R. Heinrich, V. Mullerwiebus, A. Lange, B. Deutschmann, U. Karsten, and F. Klotz, *Application of GTEM Cells for IC EMC Testing* 2008 Asia-Pacific Symposium on Electromagnetic Compatibility and 19th International Zurich Symposium on Electromagnetic Compatibility, Singapore, May 2008: p. 263-266.

29. M. Alvarez-Folgueiras, M. M. Minana-Maiques, E. Moreno-Piquero, F. Jorge-Barreiro, E. Lopez-Martin, and F. Ares-Pena, *Experimental System for the Study of Multi-frequency Dosimetry.* Proceedings of the 5th European Conference on Antennas and Propagation (EUCAP) 2011: p. 1296-1299

30. K. Malaric, J. Bartolic, and B. Modlic, *Absorber and Resistor Contribution in the GTEM-Cell.* 2000 IEEE International Symposium on Electromagnetic Compatibility, 2000. **2**: p. 891-896.

31. X. Zhou, Q. -X. Jiang, and H. -Q. Jiang, *Influences of CUT on the VSWR of GTEM cell.* 20th International Zurich Symposium on Electromagnetic Compatibility, 2009: p. 49 - 52.

32. H. X. Araujo, and L. C. Kretly, *Optimizing Impedance Matching between the Exciter – APEX and the GTEM Chamber.* 2010 IEEE 26th Convention of Electrical and Electronics Engineers in Israel (IEEEI), 2010: p. 000986-000990.

33. S. Sczyslo, H. Thye, G. Armbrecht, S. Dortmund, and T. Kaiser, *Determination of the Impulse Response of UWB Antennas Using GTEM Cells.* IEEE International Conference on Ultra-Wideband, 2009. ICUWB 2009., 2009: p. 753 - 758.

34. A. I. Yurekli, M. Ozkan, T. Kalkan, H. Saybasili, H. Tuncel, P. Atukeren, K. Gumustas, and S. Seker, *GSM Base Station Electromagnetic Radiation and Oxidative Stress in Rats.* Electromagnetic Biology and Medicine, 2006. **25**(3): p. 177-188.

35. T. Jorge-Mora, M. J. Misa-Agustino, J. A. Rodriguez-Gonzalez, F. J. Jorge-Barreiro, F. J. Ares-Pena, and E. Lopez-Martin, *The Effects of Single and Repeated Exposure to 2.45 GHz Radiofrequency Fields on c-Fos Protein Expression in the Paraventricular Nucleus of Rat Hypothalamus.* Neurochemical Research, Aug. 2011.

36. K. Malaric, A. Sarolic, V. Roje, J. Bartolic, and B. Modlic, *Measured Distribution of Electric Field in GTEM-Cell.* 2001 IEEE International Symposium on Electromagnetic Compatibility, 2001. **1**: p. 139-141.

37. S. -T. Lu, S. P. Mathur, Y. Akyel, and J. C. Lee, *Ultrawide-Band Electromagnetic Pulses Induced Hypotension in Rats.* Physiology & Behavior, 1999. **67**(3): p. 753-761.

38. M. Tkalec, Z. Vidakovic-Cifrek, B. Pevalek-Kozlina, K. Malaric, and R. Malaric, *Evaluation of Genotoxic Potential of Microwave Electromagnetic Field in Onion (Allium Cepa).* 2007 IEEE International Symposium on Electrimagnetic Compatibility, 2007: p. 1-4.

39. K. Malaric, J. Bartolic, and R. Malaric, *Determination of the Higher Order Mode Occurrence in a TEM and GTEM-cell Using Self Developed Computer Program.* 2000 Asia-Pacific Microwave Conference, 2000: p. 1027-1030.

40. R. De Leo, L. Pierantoni, T. Rozzi, and L. Zappelli, *Accurate Analysis of the GTEM Cell Wide-Band Termination.* IEEE Transactions on Electromagnetic Compatibility, May. 1996. **38**(2): p. 188-197.

41. R. N. Perez-Bruzon, A. del Moral, C. Perez-Castejon, M. Llorente, A. Vera, and M. J. Azanza, *Validation of an Original Incubator Set-up for the Exposure of Human Astrocyte Cells to X-band Microwaves in a GTEM-chamber.* Histology and Histopathology, Sep. 2011. **26**(9): p. 1187-1196.

42. G. Duranti, A. Rossi, N. Rosato, G. Fazio, G. Sacerdoti, P. Rossi, R. Falsaperla, V. Cannelli, and R. Supino, *In Vitro Evaluation of Biological Effects on Human Keratinocytes Exposed to 900 MHz Electromagnetic Field.* The Environmentalist, 2005. **25**: p. 113-119.

43. N. J. Maclver, S. R. Jacobs, H. L. Wieman, J. A. Wofford, J. L. Coloff, and J. C. Rathmell, *Glucose Metabolism in Lymphocytes is a Regulated Process with Significant Effects on Immune Cell Function and Survial.* Journal of Leukocyte Biology, Oct. 2008. **84**(4): p. 949-957.

44. R. Otton, J. R. Mendonca, and R. Curi, *Diabetes Causes Marked Changes in Lymphocyte Metabolism.* Journal of Endocrinology, Jul. 2002. **174**(1): p. 55-61.

45. I. Buhler, R. Walter, and W. H. Reinhart, *Influence of D- and L-glucose on Erythrocytes and Blood Viscosity.* European Journal of Clinical Investigation, Jan. 2001. **31**(1): p. 79-85.

46. K. B. Levine, T. K. Robichaud, S. Hamill, L. A. Sultzman, and A. Carruthers, *Properties of the Human Erythrocyte Glucose Transport Protein are Determined by Cellular Context.* Biochemistry, Apr. 2005. **44**(15): p. 5606-5616.

47. David Morgan, *A Handbook for EMC Testing and Measurement*. 1994, London, UK: Peter Peregrinus Ltd.

48. EMC Test Technologies, *GTem Emc-1500*. 2 February 2010.

49. D. C. Pande, and P. K. Bhatt, *Characterization of a Gigahertz Transverse Electromagnetic Cell (GTEM cell).* Proceedings of the International Conference on Electromagnetic Interference and Compatibility 1997, 1997: p. 31-38.

50. T. -S. Chen, *Determination of the Capacitance, Inductance, and Characteristic Impedance of Rectangular Lines.* IRE Transactions on Microwave Theory and Techniques, Sep. 1960. **8**(5): p. 510-519.

51. Kreimir Malaric, *EMI Protection for Communication Systems*. 2010: Boston : Artech House c2010.

52. C. Icheln, *The Construction and Application of a GTEM Cell*. Nov. 1995, University of Hamburg-Harburg / Helsinki University of Technology.

53. P. A. Chatterton, and M. A. Houlden, *EMC; Electromagnetic Theory to Practical Design*. May 1991, Liverpool, UK: J. Wiley & Sons.

54. James H. O'Keefe, David S. H. Bell, and Kathleen L. Wyne, *Diabetes Essentials*. 2009, Sudbury, MA: Jones and Bartlett Publishers, LLC.

55. World Health Organization (WHO), *Diabetes*. August 2011.

56. National Diabetes Information Clearinghouse (NDIC), *National Diabetes Statistics, 2011*. February 2011.

57. James H. Jandl, *Blood: Textbook of hematology*. c1996, Boston, MA: Lippincott William & Wilkins.

58. National Space Biomedical Research Institute, *Hematocrit*. 2000-2010.

59. NASA, *Electromagnetic Spectrum*. 6 January 2011.

60. Peter Stavroulakis, *Biological Effects of Electromagnetic Fields: Mechanisms, Modeling, Biological Effects, Therapeutic Effects, International Standards, Exposure Criteria*. c2003, Berlin, NY: Springer.

61. ETS-Lindgren L.P., *Microwave Absorber Selection Guide: EMC-24PCL Microwave Absorbers*. 2011.

62. Inc. Powerohm Resistors, *SXR Smoothwound Resistor*. 2012.

63. X. T. I. Ngu, *An Assessment of a GTEM Cell as a Test Environment Using Measurements and Simulations*, in *Department of Electrical and Electronic Engineering*. Jul. 2009, University of Nottingham: Nottingham, UK.

64. M. Cifra, J. Pokorny, F. Jelinek, and O. Kucera, *Vibrations of electrically polar structures in biosystems give rise to electromagnetic field: Theories and experiment.* PIERS Proceeding, Moscow, Russia, Aug. 2009.

65. S. Abdalla, *Effect of erythrocytes oscillations on dielectric properties of human diabetic-blood.* American Institute of Physics, 2011. **1**(012104).

66. S. Abdalla, S. S. Al-ameer, and S. H. Al-Magaishi, *Electrical properties with relaxation through human blood.* Biomicrofluidics, 2010. **4**(034101).

VITA

Nattaphong Boriraksantikul was born in Hatyai, Songkhla, Thailand on 5 August 1983. He obtained both his B.S. degree in Computer engineering in 2006 and his M.S. degree in Electrical Engineering in 2008 from the University of Missouri-Columbia (MU), Missouri, USA.

In 2010, he received a graduate research assistantship from the Electrical and Computer Engineering department at MU, where he pursued his Ph.D. degree. His Ph.D. research was area of RF effects on biological systems. He has also worked on several research projects, including biological effects of electromagnetic radiation on blood cells and effects of high voltage nanosecond pulses on cancer cells conjugated to metallic nanoparticles. His current research areas of interest include applied electromagnetics, antenna analysis and design, bioelectrics, and renewable energy.